LAND USE CLASSIFICATION OF THE GREATER VANCOUVER AREA: A REVIEW OF SELECTED METHODS

By

Jayati Sinha

M. Phil., Jawaharlal Nehru University, India, 1998
M. A., Jawaharlal Nehru University, India, 1996
B.A., (Hons) Burdwan University, India, 1993

A THESIS SUBMITTED IN PARTIAL FULFILLMENT
OF THE REQUIREMENTS FOR THE DEGREE OF
MASTER OF ARTS

in

THE FACULTY OF GRADUATE STUDIES

(Department of Geography)

We accept this thesis as conforming
to the required standard

THE UNIVERSITY OF BRITISH COLUMBIA
July 2001

In presenting this thesis in partial fulfilment of the requirements for an advanced degree at the University of British Columbia, I agree that the Library shall make it freely available for reference and study. I further agree that permission for extensive copying of this thesis for scholarly purposes may be granted by the head of my department or by his or her representatives. It is understood that copying or publication of this thesis for financial gain shall not be allowed without my written permission.

Department of GEOGRAPHY

The University of British Columbia
Vancouver, Canada

Date 24.07.01

DE-6 (2/88)

Abstract

Accurate and current land use information for urban areas is important for effective management and planning. Over the years, researchers/planners have relied heavily on aerial photographs for land use information of urban areas because of the limitations of deriving more accurate land use estimates from satellite remote sensing data. The main problem involved in producing accurate land use maps of cities and towns from satellite images is that urban areas consist of a complex assemblage of different land cover types, many of which have very similar spectral reflectance characteristics. This is because land use is an abstract concept- n amalgam of economic, social and cultural factors-that is defined in terms of functions rather than forms. The relationship between land use and the multispectral signals detected by a satellite sensor is therefore both complex and indirect.

In many European cities, residential areas are characterized by a complex spatial assemblage of tile roof, slate roof, glass roof buildings, as well as tarmac, concrete and pitch roads, and gardens (comprised of grass lawns, trees and plants). In North American cities, roofing materials are more commonly composed of wood and shingles. In both settings all these "objects" together form the residential areas or residential districts of town or city, but each of them has a different spectral reflectance. So, in generating a land use map from remotely sensed image, buildings, roads, gardens, open spaces will be identified separately.

Keeping this in mind, this thesis evaluates eight selected land use classification methods for the Vancouver metropolitan area, identifies the most accurate and suitable method for urban land use classification, and produces a land use map of the study area based on the most suitable method.

The study area is a part of Greater Vancouver Regional District (GVRD). It includes Vancouver, Burnaby, Richmond, Delta, and parts of seven other municipalities. The whole area is highly urbanized and commercialized. Agricultural lands are present in the southern part of the study area (which includes parts of Richmond, Delta and Surrey).

For this study four sources of data have been used. The 1996 Greater Vancouver regional District (GVRD) land use map is the basic source of land use information. A remotely sensed image of May 1999 (Landsat 7) has been used for the identification of land cover data, Vancouver and Fraser valley orthophotos (May/July 1995) have been used to locate sample sites, and aerial photos of May 1999 (1:30,000) have been used for ground verification.

Key words: Land use, land cover, urban image classification, and error matrix.

TABLE OF CONTENTS

LIST OF TABLES

LIST OF FIGURES

Acknowledgement

While doing this research, I had the honour and privilege of working with a number of exceptional people whose help and support proved to be invaluable. First and foremost, I would like to thank my supervisors Dr. Brian Klinkenberg and Dr. Graeme Wynn. Their boundless enthusiasm and excellent advise during the past two years provided a most enjoyable environment to work in. I would also like to thank Dr. Tom Hutton, my third committee member, for nourishing the whole idea right from its synopsis stage to its final form. Catherine Griffiths assisted greatly in the preparation of this thesis. Thanks are also due to all staff of the Geography Department for their generous help directly or indirectly from time to time related to their respective job pursuits.

I would also like to thank the International Council for Canadian Studies and the Commonwealth Agency of India for providing me with a most generous scholarship during my research.

Thanks go out to all those people who made my stay at UBC more enjoyable. Tara deserves my special thanks for just being there, when I needed her the most. And of course, to Naresh, my husband, I owe more, than can be expressed in a few lines. He was always the source of undiminished criticism and sustenance. Finally, I would like to thank my parents and family for supporting me during my academic career.

CHAPTER I

Urban Image Classification: An Introduction and Overview of Classification Methods

1.1 Introduction: Urbanization is now recognized as a ubiquitous phenomenon of global importance. Modern urbanization results in profound changes to the landscape, specifically the proliferation of asphalt and concrete along with the displacement of agriculture and forestland. Today over 70 percent of the population in developed countries lives in urbanized areas and almost two thirds of the world's urban population lives in less developed countries (Griffiths, 2001). As a nation's population grows, quantifying, monitoring, and managing land use becomes increasingly necessary. A temporal database documenting urban land transformation is needed by urban and regional planners, policy and decision makers, earth scientists, and global change researchers to measure trends in urban sprawl; to understand land use patterns; to monitor how land use changes affect the environment; to develop zoning policies concerning land use development; to understand the impacts of development on ecosystems; and to develop predictive modeling techniques to forecast future areas of urban growth (Cervero, 1989).

The demand for land use information has increased recently, especially in rapidly growing metropolitan areas (Homer *et al.*, 1997). Many Federal, State, regional, and local planning agencies require up-to-date land use information for the management and planning of these areas. Aerial photographs have traditionally been used to collect this information. However, aerial photographs are expensive and difficult to get on a regular basis. Satellite remote sensing can provide a method for acquiring regular, recent information about urban areas which may be particularly useful for monitoring changes within and on the fringes of urban development (Harris & Ventura, 1995). Researchers all over the world are trying to develop improved image classification techniques. The increasing number of image classification techniques developed in recent years suggests that satellite remote sensing may be the most widely used terrestrial resources survey technique through the next decade or two, especially for the analysis of land cover and its changes (Toulios, 1990). Yet the proliferation of classification techniques also suggests that no one technique is entirely satisfactory for land cover classification; there is always need to improve the techniques in order to achieve more accurate classification results.

1.2 Defining terminology: land cover vs land use mapping: *Land-cover* and *land-use* are closely related parameters, and are often confused, but they are *not* the same, and it is important to distinguish clearly between the two in any given classification design. *Land cover* can be defined as the actual materials present on the surface of the earth (all the natural and man-made features that cover the earth's surface) (Thompson, 1996). *Land use* typically refers to the human activity that is associated with a specific land-unit, in terms of utilization, impacts, or management practices (Thompson, 1996). *Land use* is therefore based upon function rather than forms. There can only be one *land-cover* type associated with a point on the earth's surface, but this cover type can be associated with several *land uses* in different locations. For example, 'grassland' may be used for communal-grazing within a conservancy area, it may be a part of recreational area (e.g., golf course), or it may be a part of residential area (e.g., lawns). Similarly, one land use can be associated with several land covers.

1.3 Aerial photographs and land use mapping: The technology of modern remote sensing began with the invention of the camera more than 160 years ago. Although the first, rather primitive photographs were taken as "stills" on the ground, the idea of looking down at the earth's surface, yielding *aerial photos* emerged in the 1840s with pictures taken from balloons for purposes of topographic mapping. During the American Civil War, balloons were used to observe enemy positions and reportedly to take photographs of them. This was the first of many times that war spurred advancements in remote sensing. From the Civil War until the First World War, people experimented with other platforms such as rockets, kites, and pigeons, but the great step forward was the invention of the airplane, a much more stable and reliable platform. During the First World War, cameras mounted on airplanes provided aerial views of fairly large surface areas that proved invaluable in military reconnaissance. By World War II the technology had become highly sophisticated. Between the wars, military research and development in remote sensing was minor, but the experiences of World War I encouraged civilian uses of remote sensing in forestry, agriculture, and geology. From then until the early 1960s, aerial photograph remained the single standard tool for depicting the surface from a vertical or oblique perspective.

Many organizations and individual researchers have been using aerial photographs for urban land use analysis since the 1940s (Kivell P.T. *et al.*, 1989). Mostly, these applications have relied upon small scale[1] aerial photos and have been utilized for land use mapping of large areas. Berlin (1971) has described much of this early usage. Some early studies of urban structure were attempted by Green (1957) and Green and Monier (1960), however, serious studies of urban land use analysis came mainly with the improvements in photography such as the widespread use of colour films (Lindgren, 1985). By the mid-1960s, more attention was being paid to the systematic use of sequential aerial photography in order to monitor patterns of urban change (Dueker and Horton, 1971). Since the mid-1970s aerial photographs have mostly been used for small area analysis, as satellite remote-sensing techniques have become the single most effective method of acquiring land use data for large areas.

1.4 Satellite remote sensing and land use mapping: Satellite remote sensing can be traced to the early days (1950s) of the space age, when both Russian and American programs began imaging surfaces using several types of sensors from spacecraft. With the development of the space program in the 1960s, satellites were being declassified for civilian use. The first systematic satellite observation came with the launch of the United States' *TIROS 1* in 1960. This was a meteorological satellite, designed to track weather

[1] Small Scale vs. Large Scale aerial photos: Geographers use these terms differently from others. A **large scale** is where *the RF (***representative fraction** or ratio scale) *is relatively large*. A 1:1200 map or aerial photo is therefore larger scale than a 1:10,000,000 map or aerial photo. The 1:10,000,000 map or aerial photo would usually be called a **small scale map** or aerial photo. This is true even though the 1:10,000,000 map or aerial photo would show a much larger area than the 1:1200 map or aerial photo. The large/small scale terminology can become confusing when talking about large versus small areas. If you are talking about a phenomenon that occurs across a large region, it is tempting to say it's a large-scale phenomenon (e.g., "the forest blight is a large-scale disease"). However, the map that would show this would be small-scale.

systems. With the launch of the first Landsat satellite (which was the first satellite to collect data on the earth's natural resources) in 1972, systematic, synoptic, repetitive, 80 m resolution multispectral images of the earth's surface were available from space. Data capture, transmission, storage and analysis technologies have improved substantially since the first Landsat. The data collected by multispectral remote sensing instruments are in a digital form, allowing for mathematical analysis and manipulations. The information content of remotely sensed data is enhanced by the ability to apply image analysis techniques to extract useful information.

Until the early 1980s, satellite sensor technology had been used with some success to monitor land use in agricultural areas; much less satisfactory results were generally reported from the monitoring of urban areas (Forster, 1985; Barnsley *et al.*, 1989). During this period the application of remote sensing techniques to urban areas was relatively crude, and was used mainly to examine urban site and transport linkages and various aspects of individual land plots (Kivell P.T. *et al.*, 1989). Initially, this was attributed to the relatively coarse resolution of early Earth-resources sensors, such as the Landsat Multispectral Scanning System (MSS) (Barnsley and Barr, 1996). These sensors tended to produce broad, composite signals from urban areas. It was quite difficult to distinguish between different urban land use categories in remote sensing images (Barnsley and Barr, 1996). Over time, higher-resolution sensors have been used to collect information on land cover. However, the use of higher-resolution data from the current generation of satellite sensors has not always yielded anticipated improvements in distinguishing land cover patterns in urban areas (Forster, 1985; Barnsley and Barr, 1996).

Since the 1970s numerous techniques for satellite image classification have been developed. Initially, two types of approaches evolved and, in spite of recent developments, these have remained as the basic options. They differ in the assumptions made about the knowledge of the scene to be classified. In what is generally called *supervised classification, a priori* knowledge of all cover types to be mapped is assumed. This knowledge is used to define 'training sites' (representative sample sites of known land cover types). The overall objective of the training process is to assemble a set of statistics that describe the spectral response pattern for each land cover type to be classified in an image. Once the statistical characterization is achieved for each land cover class, the entire image is then classified by examining the reflectance for each pixel and assigning it to a land cover class. In *unsupervised classification*, no prior information is required. Unsupervised classification methods divide the scene into more or less pure spectral clusters. In essence numerical operations are performed to group pixels according to their spectral properties (Jensen, 1986). Once the spectral clusters are generated, analysts often attempt to determine the nature of the clusters and to label them.

In recent years (between 1980 and 1995), numerous variants of these two basic classification methods have been developed. These include *decision trees* (Hansen *et al.*, 1996); *neural networks* (Carpenter *et al.*, 1997; Foody *et al.*, 1997; Bischof and Leonardins, 1998; Yool, 1998); *fuzzy classification* (Foody, 1996, 1998; Mannan *et al.*, 1998) and *mixture modeling* (Meer, 1995) for supervised classification, and classification by *progressive generalization* (Chilar et al., 1998), and *post-processing adjustments* (Lark, 1995) for unsupervised techniques.

In the beginning of satellite remote sensing, image analysis was entirely dependent on the spectral signature[2] (or spectral reflectance) of a feature. However, it was difficult to discriminate one specific urban class from another based solely upon spectral characteristics (Estes *et al.*, 1983). The fundamental problem involved in producing accurate land use maps of cities and towns from satellite images is that urban areas consist of a complex assemblage of different land cover types, each of which may have different spectral reflectance characteristics (Barnsley *et al.*, 1991; Eyton, 1993; Barnsley, 1996). For example, in many European cities, residential areas are characterized by a complex spatial assemblage of tile roof, slate roof, glass roof buildings, as well as tarmac, concrete and pitch roads, and gardens (comprised of grass lawns, trees and plants). In North American cities, roofing materials are more commonly

[2] In remote sensing, the word 'spectral signature' has a special connotation. The spectral signature of a feature comprises a set of values for the reflectance of incident electromagnetic energy in different regions of the electromagnetic spectrum (appendix 1.1).

composed of wood and shingles. In both settings all these "objects" together form the residential areas or residential districts of towns or cities, but each of them has a different spectral reflectance. So, in generating a land cover map based on the spectral reflectance of individual objects on the earth, the buildings, roads, gardens, open space will be identified separately.

Over the last few years, high-resolution sensors have been used to collect information on land cover. As the spatial resolution of the sensor increases, individual objects on the earth (e.g., buildings, roads, trees, open spaces etc.) begin to dominate the detected response of each pixel; therefore, the spectral response of urban areas as a whole becomes more complex and varied, making land cover classification more problematic (Gastellu-Etchhegorry, 1990).

Although most classification strategies have focused on the use of the spectral dimension, the spatial elements also contain important information, especially in fine resolution data (Wulder, 1998). Numerous algorithms have been developed to quantify spatial relations within images, such as texture (Gong *et al.*, 1992), pattern recognition (Wilkinson, 2000), segment homogeneity (Kartikeyan *et al.*, 1998), and various others, but the spatial dimension has not been used effectively in image classification so far.

There is a strong need to make better use of spatial information for urban image classification. The spatial information contained in the satellite images can be subdivided into two types: texture and context. *Texture* refers to the spatial variation within a contiguous group of pixels. It is defined as the characteristic placement and arrangement of spectral tones in an image. It determines overall visual “smoothness” or “coarseness” of image features, and can be a very valuable aid in identifying urban features. By contrast, the *context* of a pixel (or a group of pixels) consisted by its spatial relations with pixels in the remainder of the image. Certain classes of ground cover are likely to occur in the *context* of others (Swain *et al.*, 1981; Alosno F. G. *et al.*, 1991; Kartikeyan B. *et al.*, 1994; Stuckens J. *et al*, 2000; Barr *et al.*, 2000). In general one does not expect to find a agricultural fields in the midst of a high-density urban area[3], for example. A close-grown lush vegetation cover in such a location is more likely turf or lawn than an alfalfa crop (Swain *et al.*, 1981).

Although in the last 5-10 years land cover mapping from satellite imagery has improved, research on various issues regarding data pre-processing, classification and accuracy assessment continues. There are many aspects that remain important research questions. Perhaps chief among these is the need to develop broadly applicable, user-friendly urban land cover classification techniques for fine resolution satellite data and a procedure to generate land use maps based on land cover information.

1.5 Study Area: The study area is a part of Greater Vancouver Regional District (900 sq. km) (GVRD) (Figure-1.1)[4]. It includes Vancouver, Burnaby, Richmond, and Delta, and parts of New Westminster, Surrey, Coquitlam, Port Moody, North Vancouver, and West Vancouver. The whole area is highly urbanized and commercialized. Agricultural lands are present in the southern part of the study area (which includes parts of Richmond, Delta and Surrey).

1.6 Objectives of the study: Over the past quarter of a century, the Vancouver metropolitan area has experienced high levels of growth in population, labour force, investment, output and trade. The population of this area has increased from 827,522 in 1961 to 1,813,968 in 1996, which is a 119.3 percent increase. This situation suggests the urgency of efficient planning and management to meet the growing demand for goods and services and housing within the Vancouver metropolitan area. Management and planning of urban areas requires current and accurate information about land use for informed decision-making or policy implementation. Keeping this in mind, an attempt will be made to determine the most accurate and suitable method for urban land cover

[3] This may not be true world wide and with the rise of so-called urban farming.
[4] Due to the limited resources only a part of GVRD is used for the study. The main goal of this study is to determine a suitable land cover classification method for Greater Vancouver area and the selected study area is adequately representative of the entire GVRD.

Figure-1.1 Study area

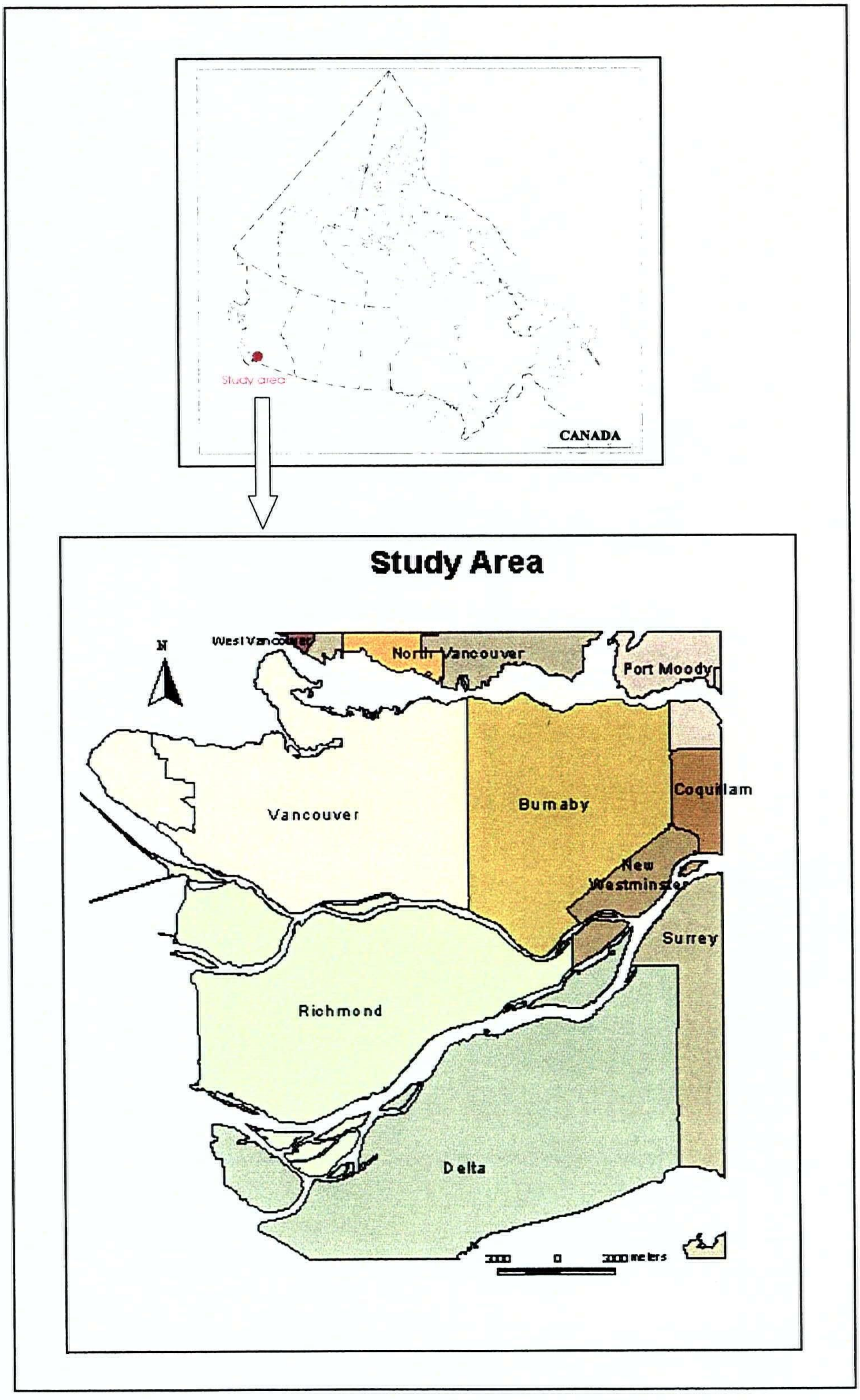

classification, which may help to generate a more accurate land use map of the Vancouver metropolitan area. Therefore, the basic objectives of the study are:

1. to review selected methods of urban land cover classification and identify the most appropriate method for use in the Vancouver metropolitan area,
2. to find out why some of the specified methods are not providing expected results,
3. to generate a land use map based on the most suitable and accurate land use classification method,
4. to investigate the comparability and accuracy level of the newly generated land use map with the 1996 land use map of the GVRD.

1.7 Research questions to be investigated: The following questions will be addressed in this study:

1. Is the 'most suitable' land use method sufficient to distinguish between different urban and non-urban features? In what way we can modify the method in order to present more accurate results?
2. What will be the possible accuracy level and reliability of the newly generated land use map of the Vancouver metropolitan area?
3. Which land use categories are not represented properly and what are the reasons for this?

1.8 Chapter scheme: This work is divided into eight chapters. The first chapter provides an overview of classification methods, introduces the objectives of the study, the research questions and the chapter scheme. The second chapter focuses on methodology and the database. Chapters 3 to 7 review selected methods of urban land use classification for the Vancouver metropolitan area. Chapters 3 reviews supervised and unsupervised land use classification methods. Three other variants of supervised and unsupervised classification are discussed in chapter 4. Image segmentation is presented in chapter 5, and methods of integrating ancillary data to improve land use classification are explored in chapter 6. Chapter 7 is a brief discussion of the role of contextual information in land cover classification. The final chapter briefly summarizes the main findings of this work and presents a land use map of the study area using the most suitable classification method.

CHAPTER II

Methodology and Database

2.1 Introduction: During the past three decades there have been significant improvements in urban image classification techniques, but no single technique yields accurate results, and none fully utilizes the data captured by the new generation of satellite sensors. More useful and suitable methods of urban land cover classification are needed. However, patterns of urbanization and metropolitan growth are not consistent throughout the world. Since the use of land varies between the developing and the developed world, particular classification methods may not necessarily be successful in capturing this variation. Therefore, this research seeks to determine the most accurate and suitable land cover classification method for the Vancouver metropolitan area.

2.2 Methods to be used: This study reviews eight methods of land cover/land use[1] classification, and generates a land use map for the Vancouver metropolitan area based on the most suitable method (figure 2.1). These eight methods are:

I Unsupervised approach:

1. Unsupervised classification
2. Image segmentation

II Supervised approach:

3. Supervised classification (using a maximum-likelihood classifier)
4. Neural network analysis
5. Fuzzy classification
6. Contextual classification

III Post-classification processing:

7. Post-classification smoothing (using modal filters)
8. Using ancillary data (agricultural and park zoning data)

---

[1] Unsupervised approach is a land cover classification while supervised and post classification approaches are land use classifications.

Figure-2.1: Different classification methods used in this study

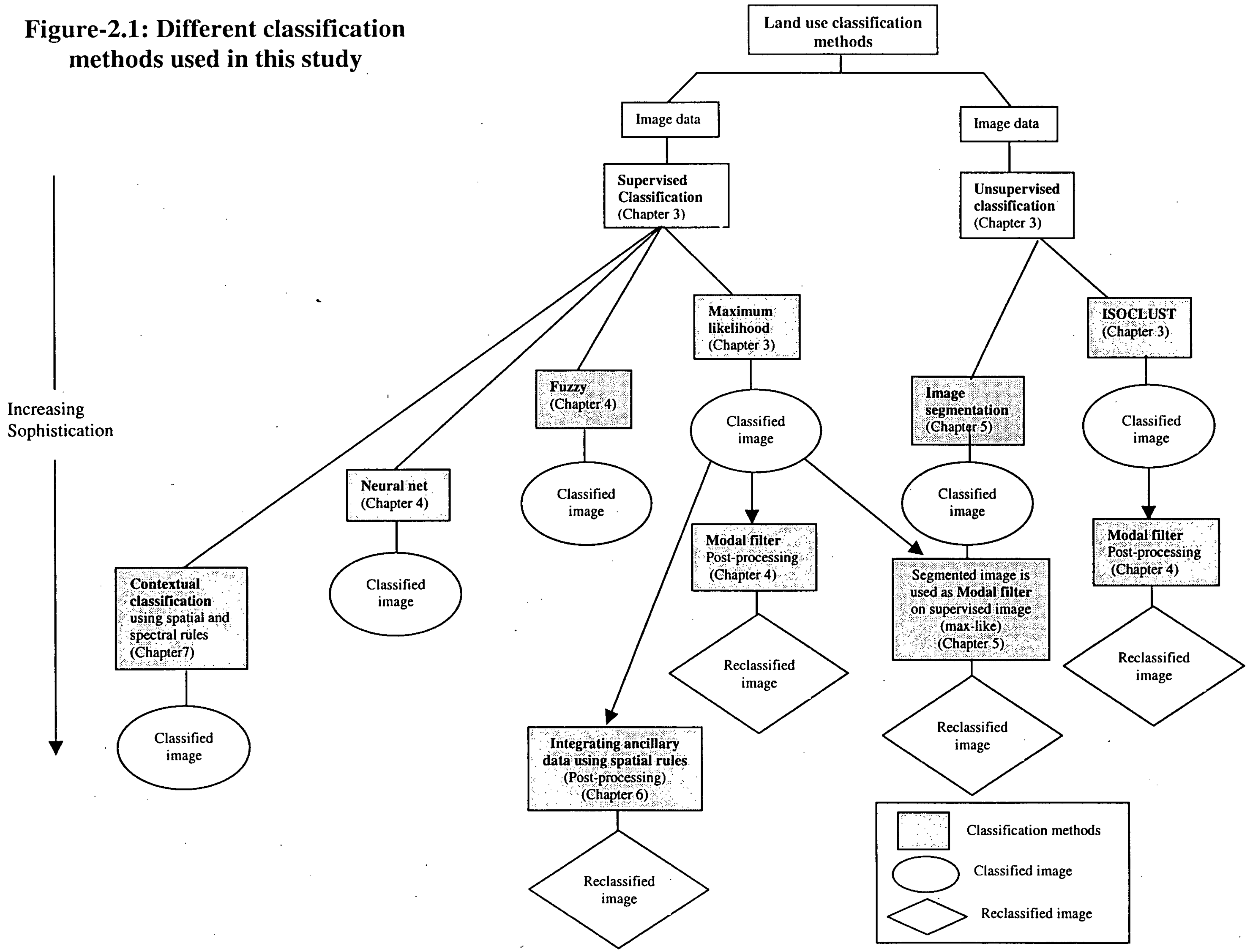

2.3 Software used for the study: A number of GIS and image processing software programs have been used in this study:

- IDRISI version 3.2 as a primary image processing software
- PCI image processing software version 6.3
- SILVICS (Satellite Image Land Vegetation Integrated Classification System) version 1.1
- ArcView GIS 3.2
- ArcInfo 8.0.2

2.4 Data sets: In this study four different data sets have been used:

1) The 1996 Greater Vancouver regional District (GVRD) land use map is the basic source of land use information. The GVRD land use map is classified into thirteen land use categories (table 2.1 and figure 2.2), which are land use zones demarcated for planning purposes. However, land cover classification techniques using satellite images are not able to distinguish between these 13 land use classes due to their spectral similarities. Thus there is a need to merge some of the classes together. Keeping in mind both spectral properties and land use issues, four different residential and institutional land use classes identified on the 1996 land use map (figure 2.2 and table 2.1) were merged into a single residential class because they are inseparable from each other in remotely sensed images due to the spectral similarity of buildings, and the driveways and lawns associated with them. The transportation land use class has been apportioned between two distinct classes: open space and industrial. It can be seen from figure 2.2 that the transportation land use class represents airport areas, bus depot and dock areas. Airport areas have been merged into the open space class due to the large content of open space associated with airport area; however, bus depot and dock areas have been merged with the industrial class because of their functional similarity. Thus the eight land use classes for this study are generated. They are: agricultural, commercial, extractive industry, industrial, lake, park, open space and residential class.

Figure-2.2: GVRD land use map, 1996
(with original 13 classes and after regrouping- 8 classes)

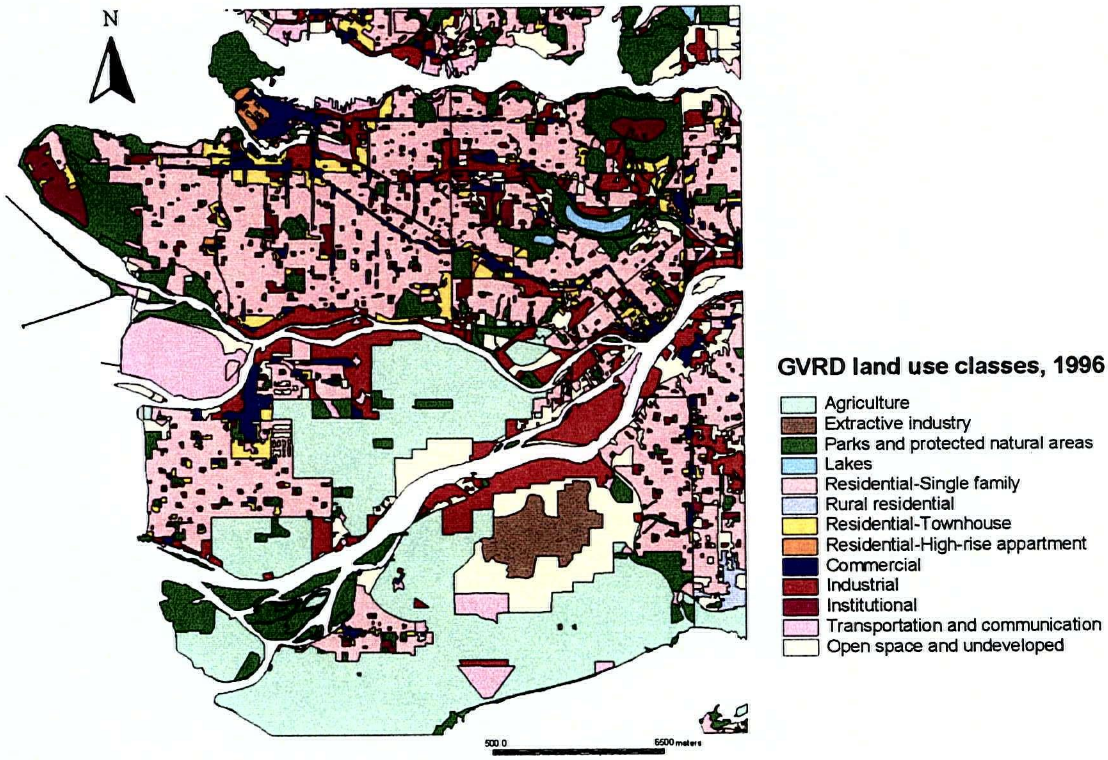

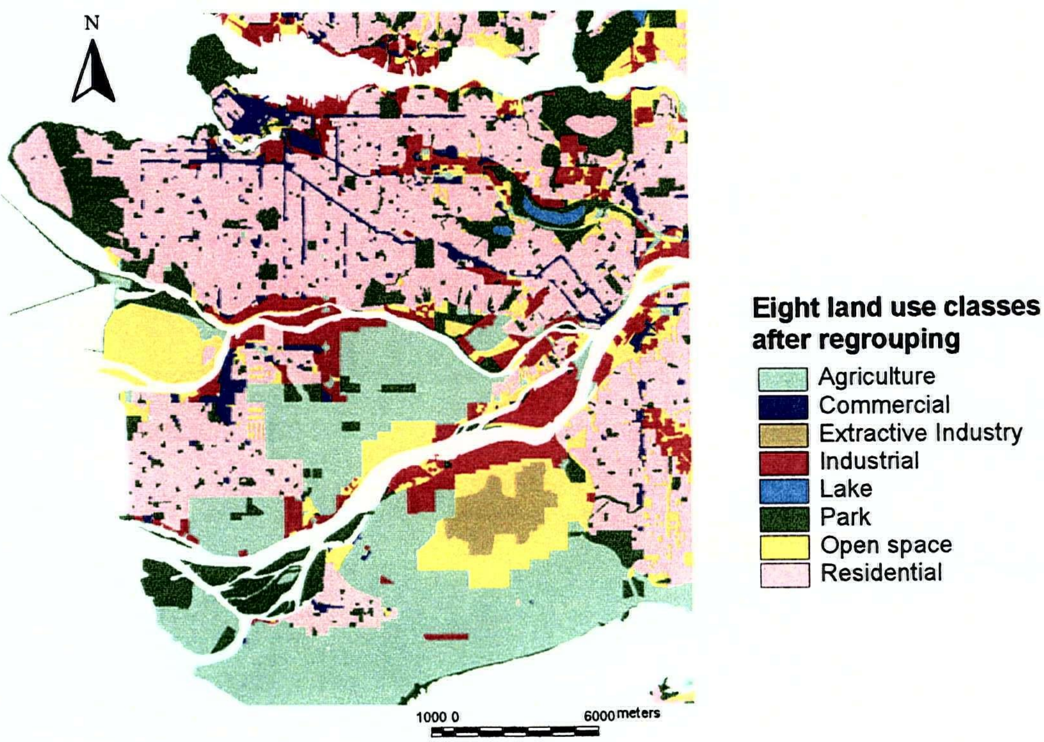

Table-2.1: Eight land use classes used for this study

Land use classes of GVRD, 1996	Eight Land cover / land use classes for this study	
1. Agriculture	Same	1. Agriculture
2. Commercial	Same	2. Commercial
3. Extractive industry	Same	3. Extractive industry
4. Industrial	Same	4. Industrial
5. Lake	Same	5. Lake
6. Park and protected national park	Same	6. Park
7. Open space and under developed	Merged	7. Open space
8. Residential -single family	Merged	8. Residential
9. Rural residential	Merged	
10. Residential townhouse	Merged	
11. Residential - high-rise apartment	Merged	
12. Institutional	Merged	
13. Transport and communication	Merged	7. Open space
	Merged	4.Industrial

2) Aerial photos of May 1999 (1:30,000) were used for ground verification.

3) 36 selected images from the Vancouver and Fraser valley orthophoto, May/July 1995 (pixel size is 4 meters and accuracy is 10 meters) were used to locate each ground truth site.

4) A remotely sensed Landsat 7 image (fused product)[2] of 1999 May was used for land use classification (table 2.2). The panchromatic band - band 8 of Landsat 7 - is characterized by a very high spatial information content (resolution of 15 m) well suited for urban analysis. The multispectral bands (bands 1 to 5 and 7, with much lower spatial resolutions, e.g., 30 m for Landsat TM) provide the spectral information for smaller scale thematic mapping applications such as land use surveys. In order to take advantage of both the high spatial information content of the panchromatic images and the essential spectral information of lower resolution multispectral images, *fusion* of these two types of images was performed in order to produce high-resolution (15 m resolution) multispectral images (except the thermal band - band 6 - which is not included in the image fusion).

[2] The principal reason of merging multi-resolution image data is to create composite images of enhanced interpretability (Welch and Ehlers, 1987; Kaczynski et al., 1995). The images should have the highest possible spatial information content while still preserving good spectral information quality (Cliche et al., 1985).

Table-2.2: Landsat 7 ETM+ Spectral Bandwidths and Resolution for both original image and LANDSAT 7 fused product (used for this study)

Bands	Wave lengths covered by	Resolution of original image	Resolution of LANDSAT 7 fused product
Band 1	450 to 520 nm	30	15
Band 2	520 to 600nm	30	15
Band 3	630 to 690nm	30	15
Band 4	760 to 900nm	30	15
Band 5	1.55 to 1.75m	30	15
Band 6	10.4 to 12.5m	60	60*
Band 7	2.08 to 2.35m	30	15
Band 8	520 to 900nm	15	15*

nm = nunometer; m = micrometer;
*Band not included in the study (band 6 and band 8). Band 6 has much coarser resolution than the rest of the bands of the data. Band 8 covers a bandwidth between .52 -.90 micrometers, which is basically an inclusion of band 2 band 3 and band 4.

2.5 Land cover accuracy assessment: Classification accuracy assessment is necessary to compare the performance of various classification techniques. Assessment of the accuracy of a classified land use map is important in many ways. The legal standing, operational usefulness, and validity of the data as a basis for scientific research are dependent on map accuracy. The development of criteria and techniques for testing map accuracy began in the 1970s (Hord and Brooner, 1976). More in-depth studies and the development of new techniques were initiated in the 1980s (Anonoff, 1985). Today, the error matrix has become the standard medium for reporting the accuracy of maps derived from remotely sensed data.

Accuracy is a measure of agreement between a reference map (assumed to be correct such as a ground truth map) and a classified land use map. The goal is to quantitatively determine how effectively pixels of an image were grouped into the correct land use classes. Most quantitative methods of assessing classification accuracy involve an error matrix built from the two data sets (i.e., the classified map and the reference map). An error matrix is a square array of numbers set out in rows and columns. The columns normally represent the reference data, while the rows indicate the classification generated from the remotely sensed data. An error matrix is a very effective way to represent accuracy because the accuracy of each category is clearly described, along with both errors of inclusion (commission errors) and errors of exclusion (omission errors), as well as summary statistics for the entire matrix.

Overall map accuracy is computed by dividing the total number of correctly classified pixels by the total number of pixels in the error matrix. Accuracies of individual categories are computed by dividing the number of correct pixels in a category by either the total number of pixels in the corresponding row or the corresponding column. When the number of correct pixels in a category is divided by the total number of pixels in the corresponding row (i.e., total number of pixels that were classified in that category), the result is an accuracy measure called *user's accuracy*. The *user's accuracy* is an indication of the probability that a classified pixel represents that category on the ground. On the other hand, when the correct number of pixels in a category is divided by the total number of pixels in the corresponding column (i.e., total number of pixels for that category in the reference data), the result is called *producer's accuracy*. *Producer's accuracy* indicates the probability of a reference pixel being correctly classified.

This study uses the IDRISI 'ERRMAT' module for accuracy assessment. In addition to the basic error matrix, 'ERRMAT' also reports the overall and per category Kappa coefficient of Agreement (referred to as K or k). The kappa coefficient represents the proportion of agreement obtained after removing the proportion of agreement that could be expected to occur by chance. The Kappa coefficient lies on a scale between 0 and 1, where the latter indicates complete agreement, and is often multiplied by 100 to give a percentage measure of classification accuracy. Kappa values are also characterized into 3 groupings: a value greater than 0.80 (80%) represents strong agreement, a value between 0.40 and 0.80 (40 to 80%) represents moderate agreement, and a value below 0.40 (40%) represents poor agreement (Congalton, 1996). The equation for the kappa coefficient of agreement is:

$$K = \frac{\text{Overall Classification Accuracy} - \text{Expected Classification Accuracy}}{1 - \text{Expected Classification Accuracy}}$$

The expected classification accuracy is the number of correct classifications that can be anticipated by chance agreement between the two data sets. It can be calculated by first using the error matrix to produce a matrix of the products of row and column totals. Then expected accuracy is computed as the sum of the diagonal cell values divided by the sum of all cell values.

2.6 Sampling in support of accuracy assessment: The overriding assumption for classification accuracy assessment is that the error matrix is representative of the entire area mapped from the remotely sensed data. Therefore, a proper sampling approach is essential in generating the error matrix. Since the verification of entire mapped areas is not always possible (especially if the study covers a large area), sampling is the only alternative for accuracy assessment of classified image. Selecting a sampling scheme that is truly representative of the ground is a critical part of image classification accuracy assessment. Designing a sample scheme includes a number of considerations, such as: (1) the spatial distribution of sample sites within a study area, (2) the number of sample sites within a study area, and (3) the size of the individual sample site.

Decisions about where to sample ground data are of great importance. There are three basic sampling schemes: simple random sampling, stratified random sampling, and systematic sampling (random systematic sampling and stratified systematic sampling)[3].

[3] **Simple random sampling** is a method of selecting the sample units out of the population, such that each element in the population has an equal chance of being selected (Cochran 1977). Simple random sampling tends to under-sample small but potentially important areas (Congalton 1988a, 1991). That problem can be overcome by using **stratified random sampling**, which is a sampling method in which the elements of the population are allocated into sub-populations (e.g. strata) before the sample is taken, and then each stratum is randomly sampled. This sampling approach can be used when specific information about certain sub-populations and increasing precision of the estimates for the entire population is desired (Cochran 1977, Clark and Hosking 1986). **Systematic sampling** is a method in which the sample units (here pixels) are selected at some equal interval over time or space. The advantage of systematic sampling is the uniform spread of the sampled observations over the entire population (Cochran 1977). The major disadvantage, on the other hand, is that the selection procedure implies that each unit in the population does not have an equal chance of being included in the sample (Berry and Baker 1968). Systematic sampling can ether be random systematic or stratified systematic. **Random systematic sampling** is a method in which the population elements are arranged in some order. The first sample is randomly located and thereafter each unit is selected systematically from around that single sampled unit using a fixed interval (Clark and Hosking 1986). **Stratified systematic sampling** combines the advantage of randomization and stratification with the useful aspects of systematic sampling, while avoiding the possibilities of bias due to the presence of periodicity (Berry and Baker 1968).

Opinions vary greatly about choices of sampling methods (e.g. Rosenfield *et al.,* 1982, Fitzpatrick-Lins 1981, Ginevan 1979, Van Genderen *et al.,* 1977, 1978, Hord and Brooner 1976). This research uses a stratified random sampling to collect the ground truth, considering each of the eight land cover classes as a separate stratum. Studies (Genderen *et al.,* 1978; Congalton, 1988) have shown that stratified random sampling provides satisfactory results using remote sensing imagery because of its ability to represent important minor categories satisfactorily.

The next step in sampling design is to determine the minimum number of sampling sites for ground truth data. Researchers (e.g. Curran and Williamson, 1985, 1986, Hatfield *et al.,* 1985, Hay 1979, Van Genderen et al., 1978, Ginevan 1979, Hord and Brooner 1976, Thomas and Allcock, 1984) have discussed the number of sample sites required to characterize a study area. Curran and Williamson (1985) indicate that the number of sample sites within a study area is dependent upon the size of the training data set and the number of classes in the final analysis. They conclude that a larger sample size than 30 (for each category) should be collected in remote sensing studies in order to keep the sampling errors low. Hay (1979) concludes that any sample of less than 30 sampling sites for each category will not provide a satisfactory guide to true error rates. Gong and Howarth (1992) suggests that the sampling size should be approximately 60. In satellite remote sensing a minimum of 40 sites *per class* is recommended for any image analysis (Thomas and Allcock, 1984). For this study an equal number of samples (60 sites) should be collected for all land use classes except for the lake class (30 sites), which occupies a fairly small area.

Most observations at ground level are made in areas rather than at points (Alford *et al.,* 1974). Therefore, decisions need to be made about the most appropriate (i.e., minimum) sample size acceptable for a valid statistical testing of accuracy of the land cover map. Justice and Townshend (1981) provide a formula to calculate the size of each sample site, in relation to the pixel size and the geometric accuracy of the imagery (eq. 1)[4].

[4] Justice, C.O., and J. G Townshend, 1981), *Integrating ground data with remote sensing*, In Terrain analysis and remote sensing, Townshend J.G., editor, pp.43, George Allen and Unwin, London.

Greater Vancouver Area: Ground Truth Sites.
(434 sample sites)

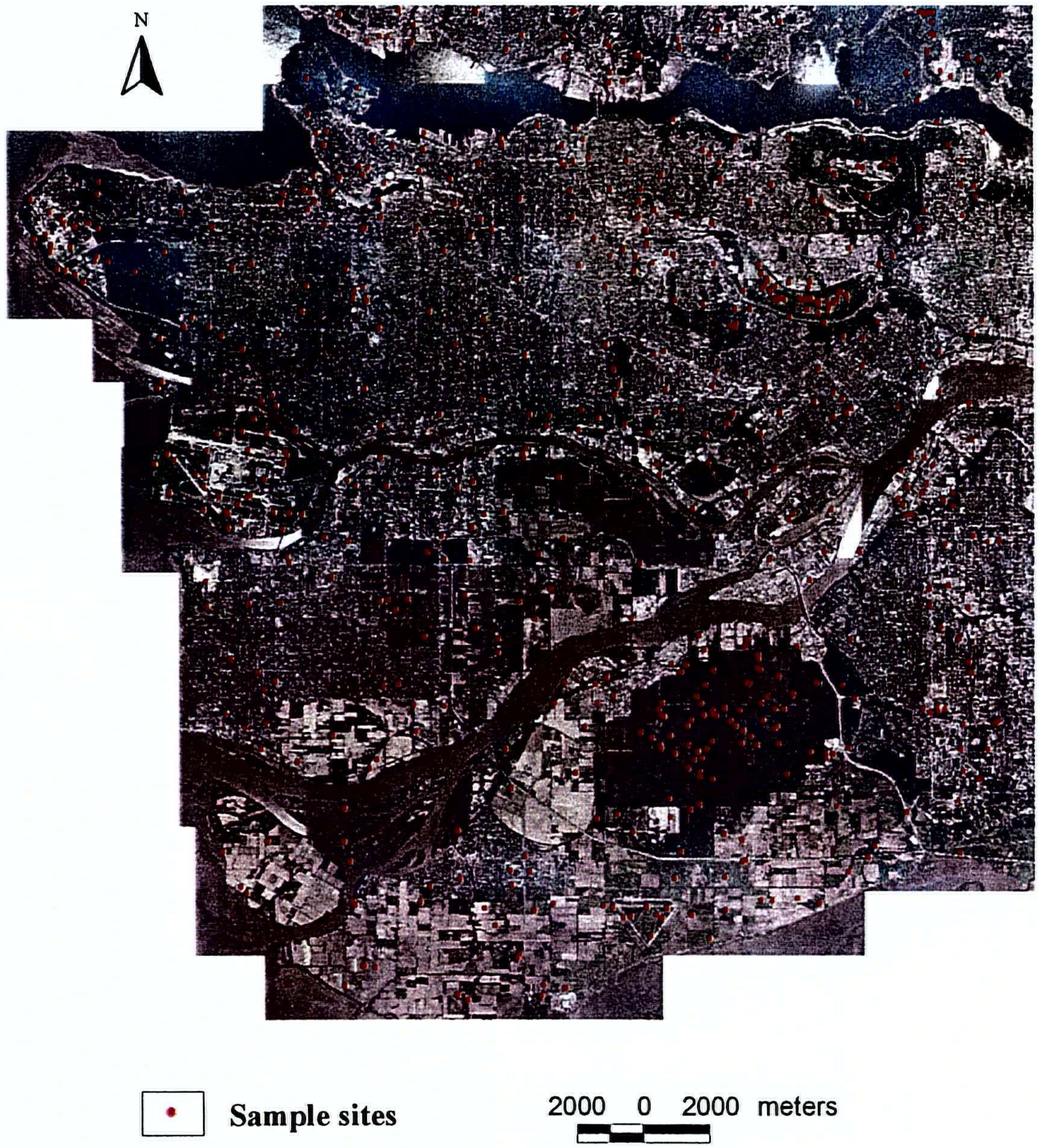

Figure – 2.3

$$A = P(1+2G) \quad \ldots\ldots\ldots\ldots\ldots\ldots\ldots\ldots \text{(eq.1)}$$

where:

A = area to be sampled

P = pixel size

G = geometric accuracy of the image (in number of pixels)

Using this formula the size of each sample site can be determined. Thus, with a geometric accuracy of 1 pixel and pixel size of 15 meters, the size should be 45 sq. meters or, in other words, 3 x 3 pixels.

After selecting the sampling method and number and size of sampling sites, the next step is to collect the ground truth information. Based on the 1996 land use map (i.e., the latest available land use map of the study area provided by the GVRD) and using the stratified random sampling method, 450 initial sample sites were selected. Aerial photos (1:30,000) of the study area dated to May 1999 were used to collect ground truth information for these 450 sampling sites in order to maintain the same time period for both image classification and ground truthing. However, these aerial photos are not georeferenced. It was important to know the exact location of each sample site before collecting the ground truth information. Thus, 1995 orthophotos (which are georeferenced) were used to identify the location of sample sites.

The resolution of the Landsat TM image (May 1999) used for the study area was 15 meters, whereas the resolution of the orthophoto was 4 meters. It was necessary to decide on a comparable sample-size for both the reference map and the classified map. Based on the formula (eq. 1) provided by Justice and Townshend (1981), a sample size of 3 x 3 pixels was required for the Landsat image (i.e., a sample area of 45 m x 45 m). To, achieve a sample size that fit both pixel sizes a sample area of 44 m x 44 m (11 x 11 pixels) was selected for the orthophoto. The sample size for orthophoto was slightly smaller than Landsat image, but given the two different pixel sizes, it was a good compromise in order to maintain the almost same area.

Table 2.3 presents the final sample sites (for each land cover class) used for the accuracy assessment. It can be seen from the table that initially there were 450 total sample sites.

Table-2.3: Number of sample sites for accuracy assessment

Land use classes	Sample sites	
	Initial sample sites	**Final sample sites**
1. Agriculture	60	76
2. Commercial	60	42
3. Extractive	60	42
4. Industrial	60	24
5. Lake	30	6
6. Park	60	55
7. Open space	60	57
8. Residential	60	132
Total	**450**	**434**

Among theses 450 sample sites, sixteen sites were eliminated due to their location either along the coastline or river. The 1996 land use map, which was used for stratified random sampling, was found to be inaccurate during ground verification. Therefore, some sample sites demarcated as industrial areas on the land use map were found after examination of aerial photos to be either residential areas or open space. Thus, after ground verification the number of final sample sites per class was changed. However, the number of sample sites for most of the classes (except for the lake class and the industrial class) was more than the recommended number. Lillesand and Kiefer (2000) suggest that the number of sample sites can be adjusted based on the relative importance of that class (i.e., more samples can be taken for important categories). Therefore, the additional samples for the residential and the agricultural classes are justified. However, for the industrial class more confidence could have been placed in result had stratified random sampling continued until the desired number of sample sites was achieved. This whole process is time consuming, and due to time limitations I did not continue to generate random sample points for industrial sites. Researchers (Curran and Williamson, 1985; Lillesand and Kiefer, 2000) have suggested that the number of sample sites can be selected with

CHAPTER III

Supervised and Unsupervised Classifications of the Vancouver Metropolitan Area

3.1 Introduction: There are two basic approaches to the classification of remotely sensed images: supervised and unsupervised classification. Supervised classification requires the analyst to have some familiarity with the study area. The analyst guides the classification by identifying areas on the image that are known to belong to each category. Unsupervised classification, on the other hand, proceeds with only minimal interaction by the analyst in a search for natural groups of pixels present within the image (Campbell, 1996). In both of these cases classification determines the category to which each pixel belongs (Eastman, 1999).

3.2 Unsupervised Classification: Unsupervised classification is a form of cluster analysis based on the DN[1] values of each pixel in an image (figure 3.1). This image classification approach allows the computer to group image data together into spectrally similar classes. It can be defined as the identification of natural groups, or structures, within multispectral data. Spectral classes are grouped first, solely on the numerical information in the data, and are then matched by the analyst to information classes (if possible).

Programs, called clustering algorithms, are used to determine the natural (statistical) groupings or structures in the data. Usually, the analyst specifies how many groups or clusters are to be looked for in the data. In addition to specifying the desired number of classes, the analyst may also specify parameters related to the separation distance among the clusters and the variation within each cluster. The final result of this iterative clustering process may result in some clusters that the analyst will want to subsequently combine, or clusters that should be broken down further.

[1] A Digital Number or DN is the value stored within a pixel or cell of an image The DN of the pixel represents the amount of light reflected back to the satellite/sensor. DN values range from 0 to 255. That is, a DN of 0 will appear as black, of 127 will appear gray, and of 255 will appear white.

Some advantages of unsupervised classification are: no extensive prior knowledge of the region is required, the chances of human error are minimized, and unique classes are recognized as distinct units. Some of the limitations arise primarily from a reliance on 'natural' groupings of different classes. Unsupervised classification identifies spectrally homogeneous classes within the data; these classes do not necessarily correspond to the information categories that are of interest to the analyst.

Figure-3.1: Unsupervised classification method

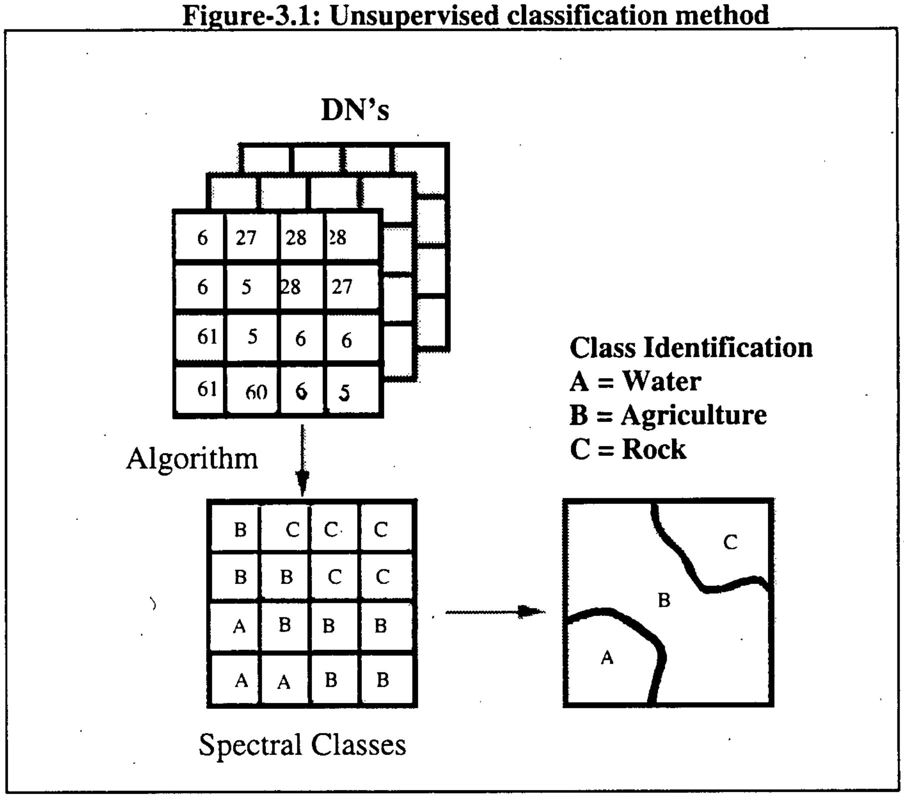

3.3 Supervised classification: Supervised classification can be defined as the process of using samples of known identity (i.e., pixels already assigned to informational classes) to classify pixels of unknown identity (i.e., to assign unclassified pixels to one of several informational classes). Samples of known identity (based on known land use types) are those pixels located within training areas (figure 3.2). The analyst identifies in the imagery homogeneous representative samples of the different surface cover types (information classes) of interest. These samples are referred to as training areas. The selection of appropriate training areas is based on the analyst's familiarity with the geographical area and their knowledge of the actual surface cover types present in the image.

The numerical information in all spectral bands for the pixels comprising these areas is used to *train* the computer to recognize spectrally similar areas for each class. The computer uses a special program or algorithm (of which there are several variations) to determine the numerical signatures for each training class. Once the computer has determined the signatures for each class, each pixel in the image is compared to these signatures and labelled as the class it most closely resembles digitally. Thus, in a supervised classification the information classes are first identified, and are then used to determine the spectral classes that represent them.

Figure-3.2: Supervised classification method

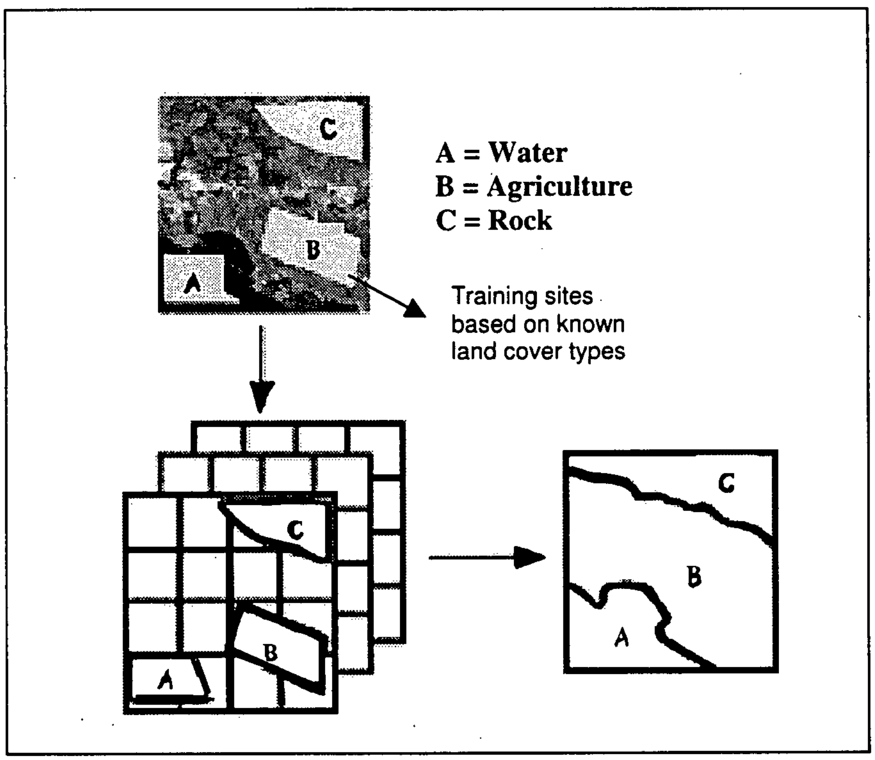

The main advantage of supervised classification is that the analyst using it is not faced with the problem of matching spectral categories on the final map with the informational categories of interest. The operator may be able to detect serious errors by examining training data to determine whether they are spectrally mixed (this is discussed under methodology, section 3.6). The major problem of supervised classification is that training data are often defined primarily on informational categories and only secondarily on spectral properties. Furthermore, the training data selected by the analyst may not be representative of conditions encountered throughout the image.

3.4 Methodology of the study: This includes the generation of false colour composites, unsupervised classifications, and supervised classification and error matrix. The study uses the following IDRISI modules to perform spectral analysis of the satellite image:

- Composite (COMPOSIT)
- Cluster (ISOCLUST)
- Maximum likelihood (MAXLIKE)
- Accuracy assessment (ERRMAT)

IDRISI cluster analysis requires composite images as an input in order to perform unsupervised classification. Thus, false colour composites were generated from the raw data using the COMPOSIT module, combining three informative bands. Generally, these include the green band, the red visible band, and the near-infrared band (that is Landsat TM bands 2, 3 and 4 respectively).

The ISOCLUST[2] module is used to produce a series of unsupervised classifications from six bands of raw data (band 6 and band 8 were excluded). This is conducted in several steps. Displaying a histogram is the first step. The histogram shows the frequency of pixels associated with each of the clusters that can be located in the image (it does a preliminary classification). Many of these clusters have very small frequencies, and thus are somewhat insignificant. For example, 22 significant clusters were identified after examining the major breaks in the histogram for the present study. Once the number of clusters to be examined has been determined, the module then classifies the image into discrete categories. At the end, there may be a need to combine some of the clusters to generate more meaningful land use classes.

[2] The ISOCLUST module is an iterative self-organizing unsupervised classifier based on a concept similar to the well-known ISODATA routine of Ball and Hall (1965) and cluster routines such as the H-means and K-means procedures.

Supervised classification begins with digitizing training sites. A *training sample* is a set of pixels selected to represent a potential information class. Spectral values for each pixel in a training site are used to define the decision space for that class. Good training site locations are generally pure in nature (i.e., not mixed up with two or more land cover classes). For example, if I want to define a commercial area, it will be important to choose an area that is not mixed with industrial or residential areas. While digitizing training sites any pixels belonging to adjacent land covers must be avoided.

This digitizing is conducted in IDRISI's colour module, using the windowing and vector drawing features. Data within each training area should exhibit a unimodal frequency distribution for each spectral band to be used. Prospective training areas that exhibit bimodal histograms should be discarded if their boundaries cannot be adjusted to yield more uniformity. Training data provide values that estimate the mean, variance, and covariance of spectral data measured in several spectral channels. These estimates approximate the mean values and the variability of band, and the interrelationships between bands for each class to be mapped.

After specifying the training sites for eight land cover classes, distributions of training area spectral response patterns were displayed graphically. Examination of the histogram output is very important when a maximum likelihood classifier is used, since it provides a visual check that the data for each class appear to be normally distributed in all bands. Training sites exhibiting bimodal histograms[3] have to be adjusted (discussed in the next paragraph) in order to improve their quality. A bimodal histogram reveals that an area encompasses two, rather than one, spectral classes, which is not satisfactory for image classification.

Figure 3.3 present an example of one such histogram. The histogram output for commercial areas for band 2 exhibits that the category is not normally distributed- in other words, the training site is not pure but rather a mixture of two different classes.

[3] While digitizing training sites I was very careful. I tried to zoom into the area as much as possible before digitizing that site. That way I was quite successful in avoiding mixtures of more than two classes.

Figure-3.3: Histogram of Commercial category

Bimodal nature of commercial training sites

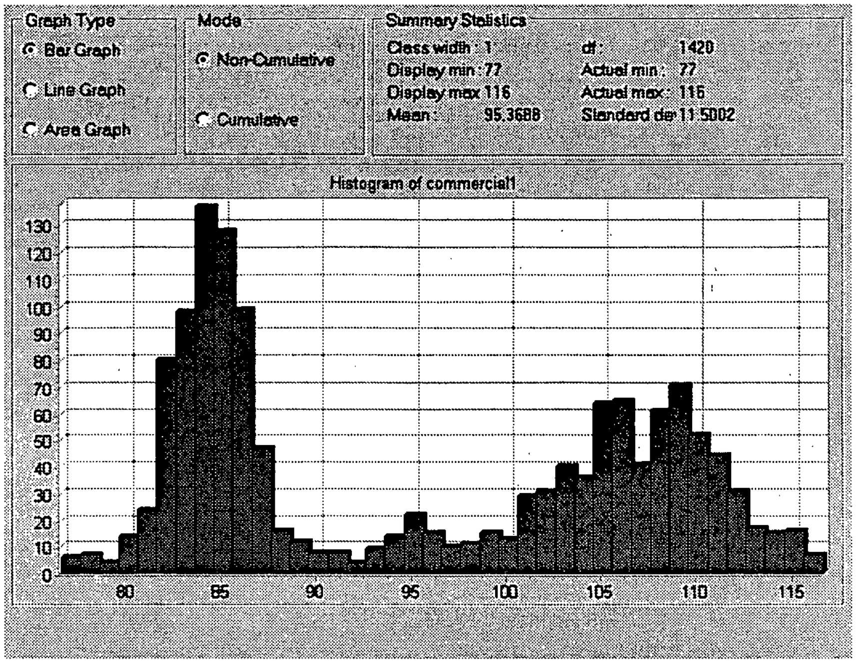

Training sites after adjustment

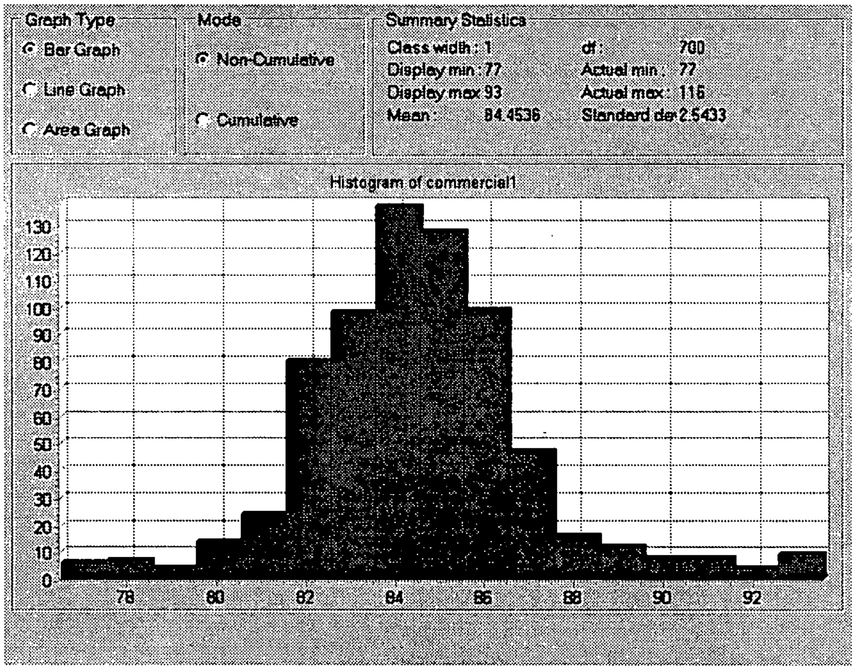

After quarrying pixels, which are known to be representative of commercial areas, I determined that DN values for pixels belonging to commercial areas vary from 70 to 93. However, the histogram of figure 3.3 presents a much wider range of DN values (from 76 to 116) for a commercial site. The pixels with DN values from 94 to 116 do not belong to the commercial class; they belong to the industrial class. So, adjustments have been made to purify the commercial training site by keeping only those pixels with DN values from 76 to 93.

In case of industrial, residential, and commercial categories, the data do not appear to be normally distributed for bands 2, 3, 4 and 5, where the distribution is shown to be bimodal. These subclasses may represent two different types of industrial sites or residential areas or commercial sites. One land use class may encompass several land covers, each with a unique spectral signature. The classification accuracy will generally be improved if each of the subclasses is treated as a separate category. Therefore 41 training sites were specified for this study (some land use classes are represented by more than one training site) in order to cover the full range of reflectance characteristics of each land use class (figure 3.4).

The MAKESIG module is used to process the training area polygons into spectral signatures representative of the intended classes. The SIGCOMP module allows the user to compare the signatures as bar graphs for each of the bands of raw data. The greater the degree of spectral separation between each signature, the better the final classified image is expected to be. To evaluate the spectral separation between categories, the signature comparison chart has been used (figure- 3.5). The fact that the commercial, industrial and high-density residential areas overlap in all most all spectral bands indicates that the categories could not be accurately classified on any single MSS band.

The next step is to classify the image. For classification the Maximum Likelihood procedure, provided by the MAXLIKE module in IDRISI, has been used. Eastman (1999) suggests that when training sites are well defined with a large sample size, the MAXLIKE procedure should be used for supervised classification. The Maximum

Figure-3.4: 41 Training sites for eight land use classes (supervised classification), inset shows nine training sites for the park class to capture the wide range of spectral signatures for different trees

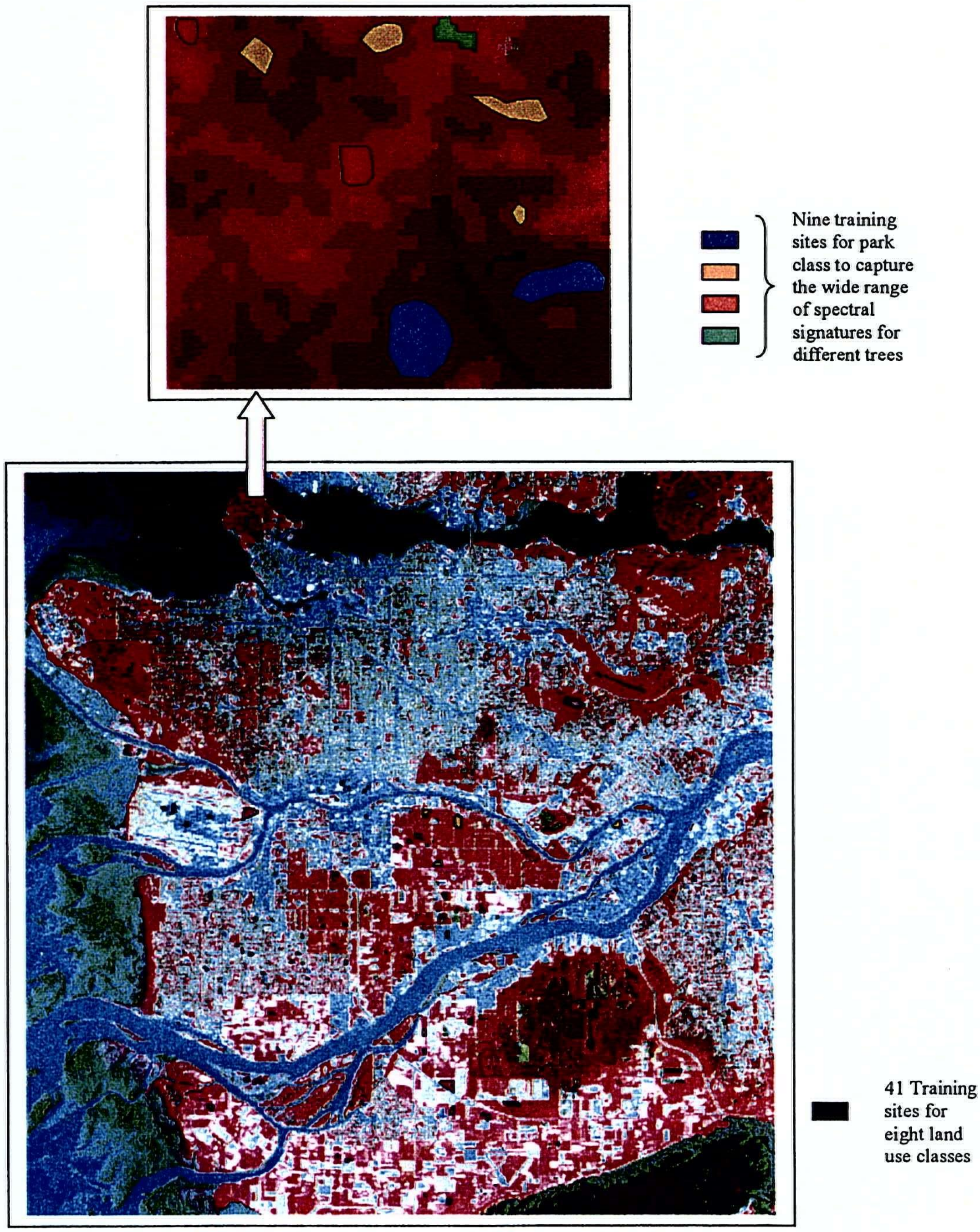

Figure- 3.5: Signature Comparison chart of eight land use classes

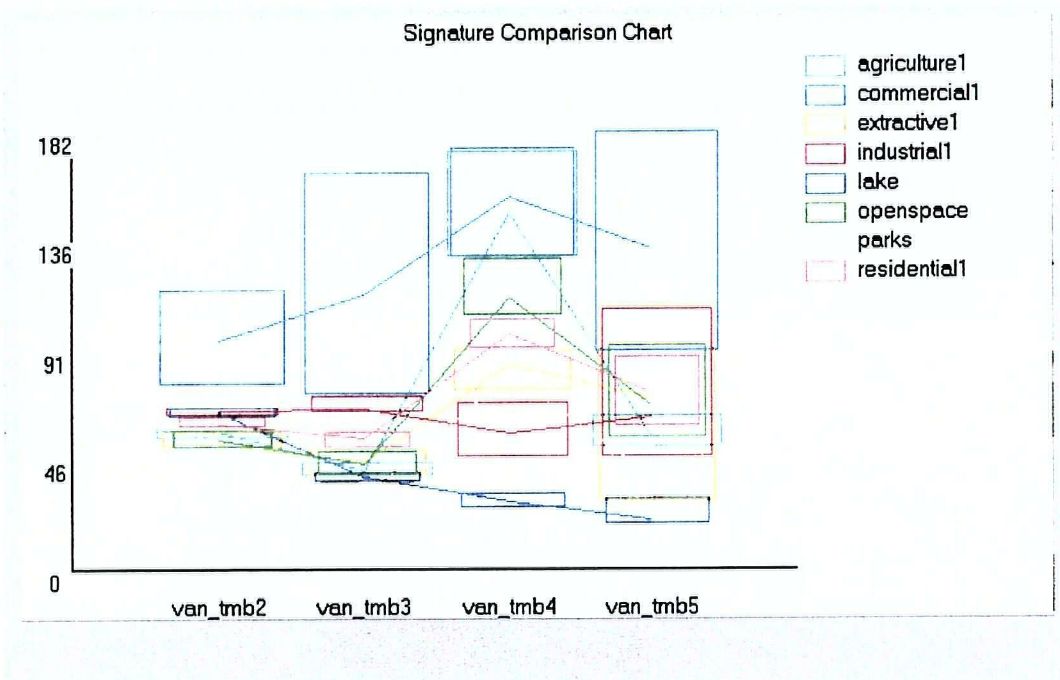

Likelihood procedure is based on Bayesian probability theory. Using the information obtained from a set of training sites, MAXLIKE uses the mean and variance/covariance data of the signatures to estimate the posterior probability that a pixel belongs to each class.

After classification, accuracy assessment is the next step. Accuracy assessment compares two maps, the reference map (assumed to be accurate) and the classified map. For the present study, ground truth data (containing 434 sample sites for eight land use classes) has been used as a reference map and has been compared with the newly generated classified maps (both supervised and unsupervised maps) of the study area.

3.5 Results of classifications: The unsupervised classification of the Vancouver Metropolitan area produced twenty-two clusters (fig-3.6). Some clusters occupy fairly large areas (e.g., clusters 1, 6, 10, 17, 20, 21) and are easy to interpret. However, some others (which occupy smaller areas) such as clusters 3, 4, 5, and 22 are more difficult to interpret. Maps and aerial photographs were used to identify these clusters.

The twenty-two classes and the corresponding land covers are shown in table-3.1. From table-3.1, it is quite apparent that some of the land cover classes are represented more than once. There is some overlapping of the classes and sometimes more than one category represents the same class. This is mainly because unsupervised classification identifies spectrally homogenous classes within the data. There is limited control over the choice of classes and their specific identities. A close inspection of table-3.1 reveals that the land use classes are not unique classes; rather they are typically a mixture of several land cover classes.

Obviously, there is a need to merge clusters in order to produce the unsupervised map with eight land use classes. For example, cluster analysis may have uncovered several agricultural categories, such as berry fields and hay fields, which I wanted to merge into a single land use class. Figure-3.7 shows an agricultural area with different crops in it.

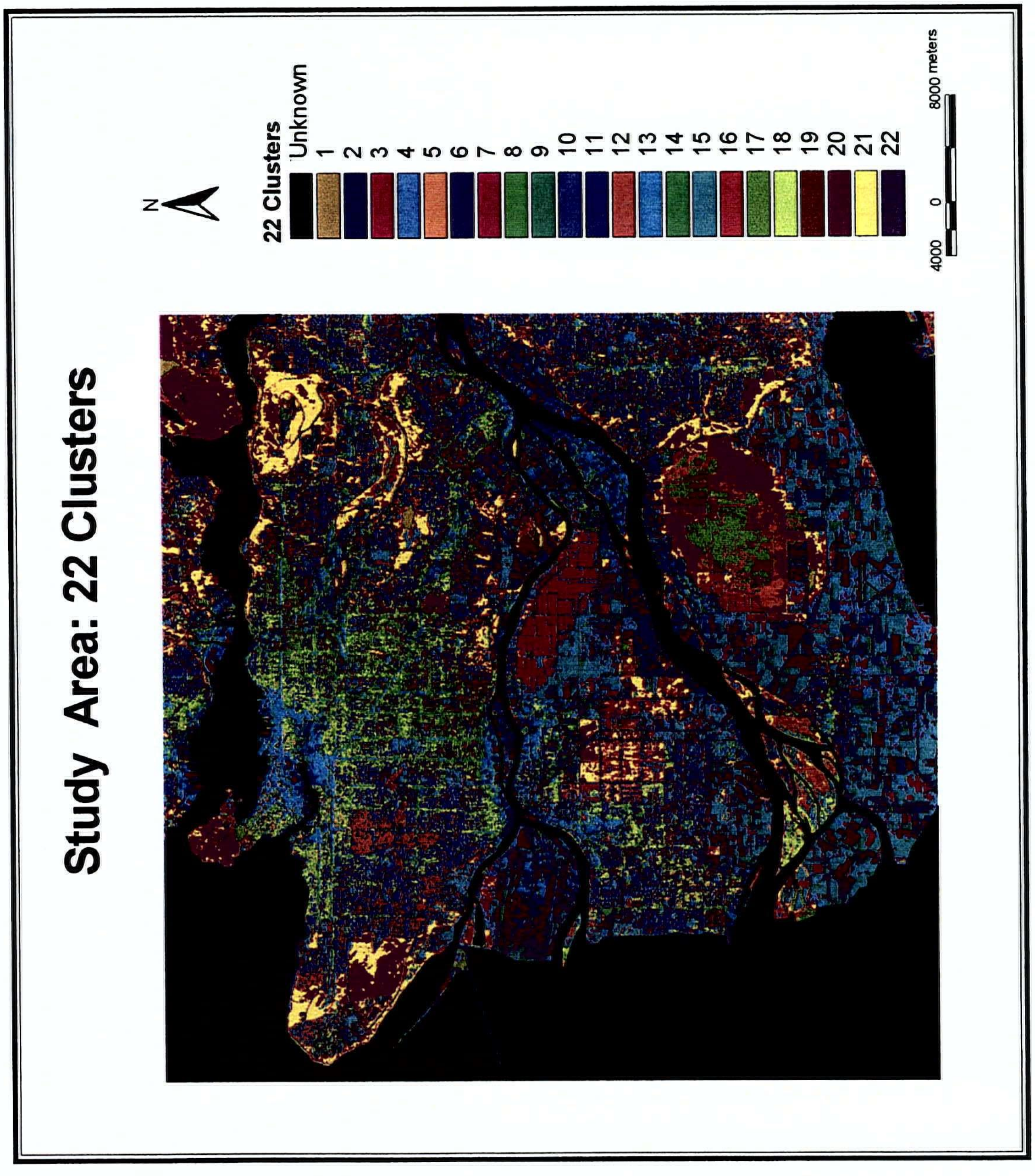
Study Area: 22 Clusters
N
22 Clusters
Unknown
1
2
3
4
5
6
7
8
9
10
11
12
13
14
15
16
17
18
19
20
21
22
4000
0
8000 meters

Figure-3.6

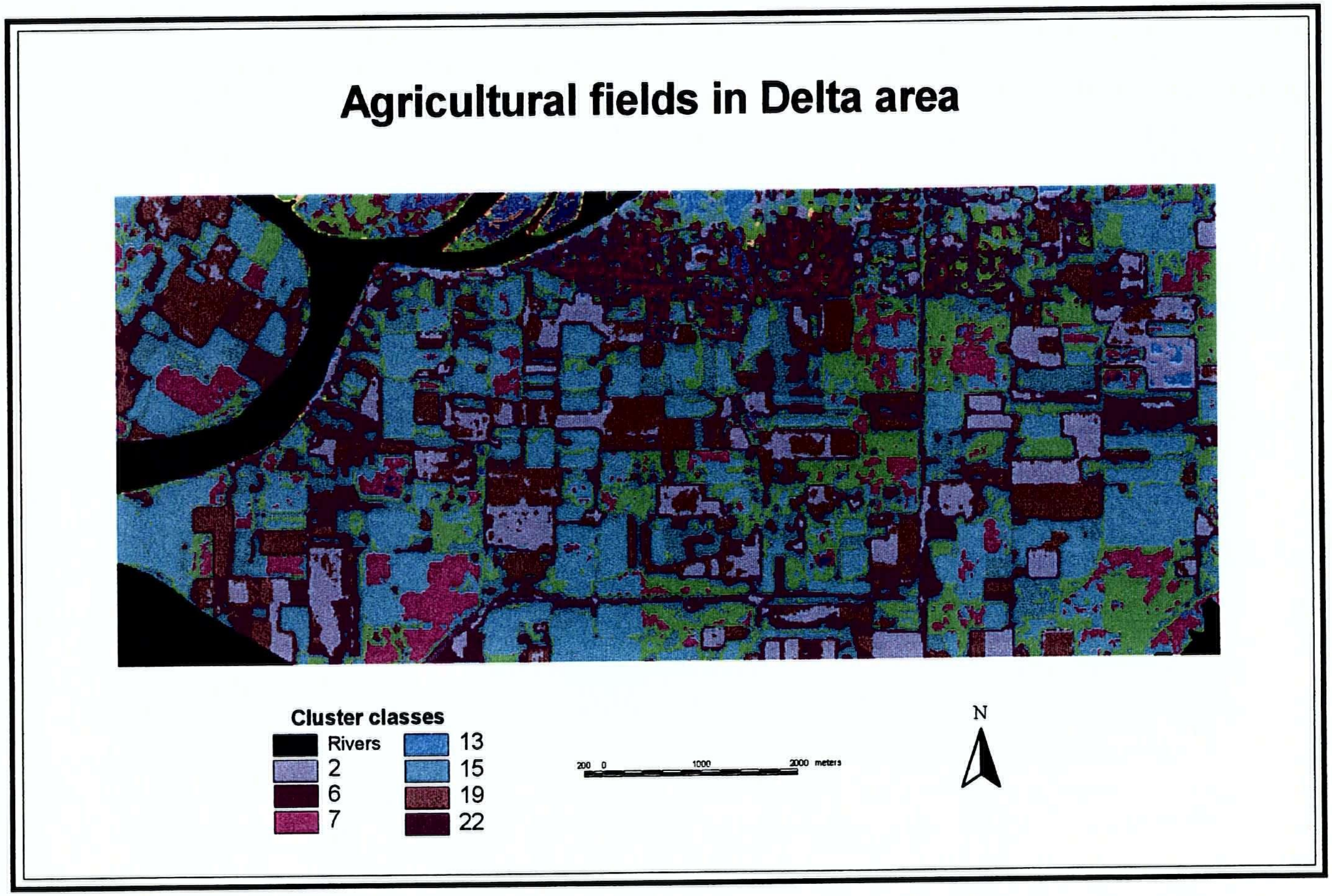
Agricultural fields in Delta area
Cluster classes
Rivers
2
6
7
13
15
19
22
200 0 1000 2000 meters
N

Figure - 3.7

Though the spectral signatures for them are different from one another, they are assigned to one information class- 'agriculture'.

Table-3.1. Unsupervised classes and corresponding Land covers and land use

Cluster ID	Land cover classes	Corresponding land uses
Cluster 1	Water body / lake	Lake
Cluster 2	Bare earth, sand piles, buildings	Parking lot / industrial area
Cluster 3	Bare earth, muddy land	Open space
Cluster 4	Grass, open fields, some trees	Cemetery
Cluster 5	Dry river channel	Open space
Cluster 6	Buildings with tree covers, roads and open space	Residential area
Cluster 7	Agricultural fields	Agricultural lands
Cluster 8	Buildings with tree cover	Residential area
Cluster 9	Bare fields could be sandy, muddy	Agricultural lands
Cluster 10	Buildings, roads	Residential area
Cluster 11	Flood plain	Open space
Cluster 12	Wet land vegetation	Partly bog area and partly residential area
Cluster 13	Buildings, roads	Built-up area, commercial areas
Cluster 14	Mud, sands along river channels, coast lines	Open space
Cluster 15	Land cover with grass, vegetation	Agricultural lands, golf course
Cluster 16	Buildings with tree cover	Residential area
Cluster 17	Emergent vegetation	Bog area
Cluster 18	Buildings, open spaces	Industrial area
Cluster 19	Bare earth	Open space and partly agriculture
Cluster 20	Coniferous trees	Park
Cluster 21	Deciduous tree	Park
Cluster 22	Open field	Park with open space

One of the objectives of this study was to come up with the most appropriate method of urban land use classification for the study area (after reviewing the eight methods of land use classification specified in chapter 1) and to compare the existing land use map (provided by the GVRD) with the newly generated land use map. Therefore, it was necessary to generate a specific set of land use classes (i.e., the eight broad land use classes for this study) that would match the GVRD land use data. Keeping in mind the purpose of the study, I regrouped some of the unsupervised classes to make the

Table-3.2. Eight land use classes after regrouping twenty-two clusters

Cluster ID	Corresponding Land covers	Regrouped land uses	Regrouped classes
Cluster 1	Water body / lake	Lake	Class 5
Cluster 2	Bare earth, sand piles, buildings	Industrial	Class 4
Cluster 3	Bare earth, muddy land	Open space	Class 7
Cluster 4	Grass, open fields, some trees	Open space	
Cluster 5	Dry river channel	Open space	
Cluster 6	Buildings with tree covers, roads and open space	Residential	Class 8
Cluster 7	Agricultural fields	Agriculture	Class 1
Cluster 8	Buildings with tree cover	Residential	Class 8
Cluster 9	Bare fields could be sandy, muddy	Open space	Class 7
Cluster 10	Buildings, roads	Residential	Class 8
Cluster 11	Flood plain	Open space	Class 7
Cluster 12	Wet land vegetation	Residential	Class 8
Cluster 13	Buildings, roads	Commercial	Class 2
Cluster 14	Mud, sands along river channels, coast lines	Open space	Class 7
Cluster 15	Land cover with grass, vegetation	Agriculture	Class 1
Cluster 16	Buildings with tree cover	Residential	Class 8
Cluster 17	Emergent vegetation	Extractive industry	Class 3
Cluster 18	Buildings, open space	Residential	Class 8
Cluster 19	Bare earth	Open space	Class 7
Cluster 20	Coniferous trees	Park	Class 6
Cluster 21	Deciduous trees	Park	
Cluster 22	Open field	Agriculture	Class 1

classification more meaningful (table-3.2 and figure-3.8). However, it was difficult to produce a final map of eight classes given the wide range of spectral signatures overlapping between classes. For example, unsupervised cluster 2 is assigned to the open space class because a significant amount of cluster 2 represents sand piles and bare earth. However, it also represents some high-rise apartments in the downtown Vancouver area.

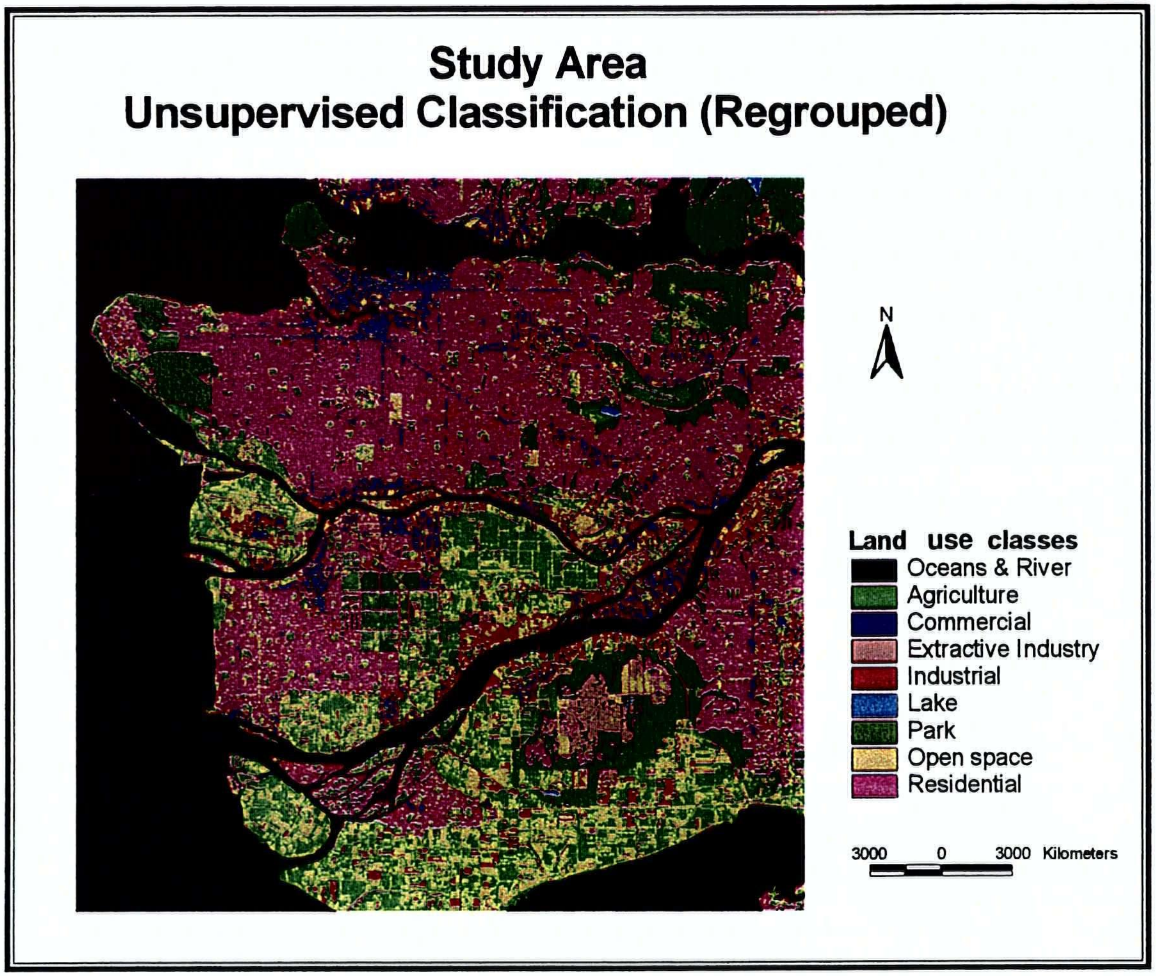
Study Area
Unsupervised Classification (Regrouped)
N
Land use classes
Oceans & River
Agriculture
Commercial
Extractive Industry
Industrial
Lake
Park
Open space
Residential
3000 0 3000 Kilometers

Figure-3. 8

Therefore, the sensitivity of unsupervised classification results depend partly on the choices made by the analyst in regrouping initial clusters. However, the results of the unsupervised classification were helpful in this study, in deciding how many training sites were necessary for the supervised classification to capture the wide range of spectral signatures to generate eight land use classes.

Table-3.3: Contingency table from unsupervised classification of Landsat TM image

Classified land uses	Ground Truth									Accuracy (%)	Commission error (%)	Omission error (%)
	Total	1	2	3	4	5	6	7	8			
1. Agriculture	507	281					5	107	114	41	45	59
2. Commercial	309	1	201		48				59	53	35	47
3. Extractive	315	20		222			46	26	1	59	25	41
4. Industrial	383	51	49		116		5	121	41	54	67	46
5. Lake	73					54	2	17		100	26	0
6. Park	575	71		28			413	16	47	83	28	17
7. Open space	593	231	11	45	16		6	177	107	35	70	65
8. Residential	1151	29	117	83	36		18	49	819	69	28	31
Total	3906	684	378	378	216	54	495	513	1188			
Overall Kappa = 51% **Overall Accuracy = 59%**												

The results of the two classifications (supervised and unsupervised) are given in table 3.3 and 3.4. The overall accuracy of the classifications was 59 percent for unsupervised and 71 percent for supervised respectively. A close inspection of both error matrices reveals that industrial, open space and agriculture classes are mostly misclassified. In particular, there was confusion between commercial and industrial classes (table 3.3, figure 3.8). A fairly large number of industrial area pixels have been classified as commercial, because of their spectral similarity (table 3.3, figure 3.10). The methodology produced the best results for the water classes, mainly because of water's clear and distinct spectral signature. The poorest results were for the open space class. Most of the open space pixels have been classified either as residential or agricultural class. Among other classes, the accuracy level for parks and extractive industry is comparatively better.

The resulting supervised-classification map is shown in figure-3.9. It can be seen from both table 3.4 and figure 3.9 that the classification results are affected by a spectral

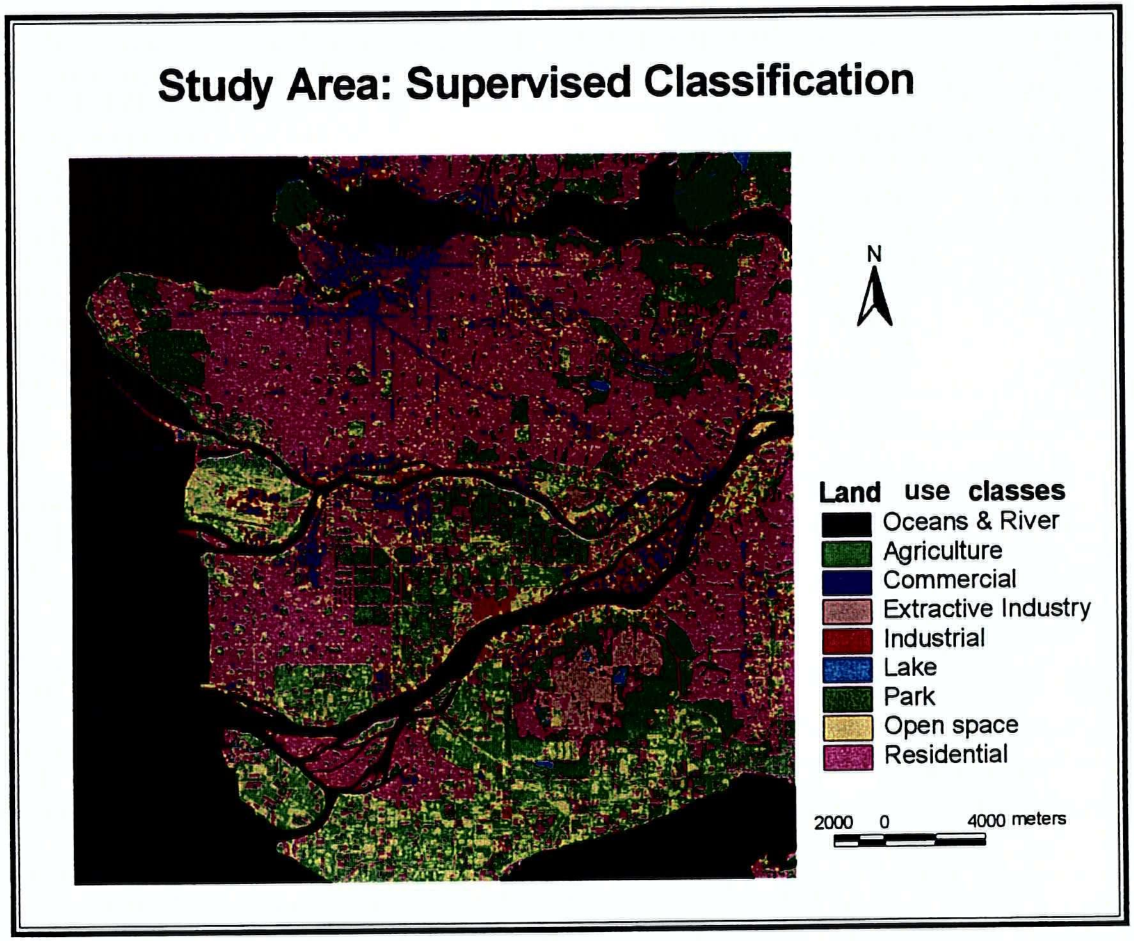
Study Area: Supervised Classification
N
Land use classes
Oceans & River
Agriculture
Commercial
Extractive Industry
Industrial
Lake
Park
Open space
Residential
2000 0 4000 meters

Figure-3.9

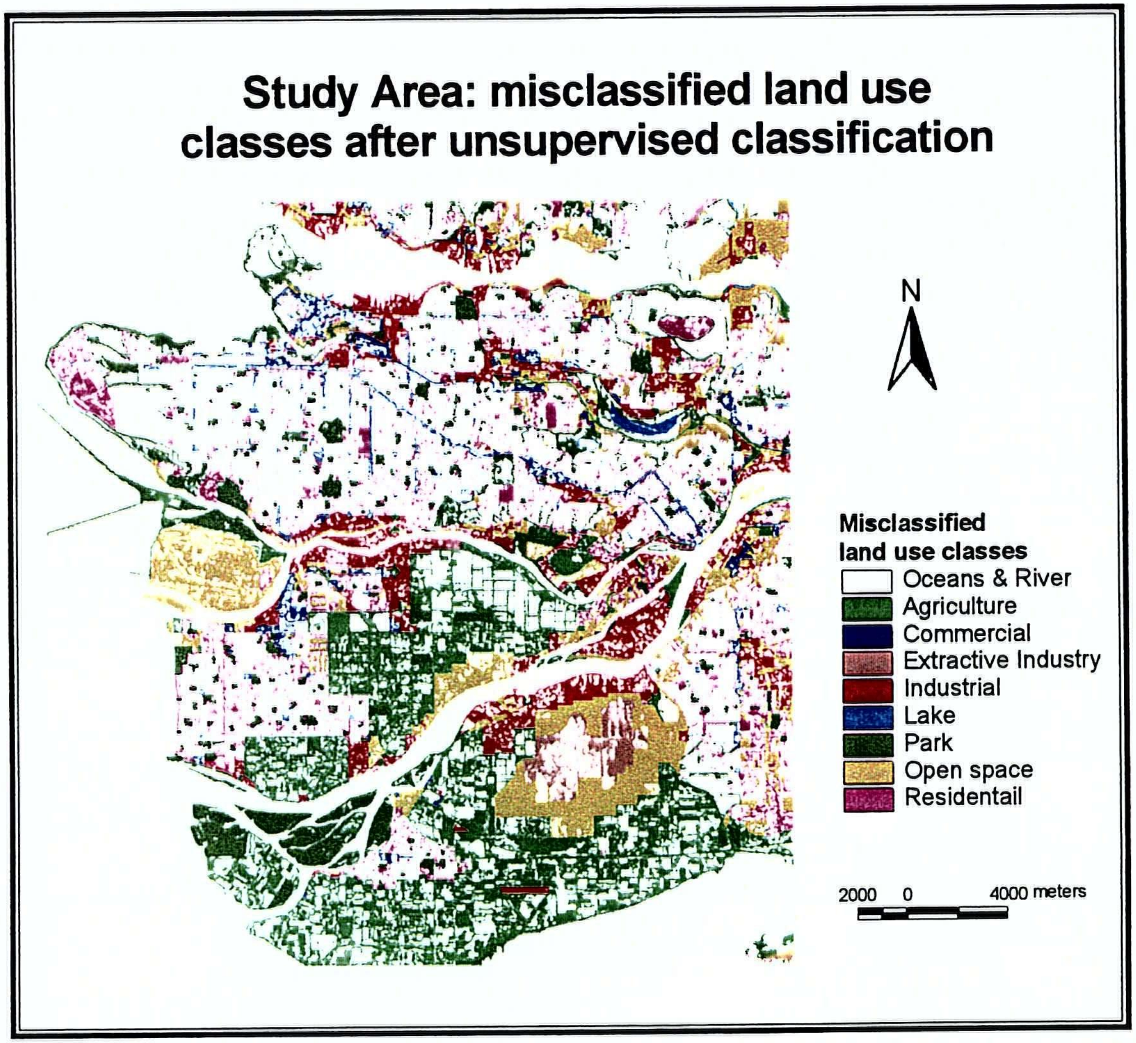
Study Area: misclassified land use
classes after unsupervised classification
N
Misclassified
land use classes
Oceans & River
Agriculture
Commercial
Extractive Industry
Industrial
Lake
Park
Open space
Residentail
2000 0 4000 meters

Figure-3.10

confusion of land cover types. Commercial areas, industrial areas, and residential areas are composed of buildings, and it is very difficult to differentiate the spectral signatures from one another. Significant confusion occurred between residential, open space and agricultural class, as evidenced by high classification commission errors (32 percent, 45 percent, and 32 percent respectively) and omission errors (16 percent, 48 percent, and 39 percent respectively) (table 3.4, figure 3.11). Viewing the classified image in conjunction with aerial photographs revealed that this confusion was mainly between cleared land (within open space agricultural areas) and construction sites (within residential areas). This is not surprising because cleared areas occur within construction sites. There was also confusion in class assignment for the vegetated classes: open space, golf course, and fallow land. The spectral characteristics of these classes are similar because they contain the same cover type in the form of grasses. The distinction between the medium and low-density residential areas is not very clear after classification. Low-density areas have more tree cover, which is again mixed up with parks, forest areas and even with the institutional areas, for example, UBC.

Table-3.4: Contingency table from supervised classification of Landsat TM image, using maximum-likelihood classifier

Classified land uses	Ground Truth									Accuracy (%)	Commission error (%)	Omission error (%)
	Total	1	2	3	4	5	6	7	8			
1. Agriculture	615	419					29	107	60	61	32	39
2. Commercial	370		219		41				38	77	21	23
3. Extractive	285			272			1	6	6	72	5	28
4. Industrial	131		4		99			13	15	46	24	54
5. Lake	59					54		5		100	8	0
6. Park	478	13		8			425	14	18	86	11	14
7. Open space	493	132	4		33		7	269	48	52	45	48
8. Residential	1475	120	79	98	43		33	99	1003	84	32	16
Total	3906	684	378	378	216	54	495	513	1188			

Overall Kappa = 65%
Overall Accuracy = 71%

During the identification of the different land uses, it was found that the spectral differences between them were not always clear. The basic reason for this identification

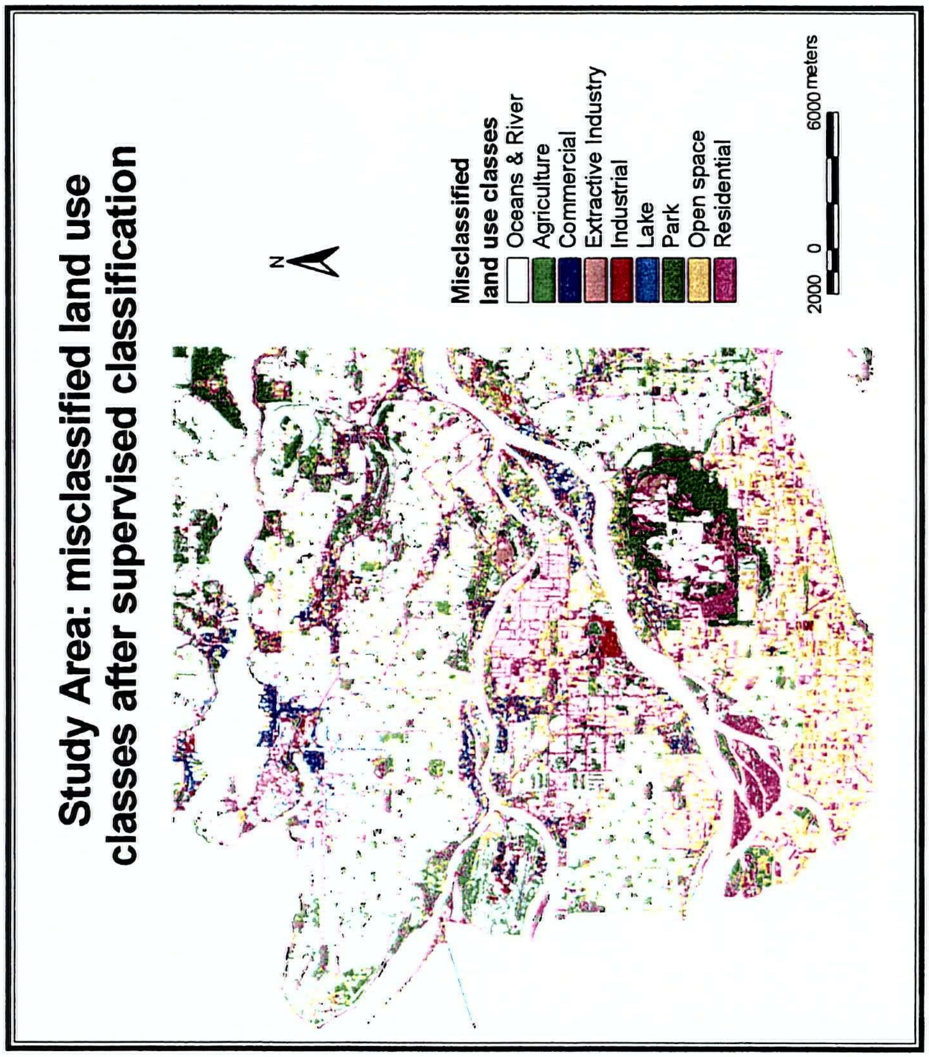
Study Area: misclassified land use classes after supervised classification
N
Misclassified land use classes
Oceans & River
Agriculture
Commercial
Extractive Industry
Industrial
Lake
Park
Open space
Residential
2000 0 6000 meters

Figure-3.11

problem is the dominance of spectrally mixed classes in the area. Many pixels contained two or more land cover types (mixed land use).

In the case of the agricultural class, most of the mis-classification has occurred between agricultural and open spaces. In some cases urban land has the same appearance as cereals and bare soil, flood plains and mud flats were easily identified; the same was true with lake areas. Both deciduous and coniferous forests were clearly demarcated. Open spaces were not very easy to identify, as they were confused with almost all other land cover classes. Both commercial and industrial classes were mixed up with each other because of the similar spectral signatures associated with both the classes.

3.6 Conclusion: Using either supervised or unsupervised techniques it is relatively simple to identify broad land cover classes such as vegetation, water, and soils. Classification becomes more difficult when a single land use class is composed of objects with varying spectral reflectances. For example, classification of urban or suburban areas is often problematic because these areas are composed of houses, trees, streets and other objects. It can be seen from figures 3.8 and 3.9 that both unsupervised and supervised classifications have produced a "salt-and-pepper" appearance (isolated and often misclassified pixels of one category are dispersed within the area of another category) after classification. A post-classification smoothing (using modal filters) has been used (and is described and evaluated in chapter 4) to reduce this speckly appearance.

In this chapter we have observed that the supervised classification technique constrained to the desired classes produces better results than the unsupervised classification. However, both supervised and unsupervised classifications consider only spectral information for land use analysis. As a result, grazing pasture, lawns and other grass associated with urban areas, and golf course have classified into one class (i.e., the same type of land cover: grass), but the land use is very different. So, the conclusion of this chapter is that spectral information alone is not sufficient to produce an accurate land cover map of a complex urban area like Greater Vancouver. Spectral signatures have their limit. Generating a better map (more accurate map) needs additional information.

CHAPTER IV

Implementing and Reviewing Three Other Methods to Improve Supervised and Unsupervised Classification for the Vancouver Metropolitan Area

4.1 Introduction: Classification is the most frequently used information extraction technique in digital remote sensing. A variety of classification mechanisms can be applied to agglomerate remotely sensed data into meaningful groups or classes. Classification units can be pixels, groups of neighbouring pixels, or the whole image.

Since 1980 numerous variants of two basic classification approaches have been developed. For supervised classification approach these include decision trees (Hansen *et al.*, 1996); neural networks (Carpenter *et al.*, 1997; Foody *et al.*, 1997; Bischof and Leonardins, 1998; Yool, 1998); fuzzy classification (Foody, 1996, 1998; Mannan *et al.*, 1998) and mixture modeling (Meer, 1995). For both supervised and unsupervised classification post-classification smoothing (Lark, 1995), and classification by progressive generalization (Chilar *et al.*, 1998) have been added to the lexicon of techniques. This chapter reviews three variants of two basic classification approaches: neural networks and fuzzy (for supervised techniques) and post-classification smoothing (for both supervised and unsupervised techniques). The reason behind this selection is that these three methods are most commonly used techniques for land use classification and are relatively simple in terms of mathematical calculations (for example, mixture modeling and progressive generalization require programming skills).

4.2 Neural Network analysis: The use of artificial neural networks (ANN) has gained increasing popularity as an alternative to statistical methods for the classification of remotely sensed images over the last few years (since the late 1980s). Their superiority to some of the classical statistical methods (e.g., maximum-likelihood classifier, bayesian and k-nearest-neighbor classifiers) has been shown in the literature (Hepner *et al.,* 1990; Bischof *et al.*, 1992; Civco, 1993; Wu *et al.*, 1994; Wilkinson *et al.*, 1994). Due to their independence from a priori statistical parameters, an artificial neural network approach has been selected for land use classification of the Vancouver metropolitan area.

An artificial neural network is composed of a large number of simple, interconnected "processors" (neurons) working in parallel within a network. Artificial neural networks attempt to parallel and simulate the functionality and decision-making processes of the human brain. In general, neural networks are referred to as mathematical models of theorized mind and brain activity (Simpson, 1990). In an artificial neural network, the processing element (PE) is the analog of the human brain's biological neuron. A processing element has many input paths, analogous to the brain's dendrites, and the information transferred along these paths is combined by one of a variety of mathematical functions, most commonly simple summation.

Neural networks can handle problems with many parameters, and work well even when the distribution of objects in N-dimensional parameter space is very complex. The major disadvantage of neural networks is that they are slow, especially in the training phase, but also in the application phase. Artificial neural network algorithms have been employed with increasing frequency in a wide range of scientific disciplines since 1985. Although the use of neural networks in remote sensing is relatively new, during the last few years the number of reported applications has been increasing steadily. The majority of applications have used an artificial neural network trained with the back-propagation algorithm (Schaale and Furrer, 1995).

One of the first papers considering the application of neural networks to the analysis of remotely sensed imagery was by Key *et al.* (1989). These authors described a system to classify merged 5-channel AVHRR data and 2-channel Scanning Multichannel Microwave Radiometer (SMMR) data over Arctic regions. In the same year, Howald (1989) used a three-layer network to classify Landsat TM data into seven land use classes. The results were compared to those from a maximum likelihood classifier. The neural network was found to produce slightly better (5 percent) overall classification accuracy. The same architecture was also used by Hepner *et al.* (1990), whose results indicated that the neural network approach could perform better (10 percent more accurate) than conventional classifiers using identical training sets.

Foody *et al.* (1995) employed neural networks trained with the back propagation algorithm to classify agricultural crops from SAR data. Their results show that in general neural networks perform better than traditional classifiers. Paola and Schowengerdt (1995) carried out detailed comparisons between maximum likelihood and back-propagation trained neural networks for the classification of urban land use from Landsat TM images. Although the overall classification accuracy figures appear to be similar in many cases, the authors also considered 2-dimensional plots of the decision surfaces of both classification methods to better explain the differences between the two classifiers in the classification maps.

4.2.1 Back-Propagation model: The back-propagation network is probably the most well known and widely used of neural network systems and is well suited for image classification because of its ability to separate image noise from image data (Schaale and Furrer, 1995). As the back-propagating neural network learns the input patterns, the network creates an intermediate output value, which is immediately compared to the target value. The difference between the intermediate output value and the target value is propagated back towards the neurons, which readjust their respective weights in order to generate an improved output value (i.e., closer to the target value).

The back propagation neural network model consists of three layers – the input layer, the output layer, and the hidden layer (Figure 4.1).

- *Input layer:* The input layer consists of one or more processing elements (number of processing units depend on the number of bands in the input data set). For example, seven-band Landsat data would require seven input processing units (i.e., seven input nodes), each corresponding to a band of the Thematic Mapper sensor. The input patterns could consist also of ancillary data (e.g., multitemporal spectral patterns, image texture, elevation and its derivatives).

- *Hidden Layer:* The hidden layer receives information from the input layer and sends information to the output layer. The connections between the layers are weighted so that the relative importance of each connection can be changed. Before training begins, these weights can be initialized with random weights or specific connections can be weighted more than others in order to take advantage of a priori knowledge.

- *Output layer:* The output layer receives data from the hidden layer. The number of inputs to the output layer is equal to the number of processing units on the hidden layer, unless the output layer is connected to the input layer.

Figure 4.1: Generalized schematic of ANN architecture. This shows the input layer, where data are presented to the network (initially with random weights), and an output layer that stores the response of the network to a given set of weighted inputs. The hidden layer could be called the layer of 'learned pattern detectors' because the activity in the hidden layer is an encoding of what the ANN has determined are significant properties of the input.

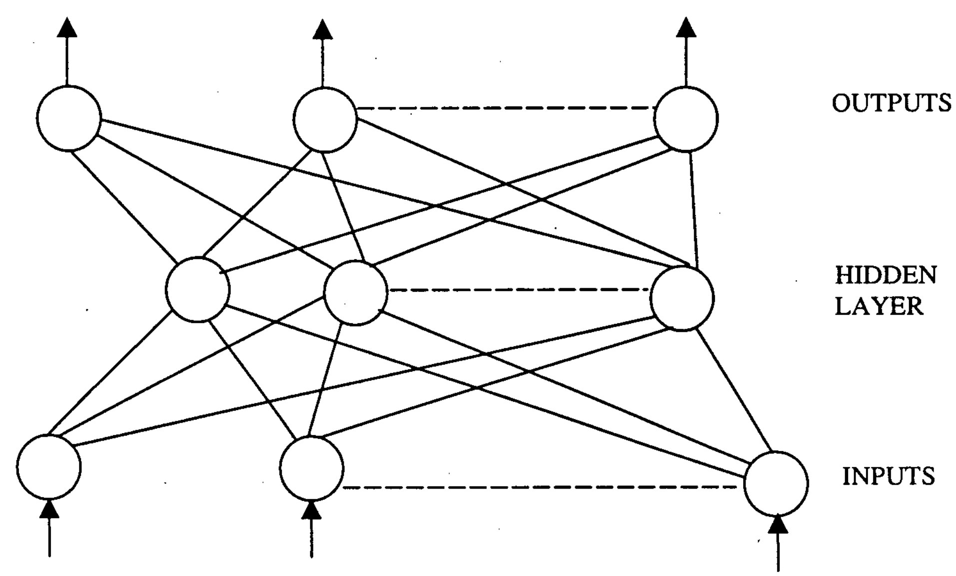

Source: Yool, S.R. (1998), Land cover classification in rugged areas using simulated moderate resolution remote sensor data and an artificial neural network, International Journal of Remote Sensing, Vol. 19, No. 1, pp. 85-96.

4.2.2 Methodology: A neural network image classification was performed with PCI image processing software (version 6.3) using a back propagation model and was compared to the maximum likelihood image classification described in chapter 3. Neural network classification is performed by PCI in three different steps. These three steps are neural network creation, neural network training, and neural network classification, and are carried out by using three different PCI module NNCREAT, NNTRAIN, and NNCLASS.

The first step of neural network classification is network creation. NNCREAT creates a neural network segment for back-propagation neural network processing. The input data for NNCREAT were 5 bands (recommended for PCI back-propagation neural network analysis) of the Landsat TM data set. These five bands were band 1, 2, 3, 4,and 5. One hidden layer was created with the maximum number of units for the input and output layers (i.e. 8 units).

The second step is to train the classifier. NNTRAIN (Neural Network Training module) trains an existing neural network segment created by NNCREAT for back propagation neural network processing using sample data from training sites. NNTRAIN continues training the neural network until one of the following three conditions is reached:

- The maximum normalized total error is less than the specified maximum total error allowed
- The maximum individual error is less than the specified maximum individual error allowed
- The number of iterations is greater than the specified maximum number of iterations

There are five user-specified network-training parameters: learning rate, momentum rate, maximum total error, maximum individual error, and number of iterations. The learning and momentum rates affect how quickly the neural network stabilizes. The learning rate specifies how fast the weights[1] are changed during training. Too low a learning rate (0.1) makes the network learn very slowly. Too high a learning rate (0.9) makes the weights and error function diverge, so there is no learning at all. The momentum rate can be used to speed up learning. A high momentum rate (0.9) trains with larger steps than a lower rate (0.1). Use of a momentum term helps reduce oscillation between iterations, and allows a higher learning rate to be specified without the risk of non-convergence.

[1] A **weight** or **connection weight** is real-valued parameters that modify the signals flowing between neural processing units or nodes in a neural network.

The maximum total error and the maximum number of iterations (i.e., number of learning cycles for training iterations) determine when training stops. After each learning cycle, the overall network error is computed. If it is greater than the user-specified maximum network error, then learning cycles continue. If the overall network error is less than the user-specified maximum network error, the current values are saved and training stops. For the present analysis, the values of the five user-specified network-training parameters are: 0.2 for learning rate, 0.9 for momentum rate, 0.01 for maximum total error, 0.001 maximum individual error, and 100 cycles for training iterations.

The final stage is to classify the image using the neural network classification module, NNCLASS. This module classifies multispectral imagery using a back-propagation neural network created by the NNCREAT program and trained by the NNTRAIN program. Once the image is classified, it is compared to the reference image (ground truth image with 434 ground-truth points), and the accuracy is tabulated (Table 4.1).

4.2.3 Results and discussions: The contingency matrix for the ANN-based classifier appears as table 4.1. The overall accuracy of the neural network classifier (using the back propagation model) was 78 percent, which was 7 percent higher than the supervised classification results. It is apparent from table 4.1 that, accuracy for seven land use classes has increased compared to the supervised classification accuracy values. The exception is the residential class, which has declined by less than 1 percent. Misclassifications have observed within the residential class, one hundred and ninety six out of 1359 pixels belonging to the residential class are misclassified as agriculture, open space, industrial, commercial, and extractive industry classes (figure 4.3). In some areas, the residential classes are found to be inseparable from the commercial and industrial classes due to the spectral similarity of buildings and the open spaces associated with them. Excellent identification of residential area is not always expected, since this area is problematic due to the mixed occurrence of houses, trees, and lawns. Here, the classifier has some difficulty separating cleared land from land under construction (this was observed when viewing the classified image in conjunction with the aerial photos), due to their spectral similarity. As a result cleared land and land under construction were often classified either as residential or industrial/commercial areas.

Table-4.1: Contingency table resulting from neural network analysis of Greater Vancouver area

Classified land uses	Ground Truth									Accuracy (%)	Commission error (%)	Omission error (%)
	Total	1	2	3	4	5	6	7	8			
1. Agriculture	678	498			0		21	100	59	73	27	27
2. Commercial	388		314		27				47	83	19	17
3. Extractive	339			317			1	6	15	84	6	16
4. Industrial	194		3		157			18	16	73	19	27
5. Lake	59					54		5		100	8	0
6. Park	487	13		7			434	13	20	88	11	12
7. Open space	457	101	4		17		6	290	39	57	37	43
8. Residential	1304	72	57	54	15		33	81	992	84	24	16
Total	3906	684	378	378	216	54	495	513	1188			
Overall Kappa = 74% Overall Accuracy = 78%												

Classification accuracy for the open space class (57 percent) is significantly poorer than that of all of the other classes (table 4.1). The ANN has assigned 223 pixels of the 513 pixels belonging to the open space class to the agriculture, extractive, industrial, lake, park, and residential classes. The spectral signatures of the open space class get mixed up with the similar spectral signatures produced by the open fields within an industrial site, the built up areas under the residential class, and bare earth/open space within parkland.

Misclassifications are observed between agricultural lands and parks. It is quite probable that spectral signatures for grasses within a park and fallow agricultural lands get confused. As a result, golf courses were misclassified as agricultural lands (figure 4.2). Generally speaking, it is difficult for any classifier to put 'grass' pixels (which can be a part of residential areas, parks, open spaces or agricultural lands) into the proper land cover class (say the open space or residential or parks); thus some misclassification is always expected unless 'grass' is identified as a separate class.

A qualitative comparison of conventional versus ANN classification indicates that the former was less able to discriminate accurately the eight land cover classes. The ANN

Study Area: Land use classes generated by neural network analysis

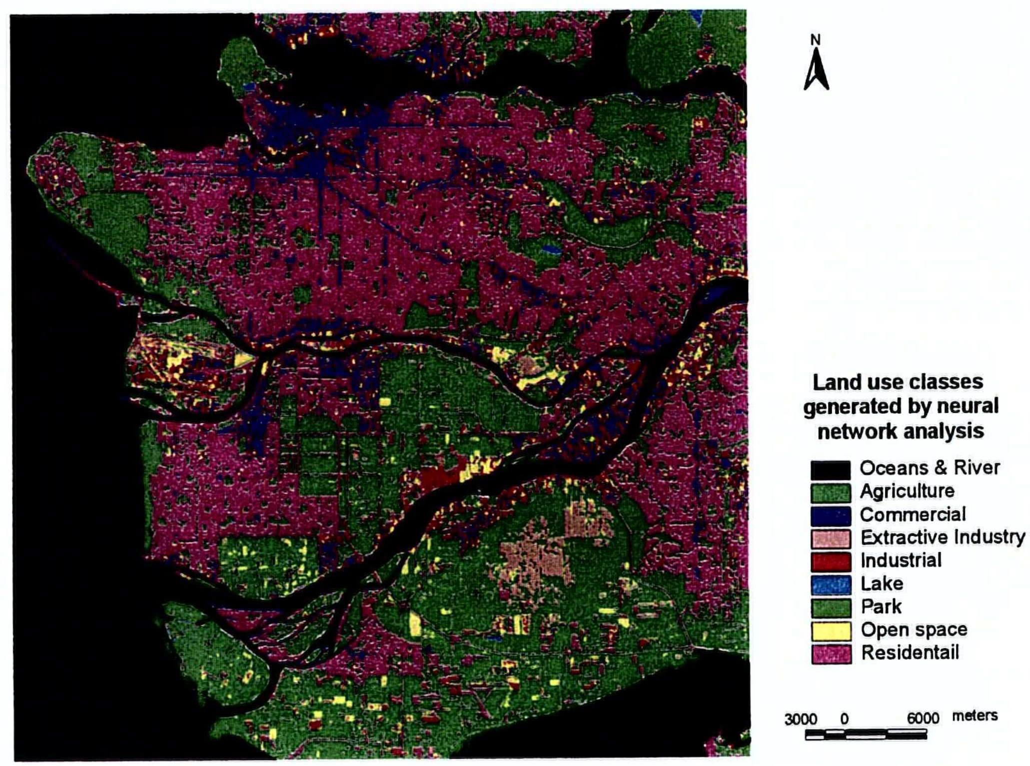

Figure-4.2

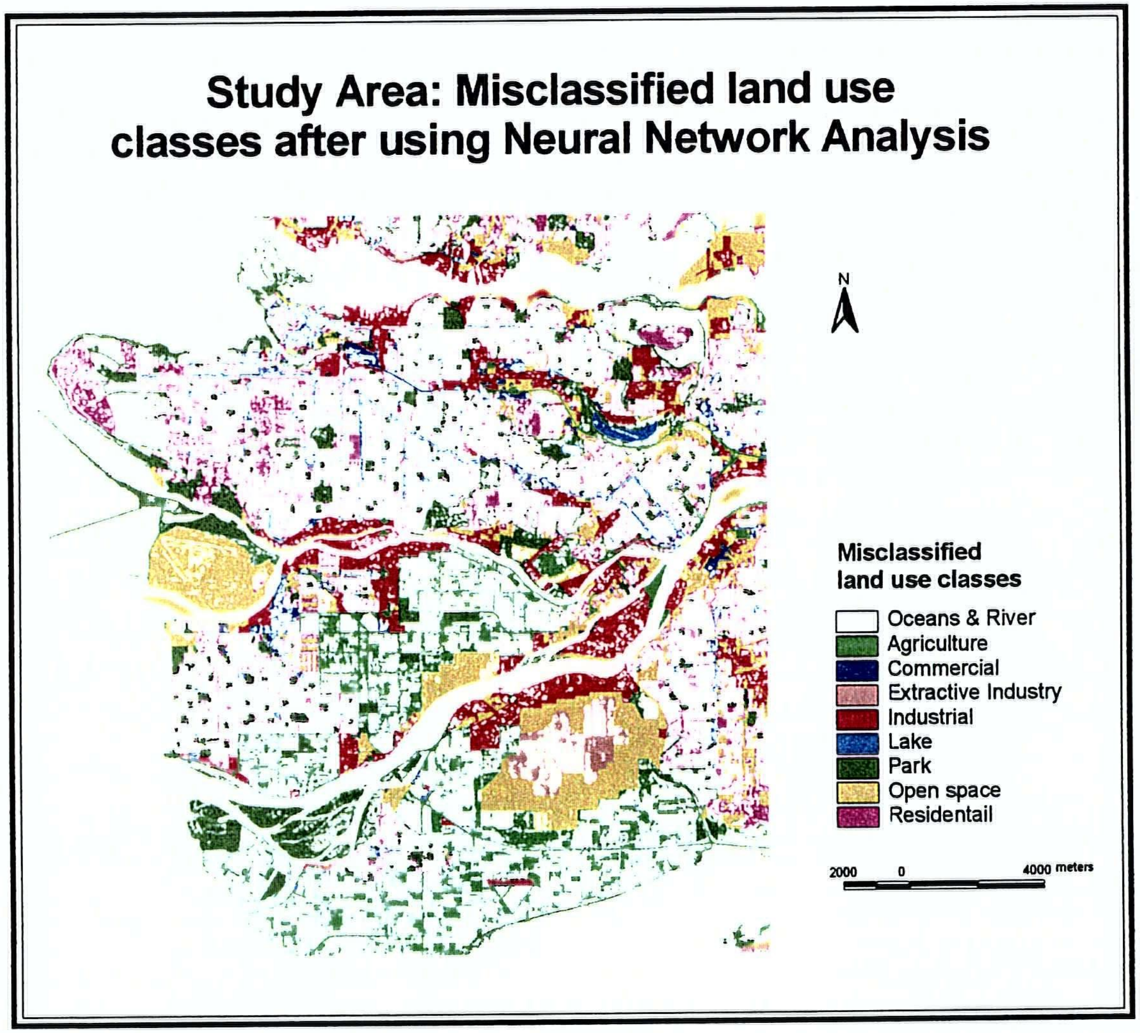
Study Area: Misclassified land use classes after using Neural Network Analysis
N
Misclassified land use classes
Oceans & River
Agriculture
Commercial
Extractive Industry
Industrial
Lake
Park
Open space
Residentail
2000
0
4000 meters

Figure-4.3

classified image (figure 4.2) is exemplified by homogeneous regions, sharp transition boundaries and continuous connected features. Figure 4.3 presents an overall idea of the misclassified pixels of different land cover classes and their distribution over the study area.

4.2.4 Conclusion: As already mentioned, neural networks are able to improve land use classification accuracy by 5 to 10 percent comparing with the conventional classification methods (Howald, 1989; Hepner *et al.,* 1990). This study confirms the effectiveness of neural network based classifiers for land use classification of the Vancouver metropolitan area. The artificial neural network technique implemented here was approximately 7 percent more accurate than a traditional supervised classification with maximum likelihood approach.

4.3 Fuzzy classification for supervised techniques: This section describes the use of supervised fuzzy classification of remotely sensed images. Conventionally, computer-assisted supervised classification requires sufficiently homogeneous training data to perform the image classification. However, such a requirement is not always feasible for an image with highly complex surface features. Moreover, traditional classification mapping with one-pixel-to-one-class algorithms normally fails to deal with the mixed pixels ordinarily caused by the mixture of land cover classes.

Fuzzy classification is based on fuzzy set theory. Fuzzy Sets are sets (or classes) without sharp boundaries; that is the transition between membership and non-membership of a location in the set is gradual (Zadeh, 1965; Schmucker, 1982). A Fuzzy Set is characterized by a fuzzy membership grade (also called a *possibility*) that ranges from 0·0 to 1·0, indicating a continuous increase from non-membership to complete membership.

A problem in remotely sensed images, and particularly with imagery of moderate and coarse spatial resolution (i.e., if the image pixel size is not fine enough to catch the spectral response from only a single land class) is that, the pixels may represent a mixture of land cover classes (referred to as mixed pixels). Where the imagery comprises many mixed pixels, it is not sensible to assign a single pixel to a single class. For example, if a pixel represents 50% open space, 50% residential area, it would be counter-intuitive to assign the pixel to, say, the residential class. In these circumstances, a traditional hard spectral classifier (for example, maximum likelihood classifier) is inappropriate and should be replaced by a fuzzy classifier where the objective is to assign one pixel to many classes in varying proportions that sum to unity.

During the last 10 years or so, researchers have increasingly applied fuzzy classifiers, such as the fuzzy c-means classifier and the mixture model, that estimate the membership of a pixel to each class. Clearly, where a pixel represents a mixture of land cover classes (common in urban areas) fuzzy classifiers provide the opportunity for greater accuracy by creating a probability function showing how likely it is that a certain pixel falls in a given class, and for this reason, fuzzy classification is now widely accepted in remote sensing as a ubiquitous solution to the problem of mixed pixels and is also tested in this section for the Vancouver metropolitan area.

Traditionally, supervised classification methods rely on the assumption that the training sites must be relatively homogeneous (i.e. not containing spectral data from another land cover class). However, this assumption is not purely in areas with highly complex land surfaces (i.e. urban areas) as mixed pixels may cause significant fuzziness in the training data. Therefore, this study focuses on developing fuzzy parameters for the training data. This approach will allow the class membership of a pixel to be partitioned between the classes. Thus, rather than being fully associated with a single class in a conventional hard classification, a pixel can have a variable degree of membership in all classes. Then the fuzzy training data will be used in a fuzzy classification.

4.3.1 Methodology: Supervised and unsupervised classifications rely on classical set theory in assigning pixels to discrete classes based on the set of fixed decision boundaries. Fuzzy set theory on the other hand attempts to improve classification accuracy by taking into account the graded boundaries that are typical of the real world. The differences in these two very different approaches are illustrated in figure 4.4.

Figure-4.4: Classification of Remotely Sensed Data Based on Hard Versus Fuzzy Logic

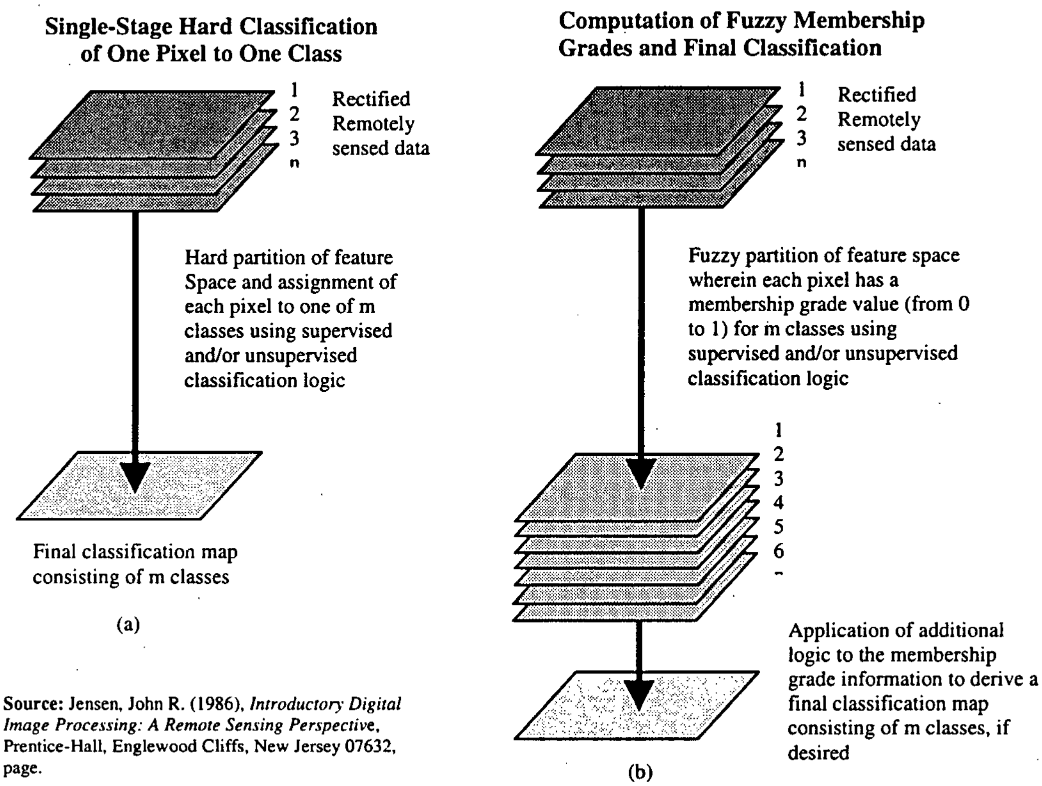

Source: Jensen, John R. (1986), *Introductory Digital Image Processing: A Remote Sensing Perspective*, Prentice-Hall, Englewood Cliffs, New Jersey 07632, page.

There are three different steps for fuzzy classification using IDRISI: (1) signature development by using FUZSIG module, (2) fuzzy classification by using FUZCLASS soft classifiers, and (3) producing a hard classification by using MAXFUZ hardeners.

The first step is to gather signature data before performing fuzzy classification. The FUZSIG module creates signatures from information contained in remotely sensed images and associated training site polygons. These signatures are used to perform a fuzzy classification of remotely sensed imagery using the FUZCLASS modules. While collecting the signatures, no assumption is made that the training sites are homogenous. Rather, it is assumed that each training site may contain pixels with varying degrees of membership in more than one class, and that this can be expressed as a fuzzy membership grade. For example, we may have an urban training site composed of 70% buildings and 30% open space. The same training site can be used as evidence for both urban and open space classes, with fuzzy membership grades of 0.7 and 0.3 respectively. The logic of the procedure is derived from Wang (1990) and is built around the concept of mixtures.

The output from FUZSIG is a set of signature files. FUZSIG gives each pixel a weight proportional to its membership grade in the determination of the mean, variance and covariance of each band for each class (Wang, 1990). Thus a pixel that is predominantly composed of buildings will have a large weight in the determination of the urban signature, but only a low weight in determining the signature for other constituents (i.e., open space). For this study new eight training sites were generated for each land use classes.

The second step is fuzzy classification using the signature files generated in the first step. The FUZZCLASS module of IDRISI was used for fuzzy classification. The FUZZCLASS module is a soft classifier based on the underlying logic of Fuzzy Sets.

There are two important parameters that need to be set when using FUZCLASS. The first one is the z-score distance where fuzzy membership becomes zero. It is assumed that any pixel at the same location in band space as the class mean has a membership grade of 1.0 (Eastman, 1999). The fuzzy set membership grade progressively decreases until it eventually reaches zero at the distance specified. This distance is specified as a z-score (standard score). For this analysis a distance of 2.58 was specified[2].

The second required parameter setting is whether or not the membership value should be normalized. Normalization makes the assumption that the classes are exhaustive, and thus the membership values for all classes for a single pixel must sum to 1.0. This normalization is required to generate true fuzzy set membership grades.

[2] Specifying a distance of 2.58 (i.e., mean $\pm$ 2.58 standard deviation) would force 1% of the pixels to have a value of 0.

The FUZZCLASS module, unlike traditional hard classifiers (e.g., maximum likelihood classifier), produces not a single classified land use map but, rather, a set of images. This set consists of one fuzzy membership image for each of the signature classes, and a classification uncertainty image. While this information describes the class composition, it does not provide any indication as to how this is spatially distributed within the pixel. The outcome is thus quite different from the classic classification algorithms, where a single land user map, containing all classes, is produced.

The final step is to produce a hard classification by using the hardeners[3] from a set of soft classification results. MAXFUZ module was used to produce a hard classification. It uses the images output from the FUZCLASS soft classifier to produce a hard decision image (where a single land user map, containing all classes) by selecting the class image that contains the maximum fuzzy membership grade and assigning that class to the output pixel. In addition, up to four levels of image abstraction can be generated. The first level image indicates the class with the highest fuzzy membership grade, the second level image shows the class with the next highest fuzzy membership grade, the third level image shows the class with the third highest fuzzy membership grade, and so on. These levels can be very useful in determining the character of a pixel since it allows one to break down the dominant and successively subordinate characteristics.

4.3.2 Results and discussions: The land use classes in the study area show a fairly complex mixture that creates difficulties in selecting a homogeneous training site for conventional supervised classification. However, since the proposed fuzzy supervised classification is able to deal with the fuzzy training data, it is acceptable to select training sites that involve more than one land cover class. The resultant classified image is shown in figure 4.5. An accuracy assessment of the classification result produces an error matrix (Table 4. 2). An overall accuracy of 80 percent was obtained.

[3] 'Hardeners' is a process by which a classic land use map can be generated from a set of images produced by fuzzy, where rules can be formulated to determine which class dominates the pixel.

Table-4.2: Contingency table resulting from fuzzy classification of Greater Vancouver area

Classified land uses	Ground Truth									Accuracy (%)	Commission error (%)	Omission error (%)
	Total	1	2	3	4	5	6	7	8			
1. Agriculture	749	623	32	5	1		1	87		91	17	9
2. Commercial	309	4	208	6	28		1	9	53	55	33	45
3. Extractive	373	7		331			15	9	11	88	11	12
4. Industrial	199		42		124			6	27	57	38	43
5. Lake	70					54	14	2		100	23	0
6. Park	590	16		14			451		109	91	24	9
7. Open space	486	16	29		35		1	365	40	71	25	29
8. Residential	1130	18	67	22	28		12	35	948	80	16	20
Total	3906	684	378	378	216	54	495	513	1188			
Overall Kappa = 69% **Overall Accuracy = 80%**												

All land use classes except the commercial and industrial had an accuracy level of more than 70 percent. A large number of pixels belonging to the commercial class have been misclassified either as residential or industrial. Figure 4.5 and table 4.2 present a hard decision fuzzy image produced by the class images (i.e., 8 land use images) containing the maximum fuzzy membership grade. However, the fuzzy classification result (especially for the commercial class and the industrial class) would have been different if the second or third highest membership grade was selected instead of the highest fuzzy membership grade.

Misclassifications were observed between the agricultural lands and the park areas while using traditional classifiers, as well as some of the more modern image classification methods (e.g., artificial neural networks); however, the fuzzy classification of the same image was able to remove most of the confusion between the agricultural class and the park class (figure 4.6). For park and agricultural classes the accuracy level was more than 91 percent. The comparatively high overall accuracy score demonstrates the potential application of the fuzzy supervised classifier to the remote sensing images with highly complex land uses.

4.3.3 Conclusion: A Fuzzy classification method for remotely sensed imagery was used in this study. The fuzziness of the training data allows the classified pixels to be

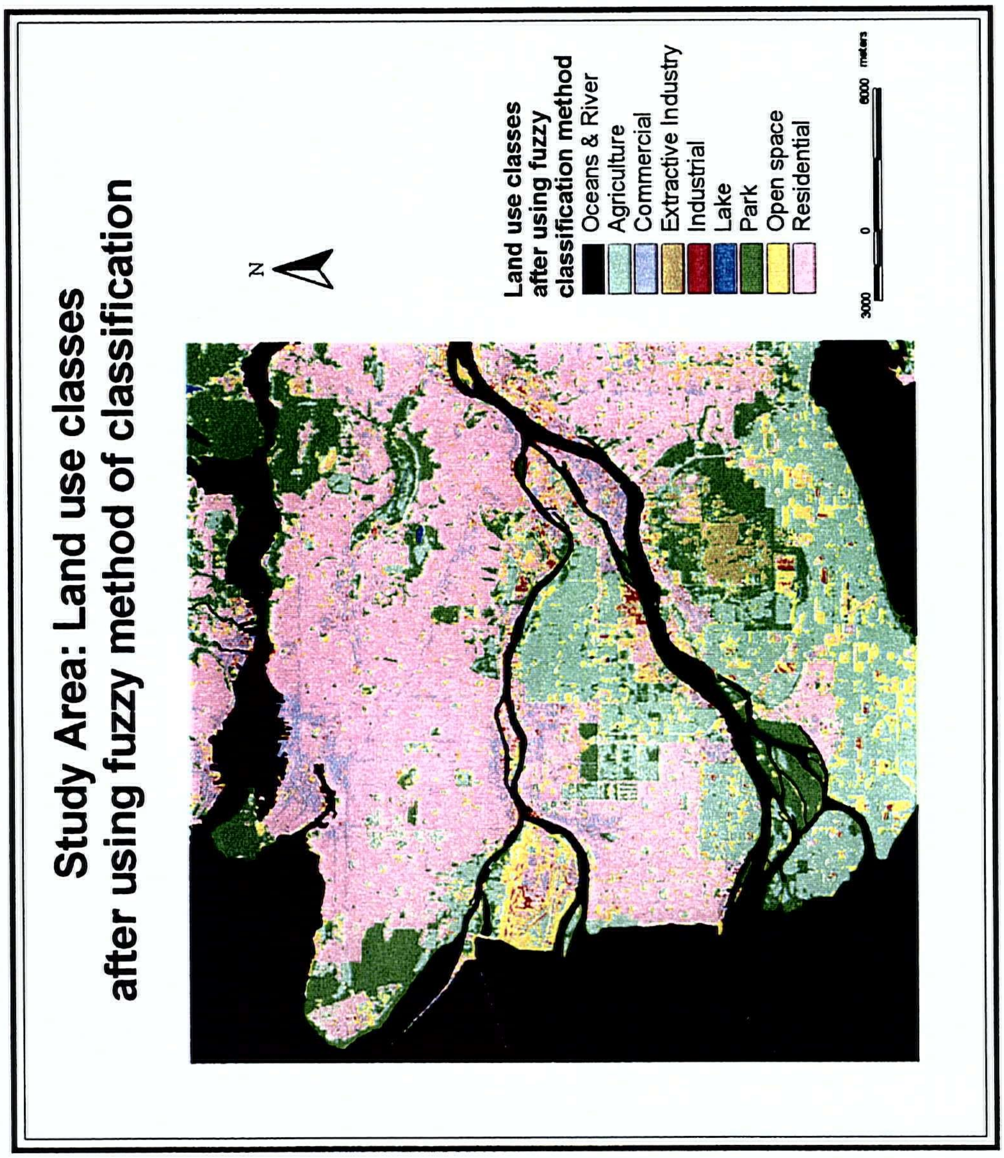
Study Area: Land use classes
after using fuzzy method of classification
N
Land use classes
after using fuzzy
classification method
Oceans & River
Agriculture
Commercial
Extractive Industry
Industrial
Lake
Park
Open space
Residential
3000
0
6000
meters

Figure - 4.5

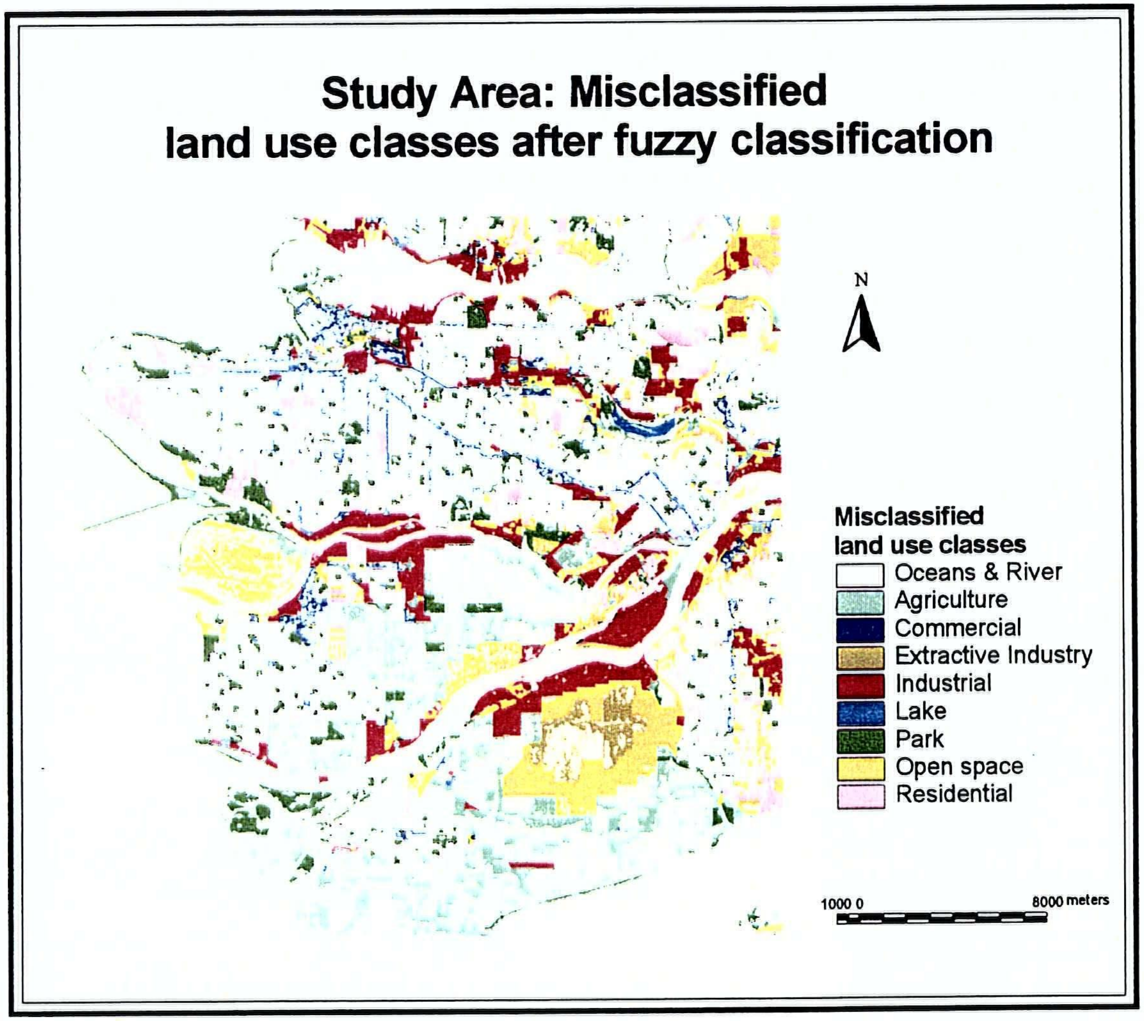
Study Area: Misclassified
land use classes after fuzzy classification
N
Misclassified
land use classes
Oceans & River
Agriculture
Commercial
Extractive Industry
Industrial
Lake
Park
Open space
Residential
1000 0
8000 meters

Figure - 4.6

presented in the form of membership values, which enabled the analysis to produce better results than did the traditional hard classifiers. Using a fuzzy set concept to map the Greater Vancouver area is useful because this area exhibits substantial variation in land use composition. Moreover, eight fuzzy images (one per land use class) produced by fuzzy soft classifiers could be used for more in depth analysis such as classification based on contextual knowledge.

4.4 Post-classification smoothing for both supervised and unsupervised techniques:
Post-classification smoothing occurs through filtering of images classified using either supervised or unsupervised algorithms. The classification process often causes a salt-and-pepper appearance resulting from spectral variability produced by pixel-by-pixel analysis (Lillesand and Kiefer, 2000.) For example, several pixels scattered throughout an urban area may be classified parks. However, for the purposes of urban land use analysis, trees and lawns associated with urban areas would be better classified into one of the urban classes forming one homogeneous area. In such situation it will be often desirable to 'smooth' the classified image to show only the broad dominant classification. A smoothing filter is often passed over the image to reduce the speckly appearance. This involves passing a window over the image whereby the central pixel of the matrix is reclassified based on the type of filter (i.e., mean, mode, weighted average) and the values within the window (the central and surrounding pixels.)

Several types of filters exist to either smooth or sharpen images. Mean (low-pass) filters are commonly used to generalize an image. These filters recalculate the central pixel of the window based on the other pixel values in the window. The median filter is excellent for random noise removal. Mode filters are good for filling gaps between polygons after a vector-to-raster conversion and for correcting "salt-and-pepper" appearances. Edge enhancement filters accentuate areas of change in continuous surfaces. High-pass filters emphasize areas of abrupt change relative to those of gradual change (Burrough and McDonnell, 1998). High-pass filters are not used for post-classification smoothing of images. For example, The Sobel Edge Detector extracts edges between features or areas of abrupt change. A user-defined filter is useful for simulation modeling.

The most popular smoothing filter in image classification is the majority or mode filter. This type of filter passes a window (3 by 3, 5 by 5, or 7 by 7 or a variable sized template or kernel) over an image in order to reclassify the central pixel in the window. The central pixel is given the value of the modal frequency (the value with the highest frequency of pixels) within the window. In other words it assigns the most common value of that neighborhood to the central pixel. For this study a modal filter was selected for post-classification smoothing because of its ability to remove "salt-and-pepper" appearances after land use classification.

A drawback of this technique is that filtering is applied all over the image. While the smoothing of misclassified pixels is desirable in urban areas, it is possible that pixels comprised of a small rural field or a house in suburban areas can be reclassified too.

4.4.1 Methodology: After classification (i.e., both supervised and unsupervised), the result usually has a "salt-and-pepper" appearance. Therefore, a post-classification smoothing is generally needed. Post-classification smoothing was used to weed out small areas that are too small to be useful units of landscape classification. The assumption was made that these small areas were really misclassifications, for one reason or another, and that they should be blended into adjacent areas (Treitz and Howarth, 1996).

Post-classification smoothing was performed by using the FILTER module (Modal filter) of the IDRISI image processing software. The modal filter, which assigns the most common value to the center pixel, is also commonly used to remove the salt-and-pepper appearance from a classified image, or slivers left after rasterizing vector polygons. For the present study a 3 by 3 modal filter was used because studies have shown that a 3 by 3 modal filter improves the classification accuracy better than a 5 by 5 or a 7 by 7 modal filters (Kettig and Landgrebe, 1976; Thomas, 1980; Booth and Oldfield, 1989). Once the post-processing smoothing was performed, the resulting image was compared to the reference image (ground truth image with 434 ground-truth points), and the accuracy was tabulated for both supervised and unsupervised classification (Table 4.3 and Table 4.4).

Table-4.3: Contingency table resulting from post-classification smoothing of supervised classification for Greater Vancouver area

Classified land uses	Ground Truth									Accuracy (%)	Commission error (%)	Omission error (%)
	Total	1	2	3	4	5	6	7	8			
1. Agriculture	663	472					26	110	55	69	29	31
2. Commercial	386		296		47				43	78	23	22
3. Extractive	278			270				6	2	71	2	29
4. Industrial	122		4		98			12	8	45	20	55
5. Lake	59					54		5		100	8	0
6. Park	479	12		6			428	15	18	86	11	14
7. Open space	433	101	4		27		5	263	33	51	39	49
8. Residential	1486	99	74	102	44		36	102	1029	86	31	14
Total	3906	684	378	378	216	54	495	513	1188			
Overall Kappa = 67% Overall Accuracy = 75%												

4.4.2 Results and discussions: After classification, many isolated pixels were observed through out the classified image[4]. This might be an accurate description of reality, but for mapping purposes, a very common post-classification smoothing was performed which produced a generalized image and removed those isolated pixels. Table 4.3 and table 4.4 present the new results of the supervised and unsupervised classifications after running a smoothing filter over them.

The overall accuracy for supervised classification, after post-classification smoothing, was 75 percent (table 4.3). The overall accuracy was improved by about four percent (from 71 percent). After post-classification smoothing, class-wise accuracy increased for almost every class, except for the park and residential classes. Possibly some of the small residential and park areas might have misclassified after running a modal filter they, which is a drawback of this method.

[4] In this section post-classification smoothing was performed for supervised and unsupervised classification, however, smoothing can be applied to any classified image, for example, fuzzy and ANN classified images.

Table-4.4: Contingency table resulting from post-classification smoothing of unsupervised classification for Greater Vancouver area

Classified land uses	Ground Truth									Accuracy (%)	Commission error (%)	Omission error (%)
	Total	1	2	3	4	5	6	7	8			
1. Agriculture	588	307		50			4	110	117	45	48	55
2. Commercial	366		234		64				68	62	36	38
3. Extractive	311			226			52	24	9	60	27	40
4. Industrial	410	45	42		136			148	39	63	67	37
5. Lake	74					54	1	19		100	44	0
6. Park	537	71		12			399	13	42	81	30	19
7. Open space	552	233	7	29			26	157	100	31	55	69
8. Residential	1068	28	95	61	16		13	42	813	68	24	32
Total	3906	684	378	378	216	54	495	513	1188			
Overall Kappa = 53% Overall Accuracy = 60%												

The overall accuracy for unsupervised classification, after post-classification smoothing, was 60 percent (table 4.4). Compared to supervised classification, salt-and-pepper appearance was much less for unsupervised classified image (figure 3.8 in chapter 3). Therefore, there was only one percent (from 59 percent) increase of classification accuracy for unsupervised classification after using a modal filter. An increase in accuracy level was observed for the agricultural, industrial, and extractive classes, while for other four classes (i.e., the commercial, park, open space, and residential classes) accuracy declined from 1 to 4 percent (i.e., comparing with the unsupervised classification results, table 3.3 in chapter 3). The reason behind this decline is that, after a running a modal filter, some of the small residential, open space and park areas might have misclassified.

The speckle-reduced output images of the study area are shown in figure 4.7 and figure 4.8. It has also been noted that visual inspection probably provides the best assessment of performance of a particular filter. It has been observed that after running a 3 by 3 modal filter on the original classification, a comparatively smoothed image of reduced speckle was generated. This still showed all the fine details and hence all meaningful information.

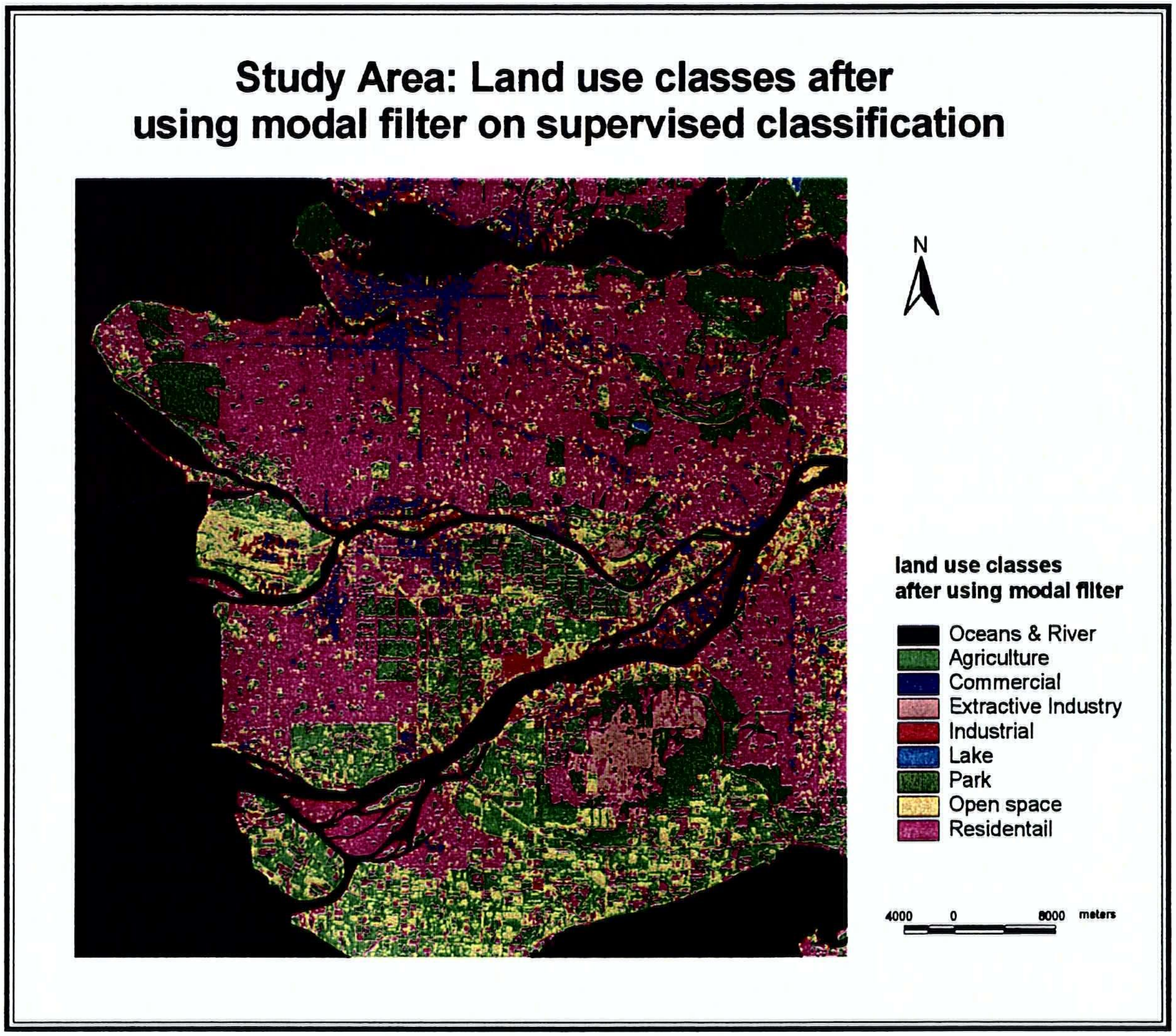
Study Area: Land use classes after
using modal filter on supervised classification
N
land use classes
after using modal filter
Oceans & River
Agriculture
Commercial
Extractive Industry
Industrial
Lake
Park
Open space
Residentail
4000
0
8000
meters

Figure-4.7

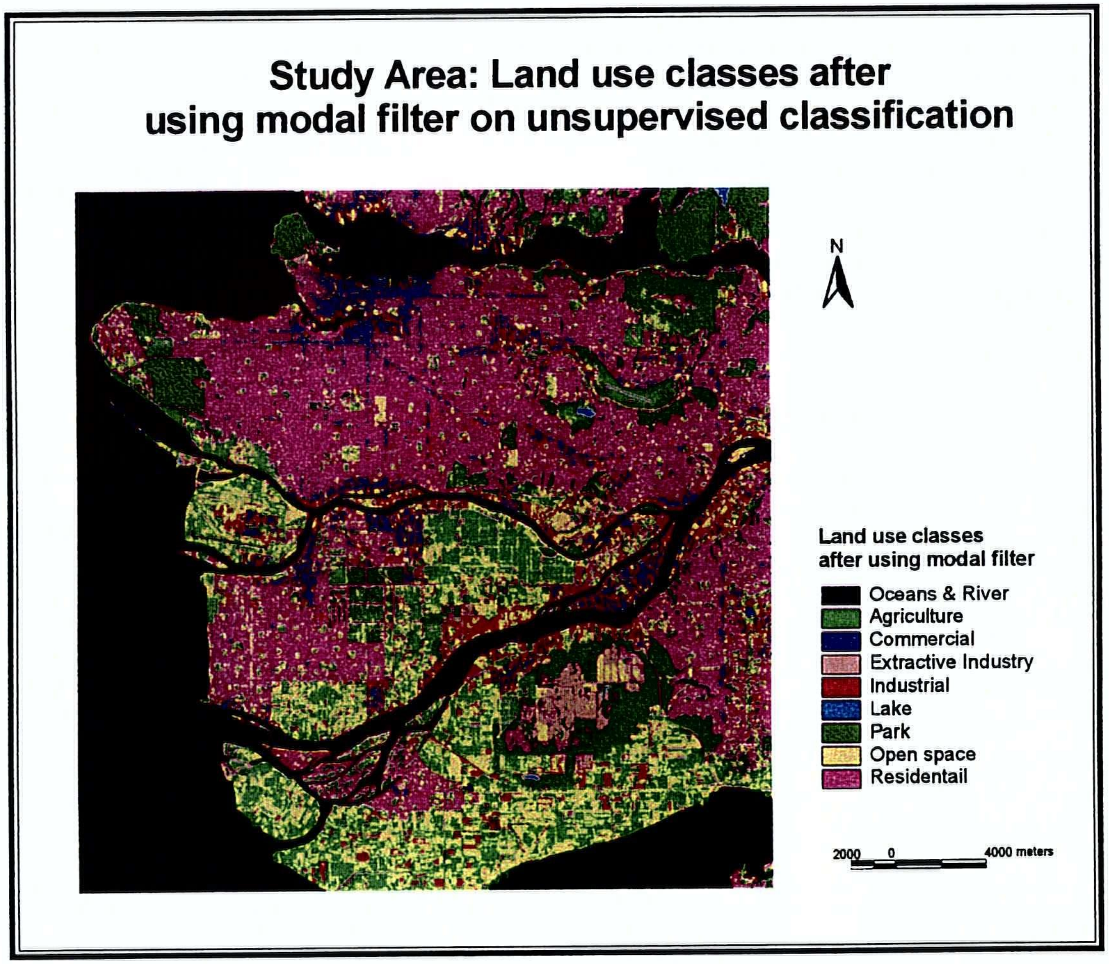
Study Area: Land use classes after
using modal filter on unsupervised classification
N
Land use classes
after using modal filter
Oceans & River
Agriculture
Commercial
Extractive Industry
Industrial
Lake
Park
Open space
Residentail
2000
0
4000 meters

Figure-4.8

CHAPTER V

Image segmentation

5.1 introduction: Image segmentation is the process of dividing digital images into spatially cohesive units, or "regions". These regions represent discrete objects or areas in the image. These regions may be later associated with information classes, but the segmentation process itself simply gives each region a generic label (region 1, region 2, etc.). For multispectral or hyperspectral remotely sensed imagery data, the regions consist of groupings of image pixels that have similar spectral values. All the pixels of a segment or region are then assumed to belong to the same information class.

Unsupervised classification (i.e., cluster analysis) is also based on spectral similarity or dissimilarity measures. 'Unsupervised' is a very general term for any sort of image classification algorithm that works automatically, that is, without much (or any) 'supervision' (control) by the user. Image segmentation is 'unsupervised' in the sense that it is based entirely on the inherent properties of the image itself, without any significant user input (apart from one or two parameters, such as gradient threshold). However, while one method (unsupervised classification) works only in spectral space, the other works in both spectral and geographic space.

Pratt (1991) argues that there is no single theory of image segmentation; rather, there are collections of *ad hoc* methods that have received some degree of popularity. Haralick and Shapiro (1985, pp101) have established the following qualitative guidelines for 'good' image segmentation: 'Image segments should be uniform and homogeneous with respect to some characteristic such as gray tone or texture. Region interiors should be simple and without many small holes. Adjacent regions of segmentation should have significantly different values with respect to the characteristics on which they are uniform. Boundaries of each segment should be simple, not ragged, and must be spatially accurate'.

Segmentation algorithms are based on either region growing/merging (Ketting and

Landgrebe, 1976), boundary detection (Marr and Hilderth, 1980), or a combination of both (Tilton, 1996). More recently (after 1990), segmentation algorithms, based on statistical models (e.g., the PICO regression model) (Acton, 1996) and Markov Field models (e.g., Bauman and Shapiro, 1994) have been proposed.

5.2 Approaches to image segmentation: Most image segmentation approaches can be placed in one of three classes:

- characteristic feature thresholding or clustering,
- boundary detection or edge finding techniques, and
- region growing.

Threshold techniques

Feature thresholding or clustering is a simple segmentation approach (no different than unsupervised clustering), computationally inexpensive and fast. Threshold techniques are based on the thresholds, which are usually selected from the image histogram. All pixels whose value (gray intensity, colour, or other) is between two values of thresholds are assigned to one region. Because the thresholds are derived from the histogram, these techniques do not take into account spatial information of the image and they do not cope well with the noise as well as with blurred edges in the image.

Boundary detection or edge-based methods

An alternative to thresholding is to find those pixels that belong to the borders of the objects. Techniques that are directed to this goal are termed boundary detection or edge finding techniques. Edge-based methods try to find the places of rapid transition from one region to another region of different brightness or colour value. The basic principle is to apply a gradient operator to the image. Gradient magnitudes are possible places of rapid transition between two different regions - what we call edges. After finding edges on the image, the edges have to be linked in order to form closed boundaries of the regions. Boundary detection does exploit spatial information through examining local edges found throughout the image. The Sobel, Prewitt and Laplacian operators are examples of edge detection approaches. For simple noise-free images, detection of edges results in straightforward boundary delineation. However, edge detection on noisy, complex images often produces missing edges and extra edges (Tilton, 1996).

Region growing

Region-based methods are complementary to the edge-based methods. Here the point is to assign pixels of the same or similar brightness or colour to the regions according to the given criteria of homogeneity (look at the neighbouring pixels of the given pixel and merge them into the region if criteria of homogeneity is satisfied). Homogeneity criteria are based on some threshold value, and thresholds depend on the image data.

***5.3 Software used for the study*:** The SILVICS (Satellite Image Land Vegetation Integrated Classification System) version 1.1 was used for Image segmentation, which implements a boundary detection or edge finding approach. SILVICS provides state-of-the-art, robust image processing tools for the spatial analysis of satellite imagery. The spatial analysis approach includes five different methods: edge preserving smoothing, re-scaling of image values, edge detection, image segmentation, and segment-based filtering. The above five steps are carried out using the SILVICS programs "Edge-Preserving Smoothing", "Re-Scaling of Image Values", "Edge-Detection", "Image Segmentation", and "Segment-based Filtering", respectively.

5.4 Methodology of the study: An outline of the image segmentation scheme using SILVICS software is presented in Figure 5.1. Detail discussions of the five steps are included later. One of the methodological constraints in using the SILVICS Image Segmentation program is that it should not be applied to extremely large images, such as full Landsat TM scenes, for the following reasons:

- The number of spatial units (segments) in a very large satellite image would be enormous. Analysis of the resulting segmented image by any SILVICS program would be very slow.
- The SILVICS image segmentation algorithm needs the entire image to be stored in memory. If this image is very large, the available memory may not suffice.

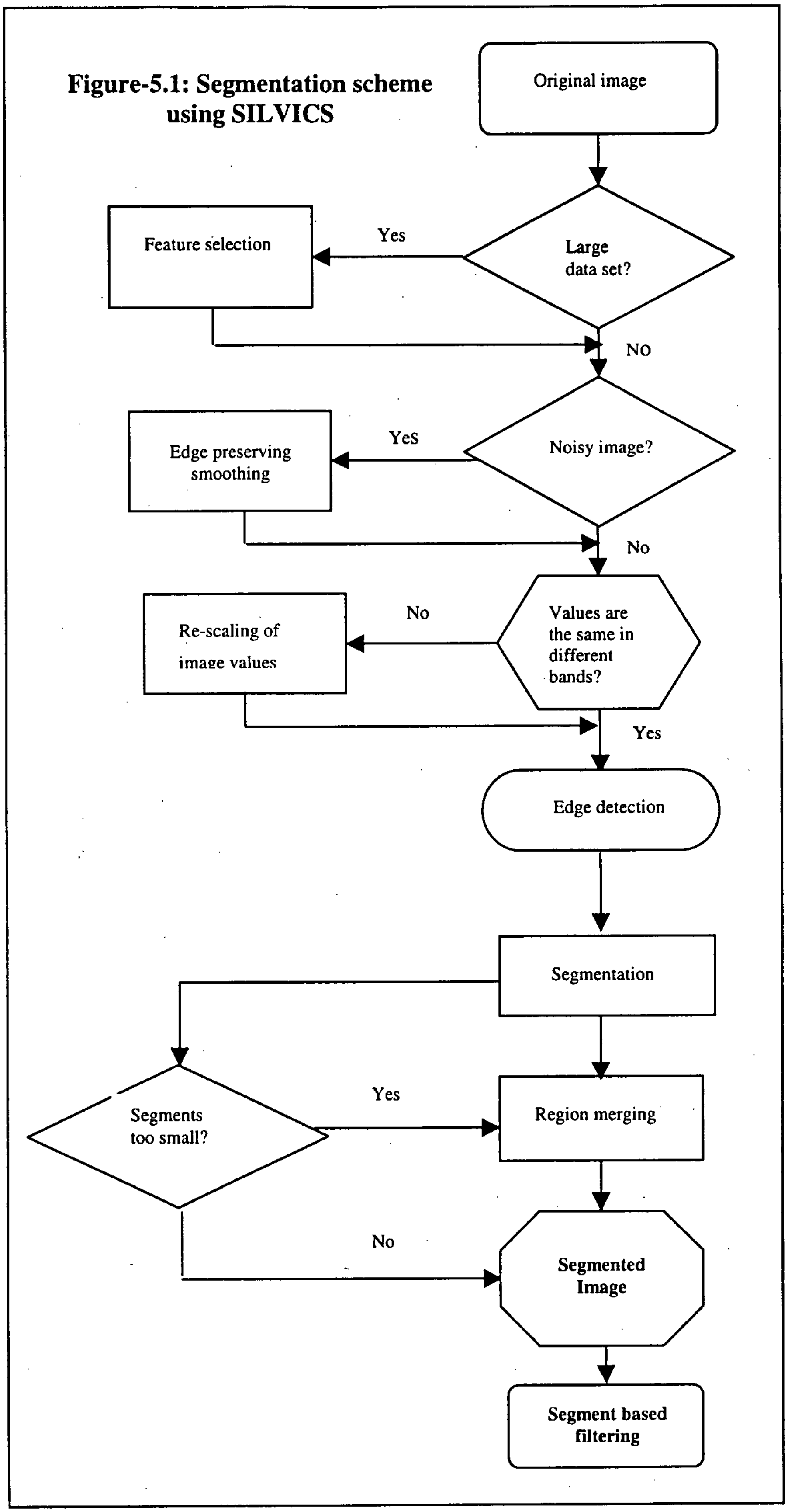

Figure-5.1: Segmentation scheme using SILVICS

For these reasons, the Image Segmentation program should be applied to carefully selected subsets of full image scenes. As the study area (2000 x 2000 pixels or 30 by 30 km) was only a part of the full image scene (184 by 172 km approximately) of Greater Vancouver Area, this was not of concern for the present study.

5.4.1 Five steps of image segmentation using SILVICS (figure 5.2):

Step1: Edge-preserving smoothing

Two problems that affect the spatial information content of satellite imagery are image noise and the blurring of edges (McCormick, 1999). Image noise is defined as random variations in image values. Image noise can be generated by many factors, such as instrument error, atmospheric interference, and the natural variability of ground features. Blurring of edges in satellite images is characterized by reduced sharpness of edges and spatial detail. When pixels at the edge between two ground features contain samples of both features, the transition between features appears blurred.

Edge-preserving smoothing helps to reduce the effects of noise in an image, without disturbing significant detail (i.e. edges). The smoothing of the satellite image is performed by using special adaptive filters. The special adaptive filter that is implemented in the SILVICS software is based on the algorithms of Nagao and Matsuyama (1979). This smoothing algorithm looks for the most homogeneous neighbourhood area around each pixel in an image, and then gives each pixel the average gray level of the selected neighbourhood area. It removes noise in a flat region without blurring sharp edges, or destroying the details of the boundary of a region. For SILVICS software this maximum homogeneity method has been used with a little modification. The original method was designed for single-band digital aerial photography. In SILVICS, the original method has been adapted for multi-band satellite images (McCormick, 1999).

For edge preserving smoothing the input was a multi-band satellite image. The output was a multi-band smoothed image. Noise is removed by the repeated use of this

5.2 Flow chart depicting the procedure followed for image segmentation

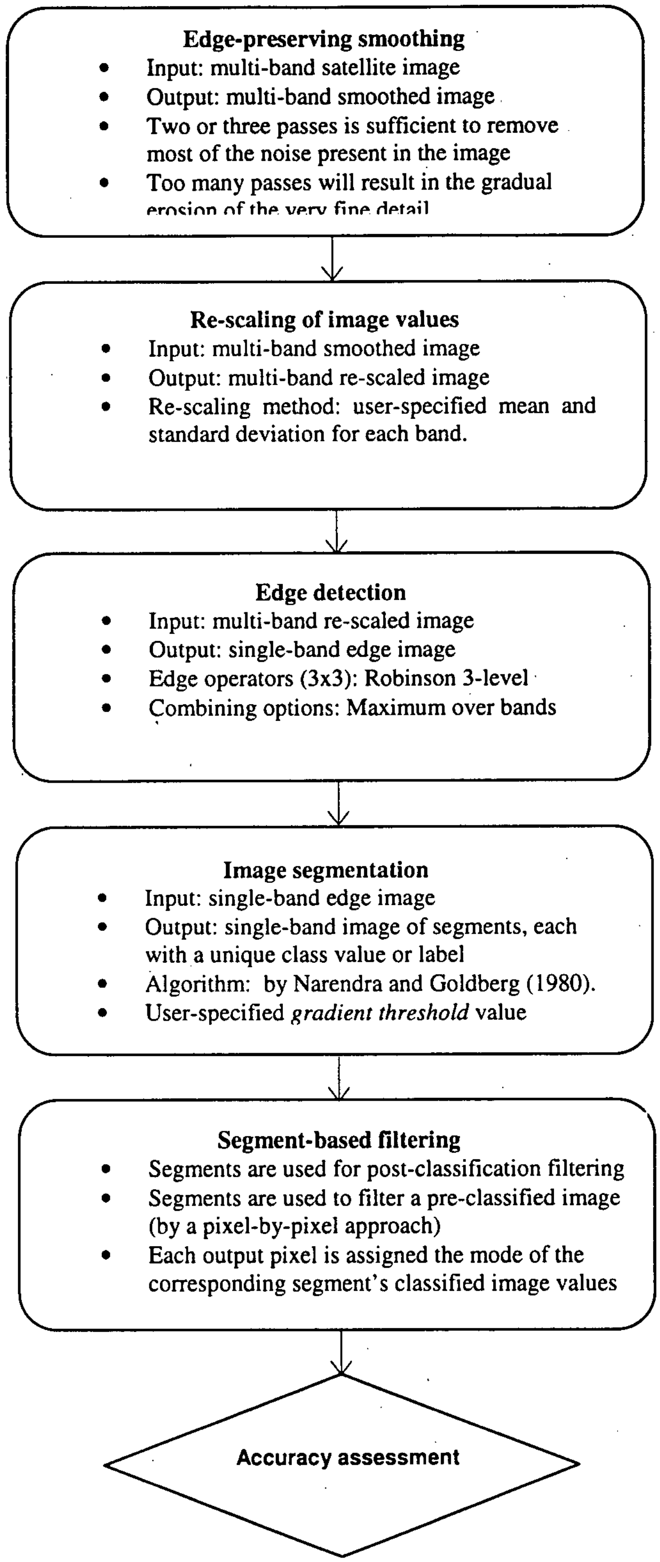

method. The degree of smoothing depends on the user-specified number of smoothing passes. Usually, two or three passes are sufficient to remove most of the noise present in a Landsat TM or SPOT image (McCormick, 1999). Too many passes will gradually erase very fine features present in an image. For the present study three passes were used for edge preserving smoothing.

Step2: Re-scaling of image values

The next step includes re-scaling image values in the different bands of the smoothed image to the same statistical distribution. According to Häme (1992), this should be done before edge detection and image segmentation. Without rescaling, some bands might have a high range of gray level values (e.g., typically TM band 4 for Landsat TM imagery), whereas other bands may have a low range of gray level values, which would further affect the detected edges and resulting segments (McCormick, 1999).

The SILVICS software provides three options for the re-scaling method:

1. *Gain, offset re-scaling method:* input bands are re-scaled by a user-specified gain and offset for each band.
2. *Minimum, maximum re-scaling method:* the input image values are re-scaled to a user-specified minimum and maximum for each band.
3. *Mean, standard deviation re-scaling method:* the input image values are re-scaled to a user-specified mean and standard deviation for each band.

For the present study the third method, that is, the mean and standard deviation method was used. The statistical distribution of the input image bands were checked before specifying the mean and standard deviation value (i.e., check whether the values in each band are normally distributed or not). This is important in order to avoid the loss of information that could result from re-scaling. The SILVICS program 'Computation of Band Statistics' was used to compute the statistical information for each band in an input image. After looking at the mean and standard deviation distribution for each band, values of 100 (mean value) and 20 (standard deviation value) were specified for the re-scaled programme. The input for re-scaling of image values was a multi-band smoothed image (generated by the previous stage) and the output was a multi-band re-scaled image.

Step3: Edge detection:

After edge smoothing and re-scaling of image values, edge detection was applied. An edge is the boundary between two regions with relatively distinct gray-level properties. Pratt (1991) has reviewed different edge detection methods. According to him there are two major classes of differential edge detection: first order derivative and second order derivative. For the first order class (after performing some form of spatial first order differentiation) the resulting gradient is compared to a threshold value. An edge is assumed to be present if the gradient exceeds the threshold value. For the second major class (i.e., second order derivative class) an edge is assumed to be present if there is a spatial change of gray-level values of the second derivatives.

Figure-5.3: Edge detection by derivative operators

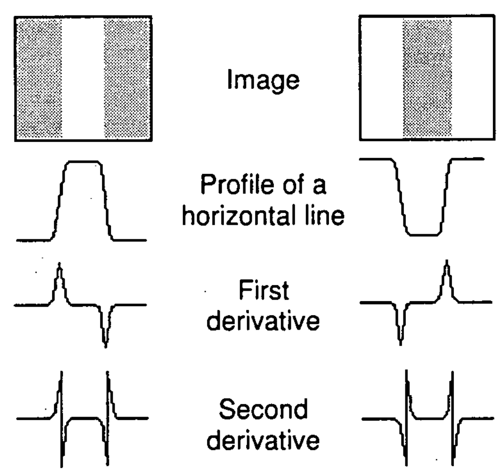

Source: http://cosmos.changwon.ac.kr/~mips/cyber/image/img7-1.html

The idea underlying most edge-detection techniques is the computation of a relative derivative operator (which will measure the instantaneous rate of change of gray level value in an image). Figure 5.3 illustrates this concept. The picture on the left shows an image of a light stripe on a dark background, the gray-level profile of a horizontal scan line, and the first and second derivatives of the profile. The first derivative is positive when the image changes from dark to light, negative when the image changes from light to dark, and zero where the image is constant. The second derivative is positive for the part of the transition associated with the dark side of the edge and negative for the transition associated with the light side of the edge. Thus the magnitude of the first derivative can be used to detect the presence of an edge in the image and the sign of the second derivative can be used to detect whether a pixel lies on the light or dark side of the edge.

The SILVICS program *Edge Detection* offers three alternative 3 by 3 edge operators that are used for the edge template gradient generation method of edge detection. The edge template gradient generation method is the most commonly used first-order derivative method. This method uses special 3 by 3 pixel windows or operators of weighting factors to compute an edge value for each pixel in an input image (Pratt, 1991). These three alternative operators are:

- Robinson 3-level
- Robinson 5-level
- User-defined

The first two edge operators[1], proposed by Robinson (1977), perform a simple averaging operation of nine pixels in a 3 by 3 grid of an image. Using the third option, the user can define any weighting factor for the 3 by 3 edge operator. SILVICS offers two options for combining the edge values of each pixel in the input image bands. These two options are: maximum over bands and sum over bands. Depending on which option is selected, the output edge value for each input image pixel is either the maximum or the sum of the edge values for the input image bands. For the present analysis the input was a multi-band satellite image (six bands, 1 to 5 and 7), and the output was a single-band edge image in which high gray-level values show points of discontinuity (i.e. edges), with stronger edges having higher edge values. The Robinson 3-level edge detection operator and the maximum over band combining methods were used.

[1] Robinson 5-level edge operator contains five integer weights between –2 and +2, whereas, Robinson 3-level edge operator contains three integer weights between –1 and +1.

Step4: Image segmentation: Next, a segmenting method is used to extract spatial units or *segments* that are defined by natural boundaries, rather than by the imagery's artificial pixel-size (McCormick, 1999). The method of image segmentation that is implemented in the SILVICS software is based on the algorithm of Narendra and Goldberg (1980). This is a simple algorithm to detect and label homogeneous areas in an image, using directed trees for region labelling. The scheme constructs the directed trees with image points as nodes, guided by an edge value computed at every point. These directed trees segment the image into disjoint regions[2].

The input for the program is a single-band image of edge values, produced by the third step of image segmentation (i.e., edge detection of a multi-band satellite image). The output of the program is a single-band image of segments, each with a unique class value or label that identifies all of the pixels in that segment. Selecting a suitable gradient threshold value is the most sensitive part of the segmentation. The larger the value of the gradient threshold, the larger the average size of the resulting segments and the smaller the total number of segments. Here, generally, a trial and error method is needed before specifying the final threshold value.

For this study I tried six different threshold values. These values were 100, 50, 30,15, 10, and 5. The first two gradient threshold values were too large to produce larger segments. As a result some of the finer details of the image were not properly represented. For example, using both 100 and 50 threshold value, the entire residential area was captured by only 5 and 12 large segments respectively. But, in reality, the residential class is not a stand-alone class, rather a mixture including some other land use classes (such as commercial areas along the major roads). These were not represented after segmentation. Using a 30 gradient threshold value, the segmentation result was better, however, the

---

[2] Algorithm of Narendra and Goldberg (1980): In this scheme, the edge operator is first applied to every point in the image to yield an edge image, which is then inverted. A modifier version of a recent graph-theoretic procedure (Koontz and Narendra, 1976) is then applied to spatially cluster the two-dimentional image points into segments that are approximately unimodal in the inverted edge value. This is accomplished by constructing directed trees with the image points as nodes. The directed trees are formed by directed links whose assignment is based upon the local edge values. The image points connected by each tree form a segment, which is unimodal in the negated edge value. This way homogeneous regions in the image are detected.

commercial and the industrial classes were not very clear. So finally I selected 15 as the gradient threshold value for the segmentation. Gradient threshold value less than 15 produced numerous smaller size segments of eight land cover classes mixed up with one another.

Step5: Segment-based filtering

The final step was to apply segmented image as a modal filter. The purpose of segment-based filtering is to incorporate the image's natural spatial units (i.e. its segments) into the image classification process. This can be done in two ways: pre-classification filtering and post-classification filtering (McCormick, 1999).

- In pre-classification filtering, the image segments are used to filter a multi-band satellite image. Each output pixel is assigned the mean or median of the corresponding segment's satellite image values. The resulting filtered image is then used as input for image classification.
- In post-classification filtering, the image segments are used to filter an image that has already been classified by a pixel-by-pixel approach. Each output pixel is assigned the mode of the corresponding segment's classified image values.

I used the second method (i.e. post-classification filtering) because, in this way, the original, unaltered satellite image values were classified. Image segments (i.e., the image produced by the fourth step) were used to filter (using a modal filter) an image that had already been classified by the supervised classification method. Each output pixel of the final image was assigned the mode of the corresponding segment's classified image values. However, in chapter 4 (post-classification smoothing) the simple modal filtering was used to remove the salt-and-pepper appearances from the classified image.

5.5 Results and discussions: Figure 5.4 illustrates the edge image produced by the *edge detection* module of SILVICS. It is assumed that an edge lies on the border of all of the important structures, so that by identifying all edges, all objects can be identified (Tilton, 1996). This assumption is not always correct, because often objects on the earth's surface merge into one another, and have no clear boundary. Basically, the idea underlining edge detection techniques is the computation of a local derivative operator. In figure 5.4, high gray-level values (i.e., the reddish pixels) present points of discontinuity (i.e. edges).

Figure-5.4 Study area: Edge Detection
(Edge detection is the prior step to image segmentation)

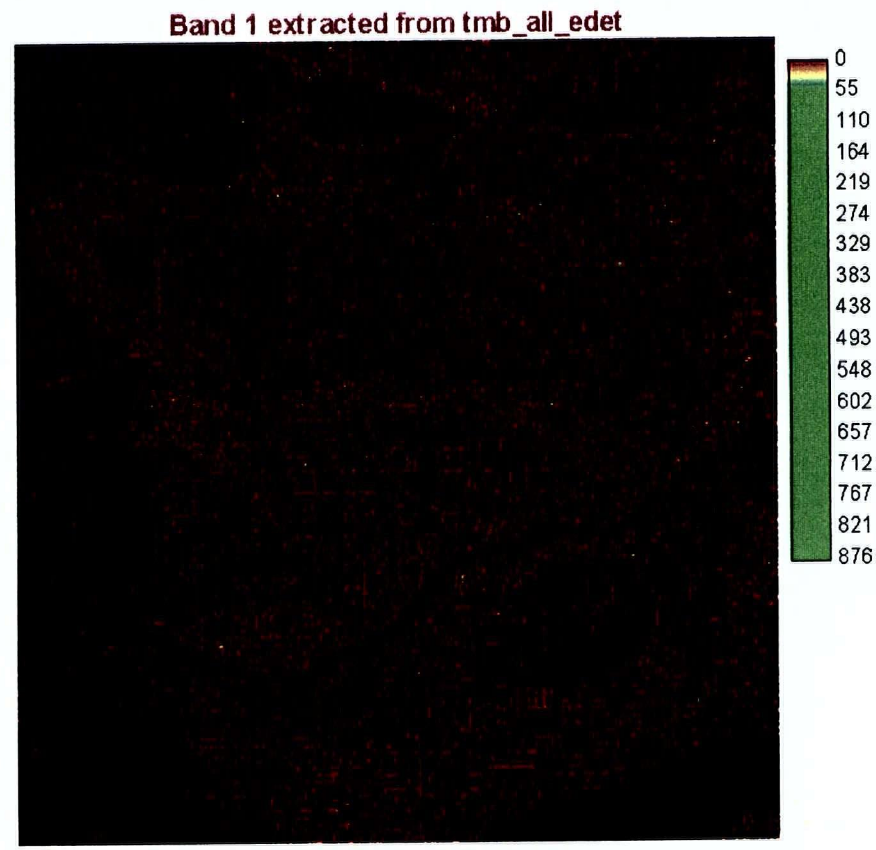

Higher edge values were observed where the edges were stronger in nature (i.e., two regions with relatively distinct gray-level properties). For example, at the Vancouver airport the spectral signatures of runways and airport buildings are different from their background (i.e., basically open fields). This produces sharp edges between these land use classes (figure 5.5). In Stanley Park, by contrast, no distinct boundaries or edges were observed except along the coast line (due to sudden change of land covers as well as spectral signatures) (figure 5.6).

Table-5.1: Contingency table resulting from image segmentation of Landsat TM image

Classified land uses	Ground Truth									Accuracy (%)	Commission error (%)	Omission error (%)
	Total	1	2	3	4	5	6	7	8			
1. Agriculture	666	601	2				17	29	17	88	10	12
2. Commercial	392	5	237		72			10	68	63	42	37
3. Extractive	345			320				13	12	85	7	15
4. Industrial	220		36		120			25	39	58	46	42
5. Lake	60					54	6			100	10	0
6. Park	525	19		6			444	9	47	90	15	10
7. Open space	434	39	21	1	4			330	39	64	24	36
8. Residential	1264	20	82	51	20		28	97	966	81	24	19
Total	3906	684	378	378	216	54	495	513	1188			
Overall Kappa = 65% Overall Accuracy = 79%												

The class-specific accuracies, the overall accuracies, and the overall kappa computed from the segmentation contingency table are presented in table 5.1. The overall accuracy for the segmented image (79 %) was eight percent more than that associated with the supervised classification (71 %). Segmentation algorithms are generally based on a piecewise homogeneous model (i.e., the internal variation is smaller than the variation between segments) (Woodcock and Harward, 1992). It was anticipated that a segmentation scheme would improve the accuracy level for homogeneous areas. The results (table 5.1, and figure 5.8) show that the segmentation scheme does indeed increase the accuracy of agricultural, extractive and park areas. The classification accuracy increases to 88 percent (from 61 percent) for the agricultural class, 85 percent (from 72 percent) for the extractive class, and 90 percent (from 86 percent) for the park class (table 5.1 and table 3.4, i.e. from the supervised classification).

Figure-5.5: Runways and airport buildings present sharp edges in Vancouver Airport Area

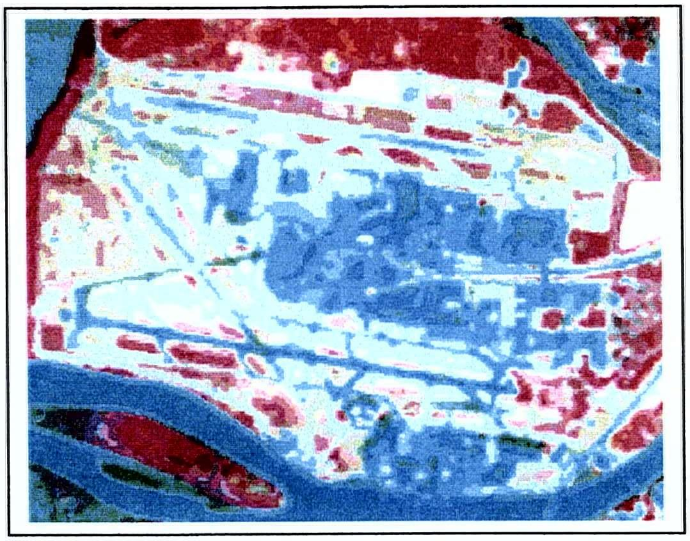

Satellite RGB image of Vancouver Airport

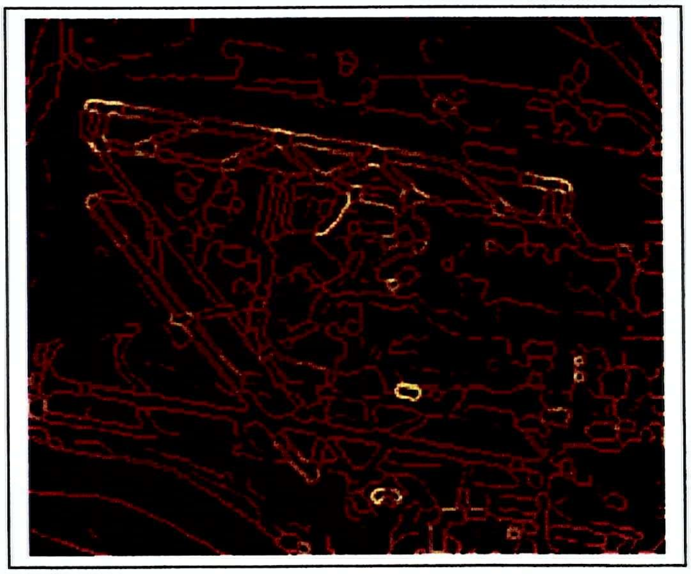

Edged image of Vancouver Airport

Figure-5.6: Stanley park area of Vancouver presents no sharp edges inside the park. Edges are observed along the coasts, lakes, marine drives.

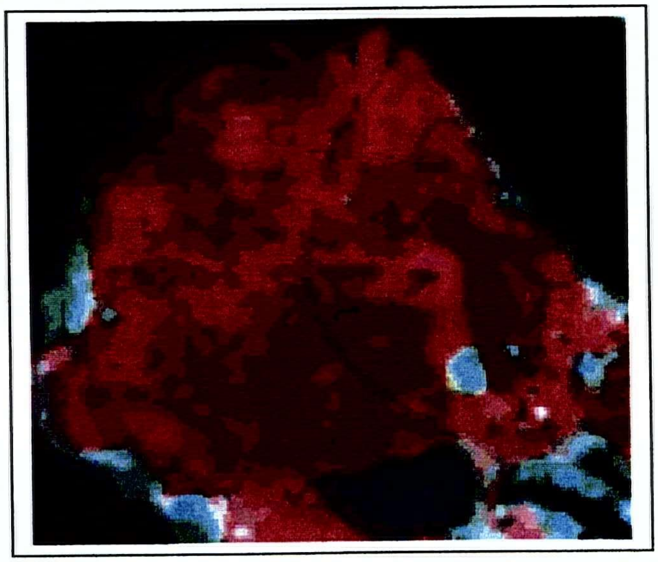

Satellite RGB image of Stanley park

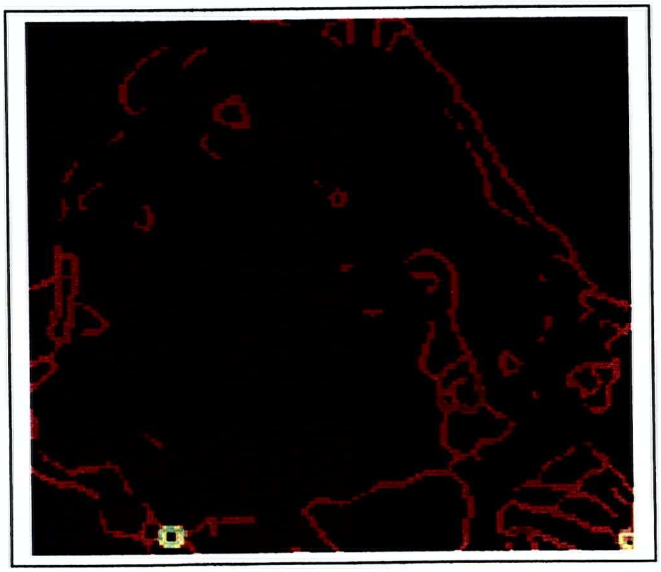

Edged image of Stanley park

Problems arise in segmenting images when the pixels are not spectrally homogeneous. It can be seen from table 5.1 that the commercial and industrial areas have low accuracy due to their highly heterogeneous land cover types. The segmenting algorithm (Narendra and Goldberg, 1980) used in this study was not very efficient in capturing the complexity of urban areas, especially for commercial, industrial, and open space classes. Due to the spectral similarity of buildings, pixels belonging to residential class were misclassified as industrial and commercial classes (table 5.1, and figure 5.9).

Schoenmakers *et al.* (1991) proposed that segmentation is complicated in remotely sensed imagery due to the existence of mixed pixels. Mixed pixels occur when a pixel contains a spectral mixture of distinct land cover types. In a per-pixel analysis[3] a mixed pixel is assigned to the class it most resembles (spectrally) on the assumption that the class occupies the majority of the surface area represented by the pixel (figure 5.7). In segmentation, the discrimination function decides whether or not to include a given pixel in the current segment. Segmentation methods look for similar characteristics in adjacent segments and join them with the current segment (e.g., segment A) if the similarity criteria are satisfied. The addition of a pixel to a segment is dependent on an automatically or manually set threshold. Mixed pixels, therefore, cause ambiguity, predominately at the boundaries of features, leading to segmentation 'flooding' (in which a feature absorbs, or floods into, a neighbouring feature).

It may be quite probable that, due to the 'flooding' effect, some of the land use classes were classified very poorly (e.g., open space, commercial, and industrial areas) (Figure 5.8). In the previous chapters it was observed that, because of spectral similarity, pixels belonging to the industrial class were often misclassified as commercial. Misclassification remains within urban areas and between commercial and industrial

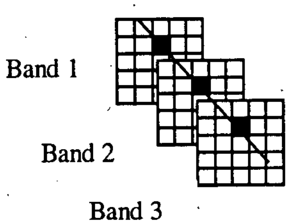

[3] Per-pixel classifiers follow a pixel-per-pixel approach

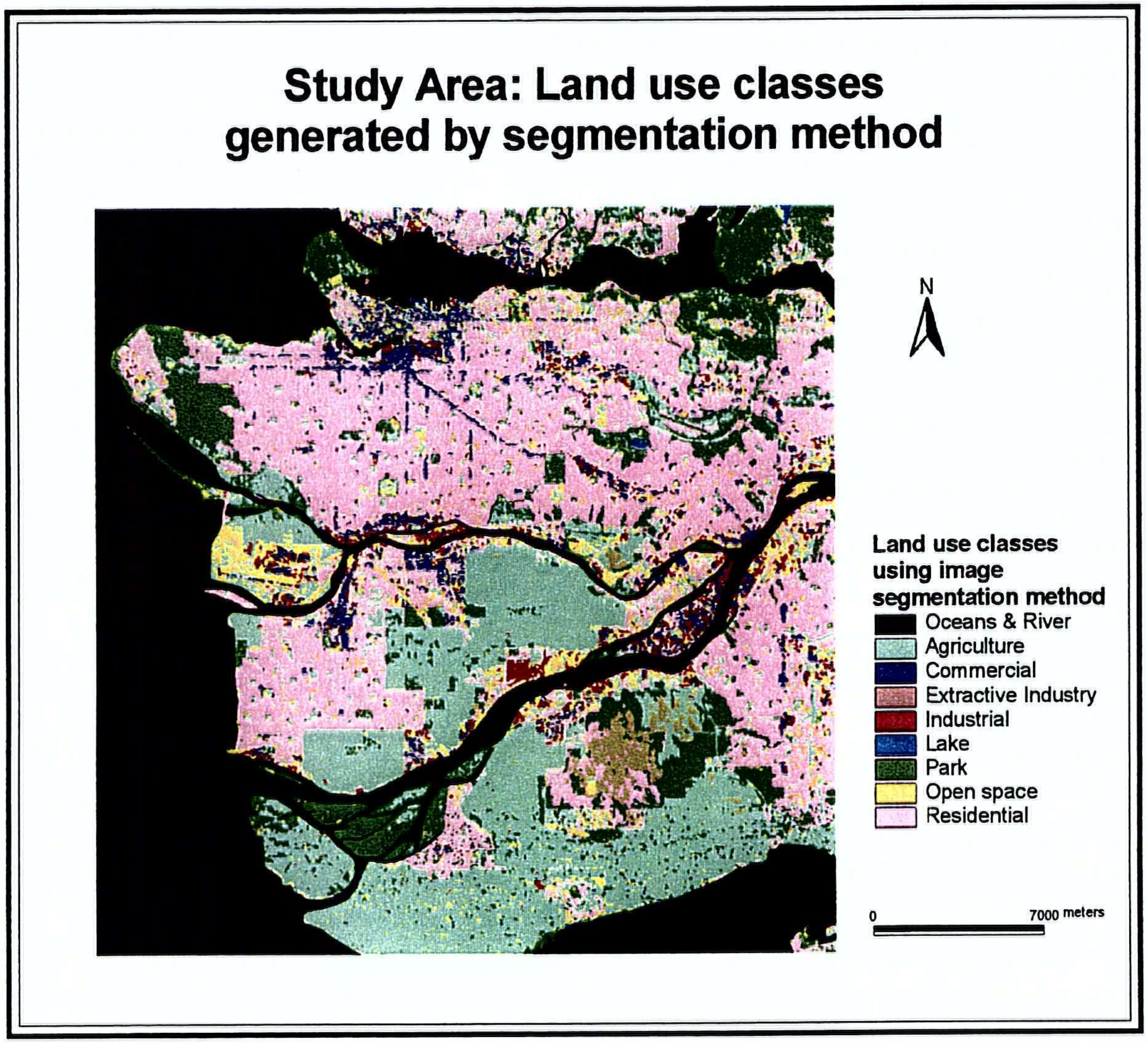

Study Area: Land use classes
generated by segmentation method
N
Land use classes
using image
segmentation method
Oceans & River
Agriculture
Commercial
Extractive Industry
Industrial
Lake
Park
Open space
Residential
0
7000 meters

Figure-5.7

Figure-5.8: Traditional per-pixel classifier is good for homogeneous areas, but not for heterogeneous areas

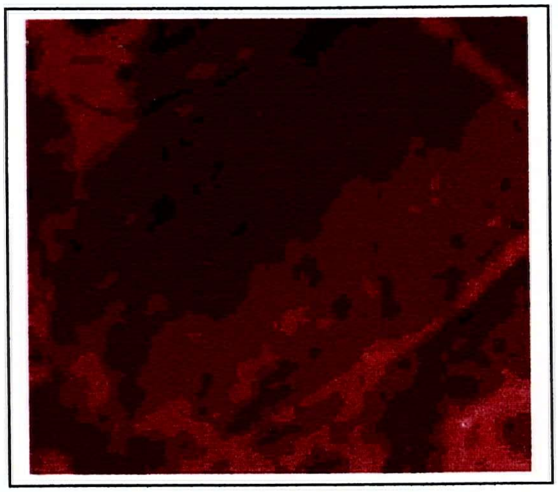

Forest

Homogeneous Spectra throughout the Image

Fairly easy to classify with per-pixel classifiers

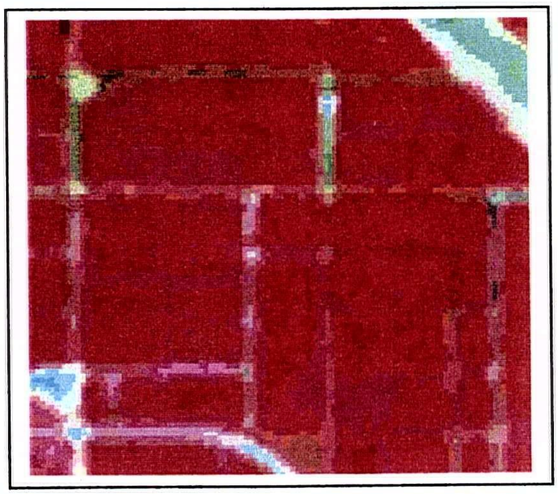

Agricultural Fields

Homogeneous Spectra throughout the Image

Fairly easy to classify with per-pixel classifiers

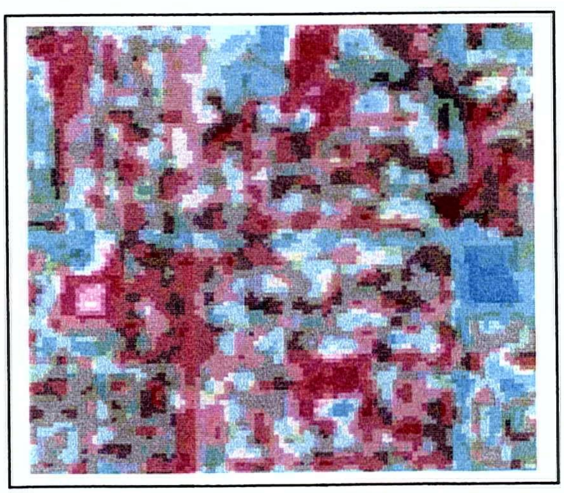

Residential Area

Heterogeneous Spectra

Difficult to classify with per-pixel classifiers

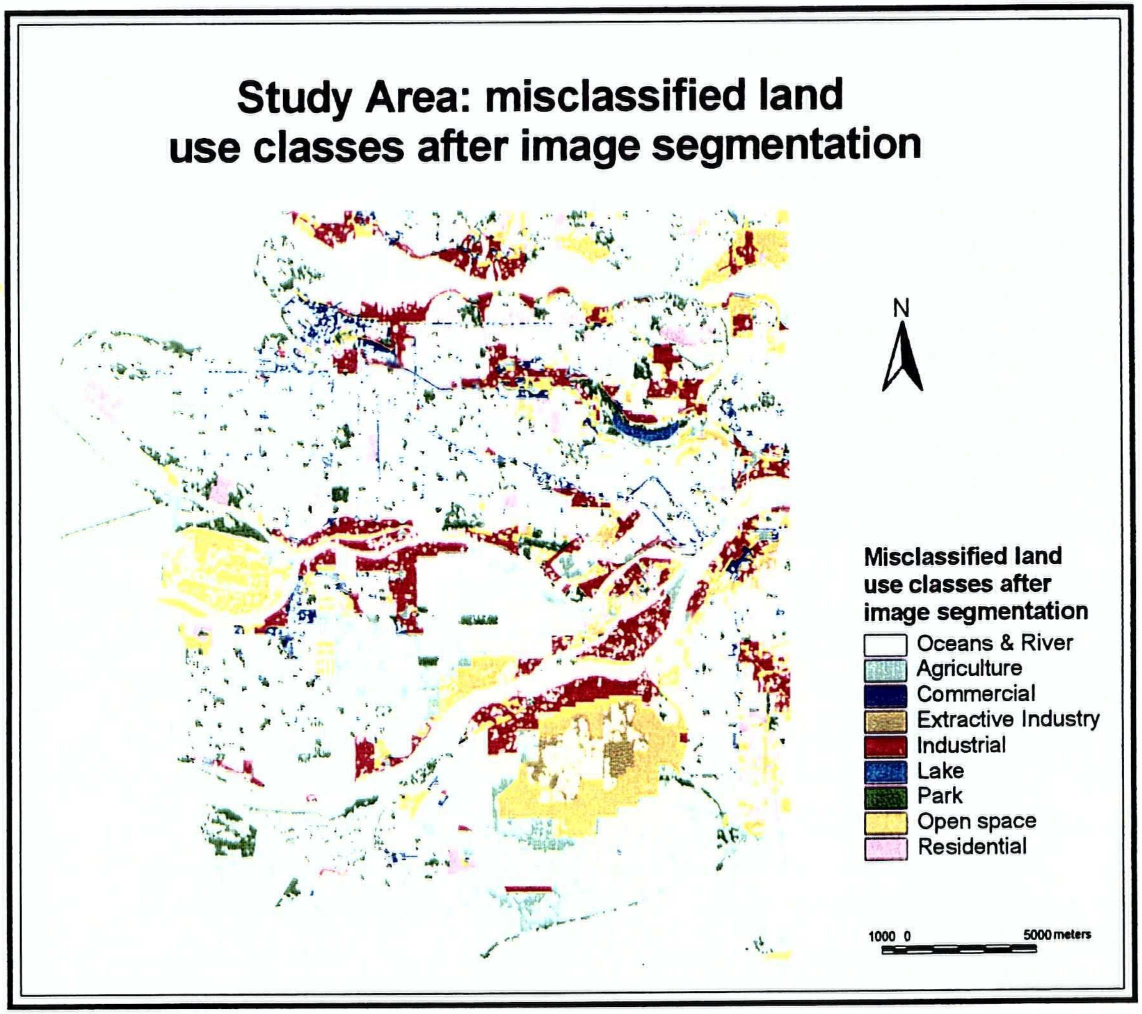
Study Area: misclassified land
use classes after image segmentation
N
Misclassified land
use classes after
image segmentation
Oceans & River
Agriculture
Commercial
Extractive Industry
Industrial
Lake
Park
Open space
Residential
1000 0
5000 meters

Figure-5.9

classes (figure 5.9). However, the accuracy level of the industrial class improves from 46 percent (supervised classification) to 58 percent (segmented image), so spatial information rather than spectral signatures might have helped identifying the industrial sites in the study area.

5.6 Conclusion: Segmentation approaches have been popular for use in extensive and/or homogeneous areas with large and regularly shaped landscape elements (e.g., large agricultural zones of the US Midwest) (Stuckens *et al.,* 2000). In our study agricultural zones, parklands, bog areas (i.e., extractive industry) have shown high levels of classification accuracy. However, the result of segmentation for urban land use classification was not very promising. There could be several ways to improve the result. Since the edge detection result was very detailed, accuracy levels might be improved by masking out the area where the edges are very dense, and then perform the segmentation. Alternatively, additional textural information might be included. Studies have shown that the addition of texture has strong benefits in threshold-based segmentations (Ryherd and Woodcock, 1996).

CHAPTER VI

The Integration of Geographic Data with Remotely Sensed Imagery to Improve Land Cover Classification for the Study Area

6.1 Introduction: Remotely sensed data are widely used in land cover classification. In classic image classification spectral values are grouped together to form classes. Sometimes two or more different features with similar spectral behaviour are grouped into the same class, which leads to errors in the final map. As mentioned in chapter 3, classifications based solely on spectral observations are often not sufficiently accurate for regional studies. Hence, improving the accuracy of classification has always been a major concern in digital image processing.

One approach to this end is the use of multi-temporal imagery to distinguish classes (Conese and Maseli 1991, Barbosa *et al.* 1996). Another is the application of the piecewise linear classifier with simple post-processing (Kai-Yi and Mausel 1993). Foody (1995) used both artificial neural networks and fuzzy logic to improve land use classification from multi-spectral image data using maximum likelihood classifiers. In chapter 3, both these methods were tested and the results indicated that both neural networks and fuzzy methods perform better than conventional classifiers. With the development of Geographic Information Systems (or GIS), the number of classification procedures using geographical data has increased. For example, Harris and Ventura (1995) integrated a classified image with information about housing and local zoning - contained in a GIS - to improve land cover classification in a small urban area of Wisconsin. Ortiz *et al.* (1997) integrated a classified image with information about soils, topography and bio-climate to improve cropland classification. Similarly, Palacio-Prieto and Luna-González (1996) employed GIS rules with ancillary data on terrain mapping units and elevation data.

Researchers note that the integration of GIS technology with remote sensing would provide increased information content and analysis capabilities, and thus be of benefit to land use planners (Nellis *et al.*, 1990). It has been recognized (e.g., Quarmby and

Cushnie, 1989; Forster, 1985; Welch, 1985) that there are many advantages to combining remotely sensed data with existing spatial and statistical data, thereby maximizing the information upon which responsible decisions for land use planning can be made. GIS technology provides the medium for this integration of spatial data, and at the same time provides a powerful tool for the quantitative analysis of land use change (Welch *et al.*, 1988).

6.2 Background: A number of methods have been developed to improve image classification using additional spatial data such as thematic maps and terrain characteristics. These methods can be generalized into three approaches:

(1) Pre-classification stratification,

(2) Classifier modification (i.e., modification during classification), and

(3) Post-classification sorting.

Improvements in classification accuracy have been observed for all three methods; however, there are constraints associated with each technique. A detailed discussion of the advantages and disadvantages of each approach was developed by Hutchinson (1982).

Stratification involves the division of the study scene into smaller areas based on single criterion or multiple criteria. This enables land covers that are spectrally similar to be classified independently (Harris and Ventura, 1995). For example, stratification of an image into urban and rural areas enables spectrally similar grassland covers to be classed as lawn and pasture in urban and rural areas, respectively. It is easily implemented, effective, and inexpensive in terms of computer time. However, this approach does not allow for gradual changes between classes and hence care should be taken when determining stratification criteria (Hutchinson, 1982).

The use of ancillary data directly in the classification process improves accuracy but also increases cost. There are two approaches to using ancillary data during classification. The first incorporates the information as a separate channel to be used during the classification process. Spooner (1991) used this approach for assessing urban change by adding a topographic quadrangle map[1] (as an additional channel) with SPOT[2] panchromatic image. Bolstad and Lillesand (1992) used this technique to improve land cover classification by combining, as two additional bands, soil texture data and topographic position data, with Landsat thematic mapper image. The second approach involves changing the *a priori* probabilities of classes based on either estimated areal composition or on a known relation between the classes and the ancillary data. Although this technique is theoretically sophisticated it requires considerable additional sampling.

Post-classification sorting allows individual pixels to be reclassified based on decision rules derived from the ancillary data. It is quick, simple, easily implemented, and efficient because it needs only to alter 'problem' classes (Harris and Ventura, 1995). It allows several categories of ancillary data to be included at once. It is a technique that is particularly suited to raster images and raster GIS (Hutchinson, 1982). A number of studies have used post-classification sorting to improve classification results. Janssen (1990) found that the inclusion of topographic data improved land use classification accuracy by between 10 to 20 percent for areas within the Netherlands. A matrix overlay analysis was used by Treitz (1992) to combine zoning data with SPOT imagery of the urban fringe of Toronto, Canada and the accuracy was improved by 10 to 12 percent. Golden and Lackey (1992) used topographic data and a post-classification model to identify and correct misclassification of forest tree species in western Oregon and Washington (accuracy was improved by 8 to 14 percent). Artificial intelligence (AI) techniques have also been investigated to integrate geographic information with spatial data (Bolstan and Lillesand, 1992).

6.3 Methodology of the study: The study involves the combination and analysis of Landsat TM data and land use zoning maps (i.e., both agricultural zoning map and city parks zoning map). An outline of the procedures used in this study is presented in Figure

---

[1] Topographic maps are called "quadrangles" because they are bounded by two latitudes and two longitudes, which approximately form a box or quadrangle.

[2] SPOT- Le Systeme Pour 'l Observation de la Terre (French Earth observation system). This satellite captures either 10 m panchromatic or 20m 3 band multispectral imagery.

6.1. Post-classification sorting was selected because of its ease of implementation, its ability to alter only those classes that were 'confused', and its suitability for use with raster data.

Figure-6.1 Flow chart depicting the procedure followed in this study

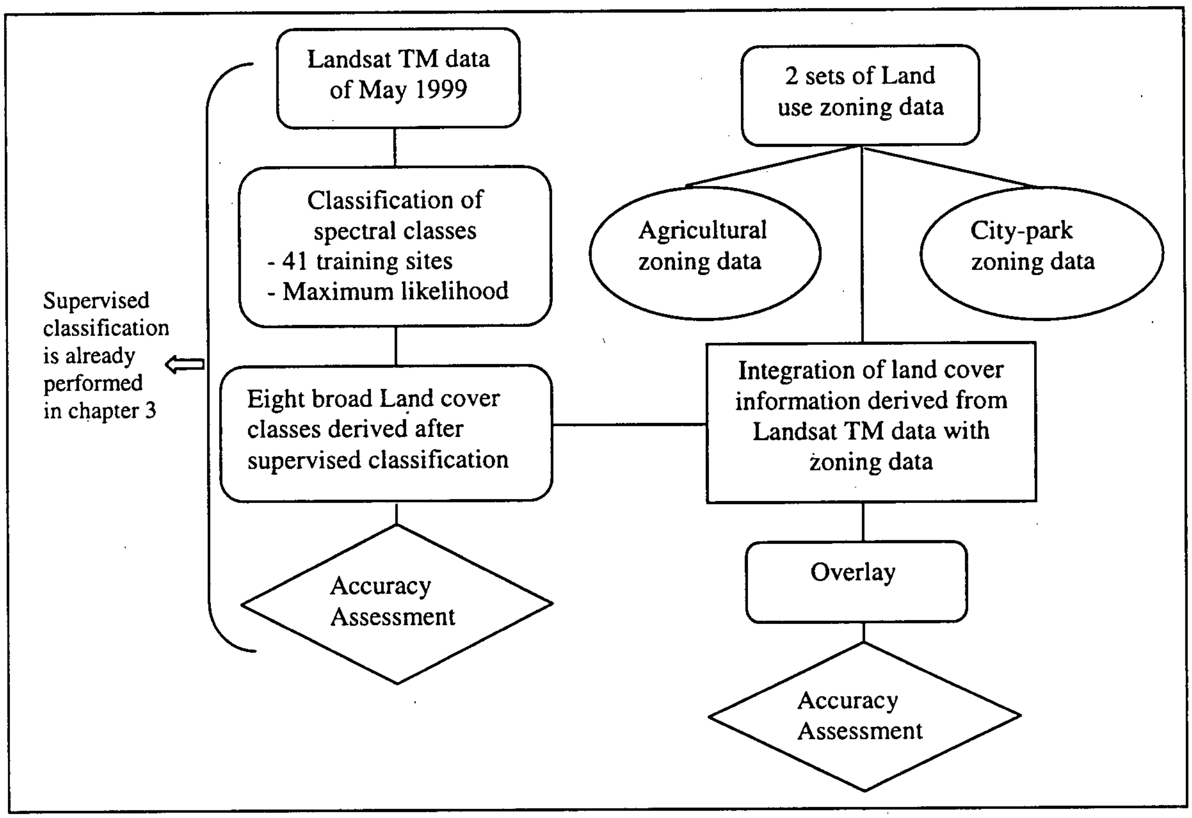

6.3.1 General approach: The objective was to derive a more accurate land cover classification using geographical data from a GIS. The misclassification of pixels caused by spectral confusion may be corrected by providing additional spatial information. The two assumptions for this approach were

- the zoning data are stored in a GIS, and
- the majority of the pixels within each zoning data have been correctly classified

Based on these assumptions, the incorrectly classified pixels (from the land cover classification) that fall within zoning data could be corrected by

- comparing the classified image with zoning data,

- determining the pixels that were misclassified,
- assigning the new label (i.e., corrected label) to the all the pixels that are within the given zoning data.

6.3.2 Data integration: A supervised classification of Landsat data for the study area has produced mixed results (chapter 3). The overall classification accuracy is 71 per cent (see Table 6.1). However, some of the land use classes (e.g., industrial, open space and agricultural classes) are very poorly classified. There is confusion between the commercial and the industrial classes. More than one third of the total agricultural pixels (omission error for agriculture class is 39 percent, table 6.1) are misclassified either as open space or residential. In an attempt to improve the results of the classification, ancillary data, in the form of agricultural and city park zoning data[3] (Figure 6.2), are combined with the classified data. Both data sets are in raster form. Post-classification sorting can be performed using any classified image (classified by either supervised or unsupervised approach), however, results from maximum likelihood classifiers were selected as most of the studies (Janssen, 1990; Golden and Lackey, 1992) have reported integrating ancillary data with maximum likelihood classified image.

Table-6.1: Contingency table resulting from supervised classification using maximum likelihood classifiers

Classified land uses	Ground Truth									Accuracy (%)	Commission error (%)	Omission error (%)
	Total	1	2	3	4	5	6	7	8			
1. Agriculture	615	419					29	107	60	61	32	39
2. Commercial	370		291		41				38	77	21	23
3. Extractive	285			272			1	6	6	72	5	28
4. Industrial	131		4		99			13	15	46	24	54
5. Lake	59					54		5		100	8	0
6. Park	478	13		8			425	14	18	86	11	14
7. Open space	493	132	4		33		7	269	48	52	45	48
8. Residential	1475	120	79	98	43		33	99	1003	84	32	16
Total	3906	684	378	378	216	54	495	513	1188			
Overall Kappa = 65 Overall Accuracy = 71%												

[3] Agricultural zoning data (1999) was produced by the Ministry of Agriculture, Food and Fisheries, and the City Park zoning data source was the BC Land Use Coordination Office.

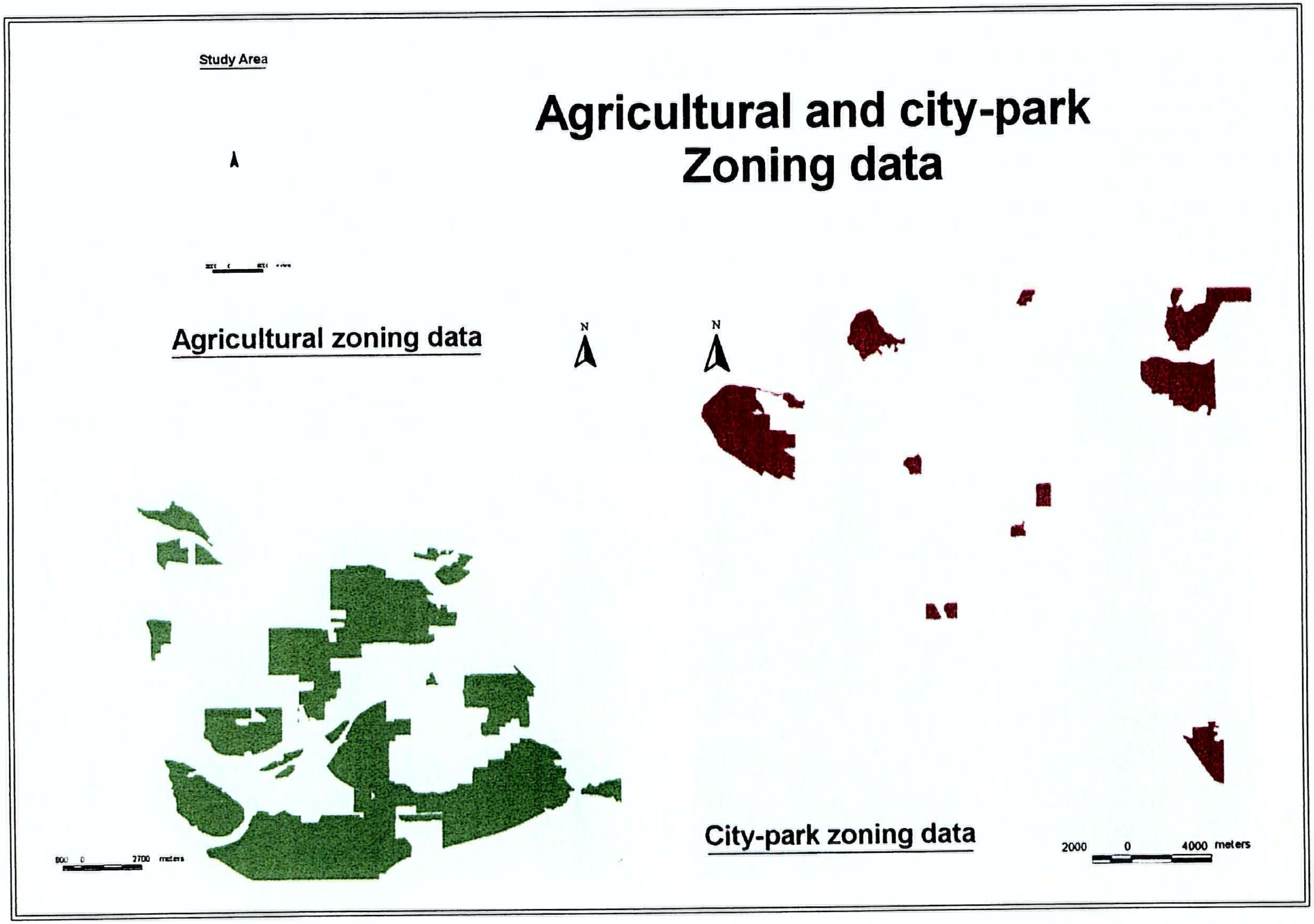
Study Area
Agricultural and city-park
Zoning data
Agricultural zoning data
N
N
2700 meters
City-park zoning data
2000
0
4000 meters

Figure- 6.2

Post-classification sorting of the land cover classes is performed using the overlay GIS modeling capabilities of IDRISI. An overlay module allows the analyst to select only those class combinations, arising through the combination of the source data sets, that are relevant to the study (Treitz *et al.*, 1992) using set rules.

Where confusion between two classes exists, rules are used to separate classes with significant overlap. As already mentioned, a significant number of pixels belonging to agricultural areas were misclassified either as open space or residential areas. However, within the ALR (Agricultural Land Reserve) of BC, residential, commercial or industrial (except industries related to agricultural products, e.g., food processing industries) developments are not permitted[4]. Zoning data enabled me to reduced this confusion between spectrally similar agricultural fallow lands, open fields, and some of the residential areas through enforcement of this rule: '*if the zoning is agriculture and the classification is open space or residential, then re-code as agriculture*'. Similarly, confusions were observed between park and open space areas. This rule - '*if zoning is park and the classification open space, then re-code as park*'- was used to identify such misclassified park areas.

The accuracy of the final output was measured by comparing the classified map with 434 ground truth sites and the results are presented in table 6.2.

6.4 Results and discussions: The integration of the zoning data with the supervised classification of Landsat TM imagery improved the accuracy of the classification. The overall classification accuracy was increased by eleven percent (from 71 percent to 82 percent) (Table 6.2) even though only 27 percent of the pixels were subject to modification. The confusion between classes that were cross-classified in the image (e.g., open space, agricultural, residential areas) was generally reduced considerably (Figure 6.3).

[4] Farm Practices Protection (Right to Farm) Act, Planning for agriculture, Ministry of Agriculture and Food, 2000.

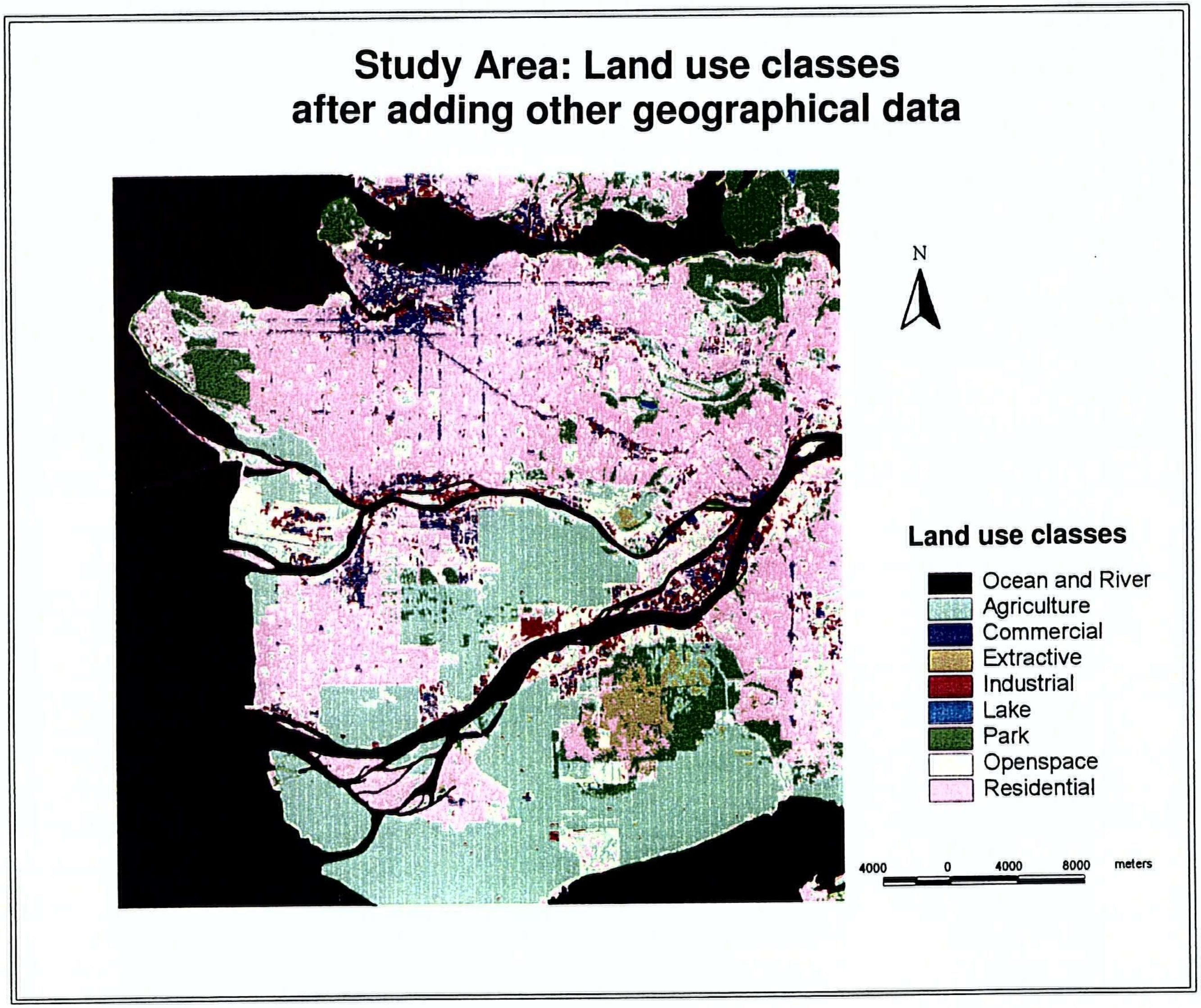
Study Area: Land use classes
after adding other geographical data
N
Land use classes
Ocean and River
Agriculture
Commercial
Extractive
Industrial
Lake
Park
Openspace
Residential
4000
0
4000
8000
meters

Figure- 6.3

The assumption that agriculture and city park zoning data would improve the classification accuracy of agriculture, open space and park classes is supported by this study. The accuracy level for the agricultural class was increased from 61 percent (maximum likelihood classifiers) to 95 percent after adding agricultural zoning data to the classified image. This also helped to increase accuracy for the open space class, as the number of misclassified pixels belonging to open space was also reduced. The inclusion of city park zoning data improved the accuracy of the park class from 86 percent to 90 percent; however, misclassifications remained between park and residential land cover. This is understandable because spectral characteristics of trees in park areas and residential areas are identical.

Table-6.2: Contingency table resulting from modification of supervised Landsat TM classification with zoning information (eight land cover classes)

Classified land uses	Ground Truth									Accuracy (%)	Commission error (%)	Omission error (%)
	Total	1	2	3	4	5	6	7	8			
1. Agriculture	690	649					9	17	15	**95***	6	5
2. Commercial	370		291		41				38	77	21	23
3. Extractive	285			272			1	6	6	72	5	28
4. Industrial	131		4		99			13	15	46	24	54
5. Lake	59					54		5		100	9	0
6. Park	498	13		8			445	14	18	**90***	11	10
7. Open space	463	12	4		33		7	359	48	70	22	30
8. Residential	1410	10	79	98	43		33	99	1048	89	26	11
Total	3906	684	378	378	216	54	495	513	1188			
Overall Kappa = 74%, Overall Accuracy = 82%												

* Agricultural and park zoning data used for post-classification processing

Misclassifications were observed between industrial and commercial land covers due to their spectral similarity. Inclusion of commercial or industrial zoning data would help to reduce the overlap between these two classes with the rule *if the zoning is commercial and the classification industrial, then recode as commercial.* However, this rule was not tested in this study. In this chapter only two rules were applied to a limited subset of the data and the classification results were improved by 11 percent, the improvement in accuracy could be greater if rules for all the classes are applied.

6.5 Conclusion: The use of ancillary spatial information to improve an urban land cover classification (using supervised method) has been demonstrated in this study. The overlay analysis technique is a convenient method for combining land cover and additional information from two separate data sets. In fact, this chapter shows that combining data from a variety of sources can actually enhance the accuracy level of land use classification. However, the sensitivity of post-classification sorting is dependent on the accuracy level of zoning data, since inaccurate zoning data may decrease the over all classification accuracy.

This technique for classification improvement requires that the analyst have a detailed understanding of the study area, the land cover classes of interest and their relation with ancillary data, before attempting to improve the classification. The general process of developing rules depends on the kind of ancillary data available. Some information about misclassification of land cover classes, such as commission and omission errors from error matrix, will be useful in developing rules.

CHAPTER VII

A brief discussion on contextual information to improve land cover classification in the study area

7.1 Introduction: Satellite images always contain three types of information: Firstly, spectral information resulting from the interaction between the electromagnetic spectrum and the materials that can be found on the earth's surface. Secondly, temporal information derived from the satellite's revolution around its orbit, which allows one to study the evolution of the spectral signatures of the earth's surface and to monitor their temporal changes. However, a single image does not provide temporal information, only sequences of images do. Thirdly, spatial information that represents the spatial organization of pixels that make up the image obtained by the sensor.

The first two types of information have been used most frequently in traditional image processing techniques (such as supervised and unsupervised classification). Spatial information has not been employed by most of the image processing classifiers based on pixel-by pixel strategies. A disadvantage of pixel-by-pixel classifications is that the imagery's valuable spatial information (i.e., the possible relations that may exist between one pixel and its neighbour) is ignored.

The spatial structure of images is an indication of the relation between the environment and the spatial resolution of the sensor (Stuckens *et al.*, 2000). If the spatial resolution (i.e., pixel size) of an image is considerably finer or smaller than the objects in the scene, most of the pixels of the image will be highly correlated with their neighbours[1] (Kartikeyan *et al.*, 1994; Alonso and Soria, 1991). In other words, due to the spatial

[1] For example, if (i,j) and (m,n) are two neighbouring pixels and if (i.j) belongs to class k then there is a high probability that (m,n) also belongs to the same class. The decision that a pixel belong to a certain class therefore is taken based not only on the observation X_{ij} at (i.j) but also on all X_{mn} where (m,n) is a neighbour of (I,j).

autocorrelation[2] the knowledge that a pixel belongs to a certain class increases the chances that its neighbouring pixels belong to the same class (Stuckens *et al.*, 2000). The main reason for not using the spatial information is that the spectral information can easily be analysed pixel by pixel whereas the spatial information normally uses several pixels during the computational process and the application of complex mathematical techniques. While traditional classification methods ignore this information, contextual classifiers specifically try to incorporate this information during the classification process.

A number of studies have used contextual classification techniques to improve urban land cover classification accuracy. Alonso and Soria (1991) used contextual information jointly with spectral information to improve urban land use classification of satellite images in central Spain. Classification accuracy was improved by 10 percent. A contextual model (based on compound decision theory) was used by Swain *et al.* (1991) to test the effectiveness of contextual classifiers in the southeast part of Indiana. A significant improvement in classification accuracy was observed both for urban and agricultural areas. Fuller and Jones (1996) found that the inclusion of contextual techniques improved land cover classification accuracy by between 4 and 7 percent for areas within the Great Britain. However, classification accuracies do not necessarily improve dramatically. Thunnissen *et al.* (1992), for example, report an improvement of only 2 percent compared to a pure per-pixel classifier.

7.2 Methodology of the study: Contextual classifiers consider simultaneously the spectral and spatial characteristics of the images to achieve more accurate classification results. One way of incorporating spatial information into the classification strategy is to hypothesize that the ground cover associated with a given pixel (i.e., its 'class') is not independent of the classes of its neighbouring pixels. Therefore, it is more likely that

[2] Spatial autocorrelation tests whether the observed value of a variable at one locality is independent of the values of the variable at neighbouring localities. If dependence exists, the variable is said to exhibit spatial autocorrelation.

more often wheat grows in the neighbourhood of a barley-growing region than in the middle of a high-density urban area.

PCI image processing software (version 6.3) was used to perform a contextual classification of the study area. The frequency-based contextual classification programmes (proposed by Gong and Howarth, 1992) of PCI perform multispectral image classification based on training sites and using a moving window. This is distinct from post classification smoothing using a modal filter (chapter 4), which is generally needed to weed out areas that are too small to be useful units of land cover classification. In post-classification smoothing 3 x 3 modal filters are used to reduce the speckly appearance of classified image. In contextual classification, contextual information is extracted from the pixel's immediate neighbours by imposing a search window and by computing a contextual parameter within that window based on both spectral and spatial information. That value is then assigned to the original pixel (Stuckens *et al.*, 2000). Although a 3 x 3 window (i.e., 3 x 3 pixel kernel) is the most commonly used moving window, this size can be changed. For images with complex class patterns (such as in urban areas), or large land cover entities, the window size should be larger (Hodgson, 1998). On the other hand the standard windows size (i.e., 3 x 3) is appropriate for images with homogeneous class pattern or with less complexity. Contextual classifiers are usually better suited for complex land use classification and are more computationally efficient than most other classifiers.

Contextual classification is performed in two different steps:

- REDUCE creates a grey level vector reduction image based on sampling a set of input bands under a user-specified window or bitmap (MASK). When a pixel window of a given size is moved all over an image(s), one can generate a frequency table for each pixel in the image(s), except for those pixels close to the image boundary. The frequency is defined as the number of times a pixel value, say 'v', occurs in a specified pixel window. For a single-band image, 'v' represents a grey level and for multi-band images a grey-level vector. The number of frequencies in a frequency table increases linearly as the number of grey levels in an image increases, and exponentially as the number of spectral bands increases. For a single-band image quantized into 'n' grey levels, one can produce grey-level frequency tables with a maximum number of 'n' frequencies in each table, however, the maximum number of frequencies in a frequency table will increase to n^m when 'm' spectral bands having the same number of grey levels are used. It requires a large amount of random access memory (RAM) in a computer to handle the n^m frequencies. For this reason, the number of grey-level vectors in multi-band image has to be reduced. The REDUCE program uses the algorithm described by Gong and Howarth (1992). The output grey level vector reduction image is used in the next step to perform a supervised classification of multispectral imagery, using user-specified training sites.

- CONTEXT inputs the grey level vector reduction image (must be 8-bit bands) created by the REDUCE program, and a set of training sites (these are the same training sites used in supervised classification), and creates a classification image under the specified output window. Each input training site can be assigned a unique output class value for the classification image. The contextual classifier uses a pixel window of specified size around each pixel.

The success of the frequency-based contextual classification (proposed by Gong and Howarth, 1992) depends heavily upon use of an appropriate moving window size (i.e., the pixel window size when performing contextual classification on each pixel). The contextual classifiers of PCI software offer a variety of odd-integer moving window sizes between 3 and 21. If the window size is too small, sufficient spatial information cannot be extracted to characterize a land use type. If the window size is too large, much spatial information from other land covers will be included. In general, contextual classification performs better when specifying a larger window size, especially if the original input image contains complicated mixed classes (such as residential, commercial or industrial areas). However, frequency-based contextual classifiers cannot classify pixels along the

Figure-7.1: Contextual classification scheme

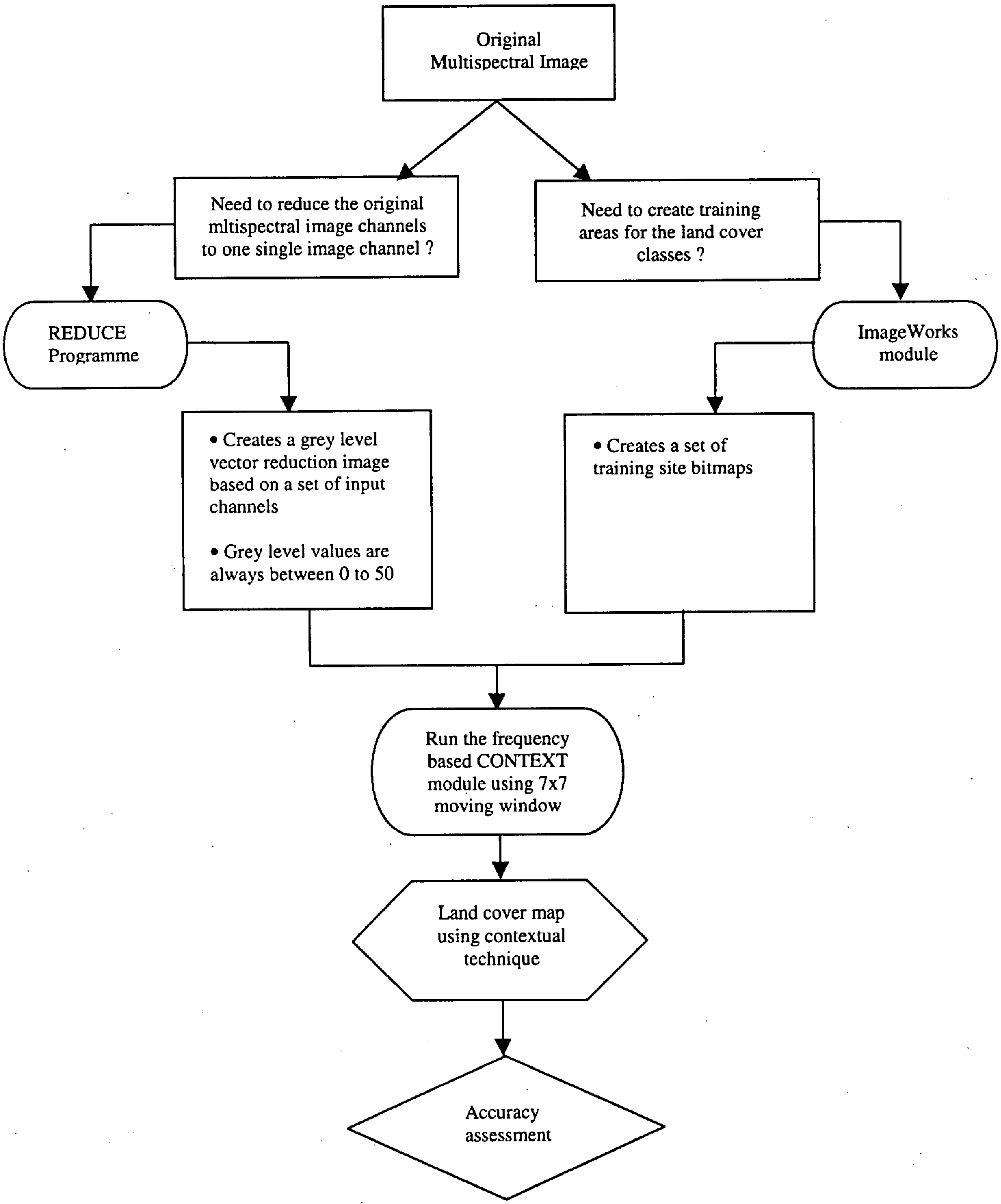

edges of the image [the edge width is calculated using this formula: (Pixel Window Size – 1)/2][3]. As a result, the output pixels along the edge are set to zero to indicate unclassified or unknown pixels. Otherwise, these edge pixels are not changed.

The window size for this study was selected based on an examination of the results of several trials, using a range of window sizes from 3 x 3, 5 x 5, 7 x 7, 9 x 9 and 11 x 11. The 3 x 3 and 5 x 5 windows were appropriate for the agricultural, the park and the extractive classes, however, the urban classes were not clearly distinguishable from one other. The larger window sizes (i.e. 9 x 9 and 11 x 11) were able to extract the urban classes (i.e., residential, commercial and industrial areas) more efficiently than the 3 x 3 and 5 x 5 windows, however, the homogeneous areas (i.e., agricultural areas, parks, extractive areas) were not classified well. Generally, larger window sizes are recommended for the urban areas, however, pixel window sizes larger than 11 x 11 were not examined in this study as they include too much adjacent information from other land cover classes. As the study area comprises both urban and non-urban land uses, the pixel window size used for this study is set to 7 x 7 considering the efficient information extraction for both urban and non urban classes and assuring a small proportion of boundary pixels. As the pixel window size was set to 7, the output classified image contains zeroes for (7-1)/2 = 3 pixels along the border of the image, since these pixels cannot be classified. Figure 7.1 presents an outline of the contextual classification scheme.

7.3 Results and discussion: Table 7.1 represents the accuracy of the classification performed on the Landsat image, using a contextual classifier. The overall classification accuracy is 85 percent. All land use classes except for the open space class present more than 80 percent classification accuracy. A fairly large number of pixels belonging to the

[3] For example: If the window size is set to 21 the output classified image contains zeroes for (21-1)/2 = 10 pixels along the border of the image which cannot be classified. Whereas, if the window size is set to 3, the output classified image contains zeroes for (3-1)/2 = 1 pixels along the border of the image which cannot be classified

open space class have been mis-classified as residential and agricultural classes (table 3.3, figure 3.10). The resulting contextual-classification map is shown in figure-7.2. It can be seen from both table 7.1 and figure 7.2 that the integration of both spectral and spatial informations during classification has reduced the confusion between the commercial and the industrial classes.

As mentioned at the beginning of this chapter, the classification accuracy obtained from the classification of satellite images using pixel-by-pixel conventional methods can be improved if the contextual information is included for the purposes of classification. Here, a comparison has been made between these two types of classification techniques (maximum-likelihood classification and contextual classification) and the final outcome from contextual classification.

Table-7.1: Contingency table resulting from contextual classification of Landsat TM image

Classified land uses	Ground Truth									Accuracy (%)	Commission error (%)	Omission error (%)
	Total	1	2	3	4	5	6	7	8			
1. Agriculture	685	596	4		1		4	56	24	87	13	13
2. Commercial	432	22	314		24		3	33	36	83	27	17
3. Extractive	317	1		303			4	3	6	80	4	20
4. Industrial	192	4	3		176			9		81	8	19
5. Lake	56					54	2			100	4	0
6. Park	482	9	2	5			450	12	4	91	7	9
7. Open space	442	28	12		6		6	354	36	69	20	31
8. Residential	1300	24	43	70	9		26	46	1082	91	17	9
Total	3906	684	378	378	216	54	495	513	1188			
Overall Kappa = 77% Overall Accuracy = 85%												

In chapter three, the result of supervised classification (using maximum-likelihood classifier) was discussed in great detail. From figure 3.6 (from chapter three) it can be seen that all the urban land use classes are inter-mixed. In agricultural areas, field boundaries have been classified into urban land use classes by the MCL. The entire map looks rather fragmented. The greatest confusion was between industrial and commercial classes, and among agricultural, park, golf course and open spaces. Because of their spectral similarity, the industrial class was mixed up with the commercial class. The open space class had been partly allocated to the agricultural, residential, industrial and park

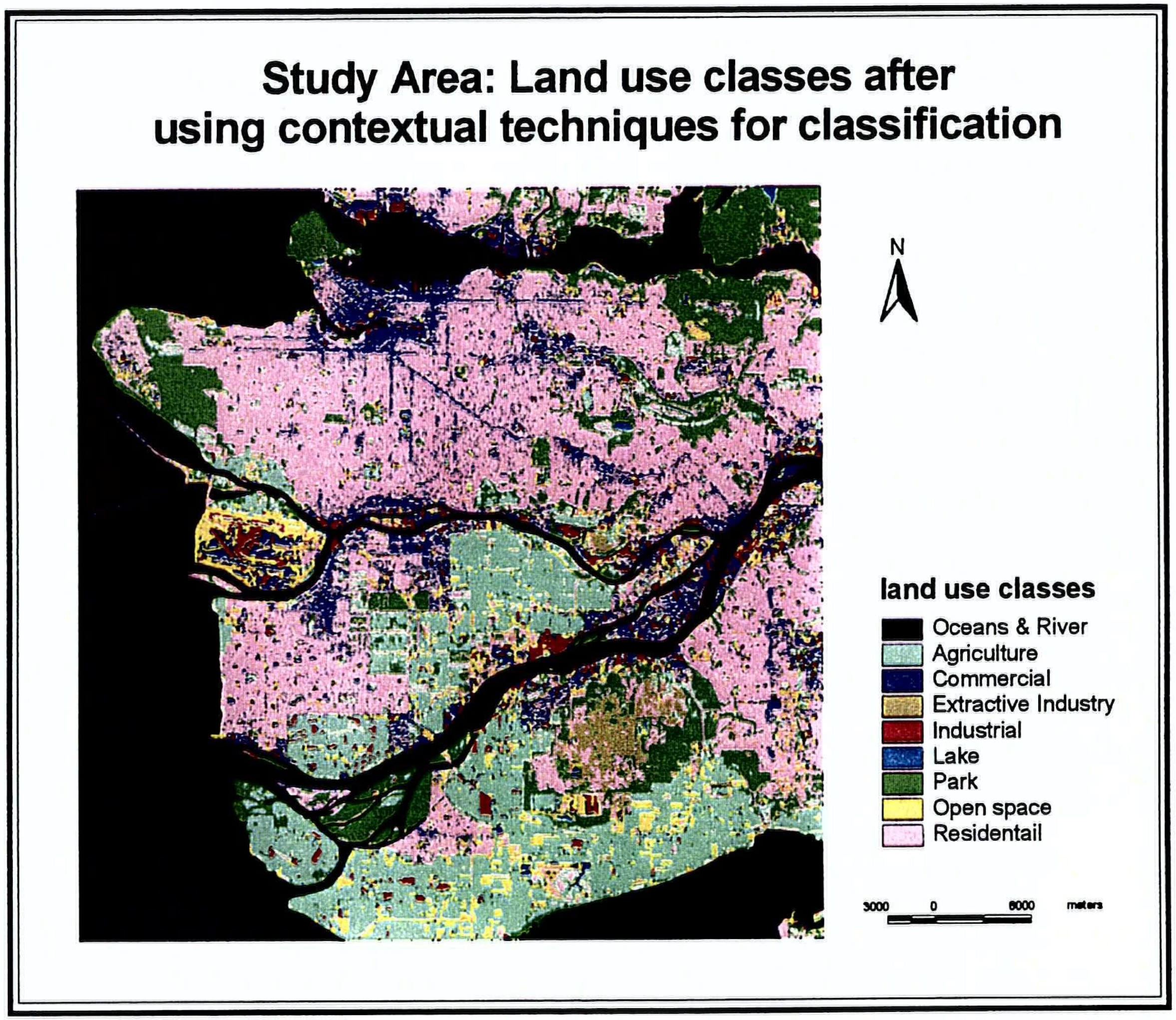
Study Area: Land use classes after
using contextual techniques for classification
N
land use classes
Oceans & River
Agriculture
Commercial
Extractive Industry
Industrial
Lake
Park
Open space
Residentail
3000
0
6000
meters

Figure-7.2

classes. The overall accuracy for supervised classification was 71 % (overall kappa was 0.65) (table-7.2).

Table-7.2: Contingency table resulting from supervised classification of Landsat TM image, using maximum-likelihood classifier.

Classified land uses	Ground Truth									Accuracy (%)	Commission error (%)	Omission error (%)
	Total	1	2	3	4	5	6	7	8			
1. Agriculture	615	419					29	107	60	61	32	39
2. Commercial	370		219		41				38	77	21	23
3. Extractive	285			272			1	6	6	72	5	28
4. Industrial	131		4		99			13	15	46	24	54
5. Lake	59					54		5		100	8	0
6. Park	478	13		8			425	14	18	86	11	14
7. Open space	493	132	4		33		7	269	48	52	45	48
8. Residential	1475	120	79	98	43		33	99	1003	84	32	16
Total	3906	684	378	378	216	54	495	513	1188			
Overall Kappa = 65% Overall Accuracy = 71%												

It can be seen from table 7.1 that the overall kappa for frequency-based contextual classification has increased to 0.77 and the overall accuracy has increased to 85 percent. Confusion between commercial and industrial land uses is substantially reduced. It was anticipated that the use of a contextual classifier would reduce the confusion in the open space class. However, just the opposite effect was observed. Although the use of a contextual classifier has produced significant improvement for most of the classes, misclassifications of open spaces have increased. Inspection of the aerial photography in areas of misclassification indicates that it was probably the size of the open spaces that played a key role, while looking at the neighbouring pixels in a 7 x 7 moving window. It can be seen in figure 7.2 that the land cover classes appear to be homogeneous. The differences between this map and the one obtained by the MCL (figure 3.6 in chapter three) are readily apparent. The 'pepper and salt' effect of figure 3.6 has been reduced dramatically. Confusion between urban and non-urban classes has been reduced. Industrial areas were classified without too much assignment of pixels to commercial and residential classes.

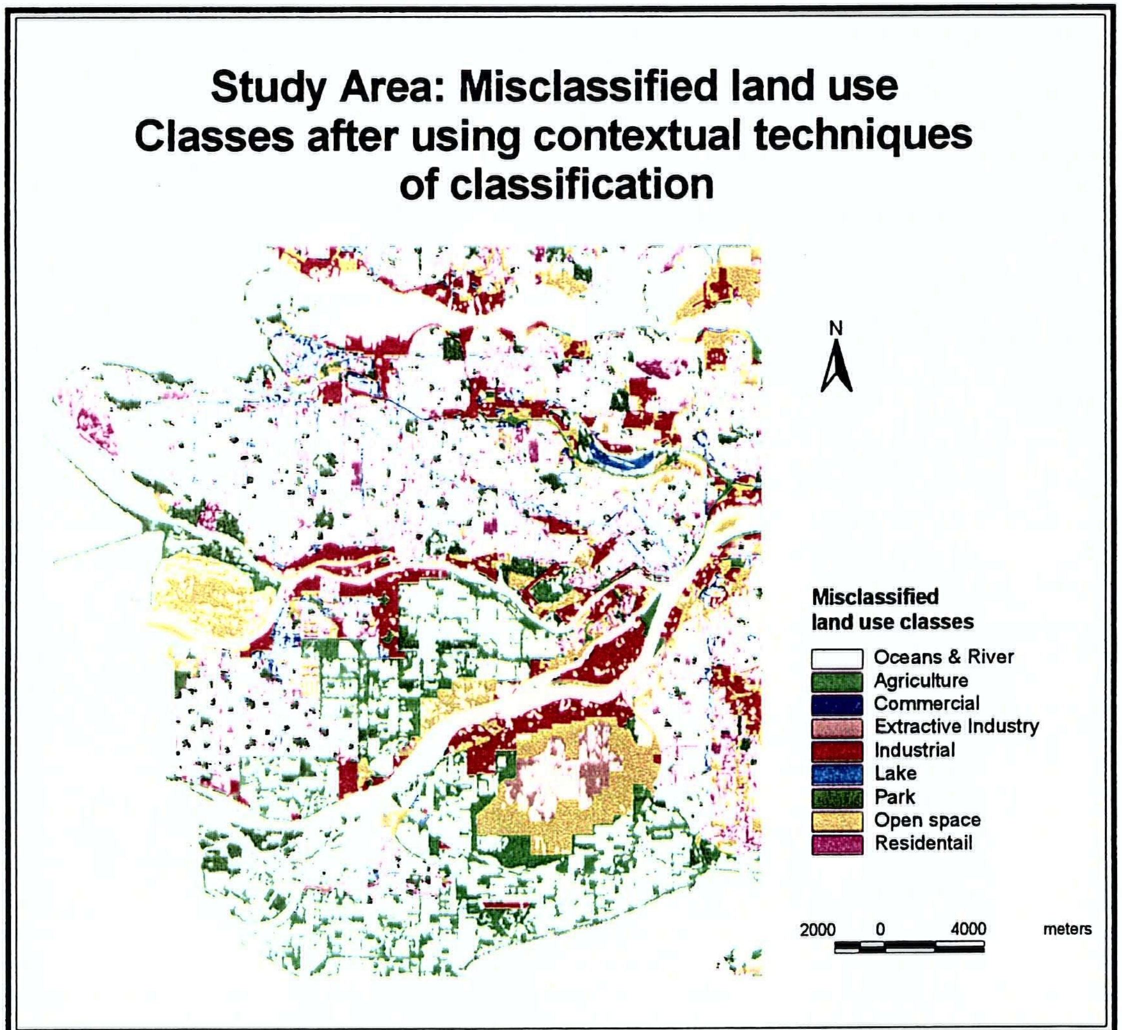
Study Area: Misclassified land use
Classes after using contextual techniques
of classification
N
Misclassified
land use classes
Oceans & River
Agriculture
Commercial
Extractive Industry
Industrial
Lake
Park
Open space
Residentail
2000
0
4000
meters

Figure-7.3

Figure 7.3 presents an overall idea of the misclassified pixels of different land use classes and their distribution over the study area. It can be seen from this map that the number of misclassified pixels has been reduced for almost every land use class. The open space is the only class in which the number of mis-classified pixels has increased.

7.4 Conclusion: In conclusion, the general objective of this chapter (that is to improve land use classification accuracies) has been achieved. In general, the frequency-based contextual classification methods are particularly effective in identifying spatial heterogeneous land use classes. This fact was observed in different urban landscapes of the study area. Frequency-based contextual classification has significantly improved the land use classification results when compared with the supervised classification results. It is important to note that, although contextual information has substantial value in urban land use classification, use of appropriate contextual classifiers is primarily dependent upon the analyst's knowledge of the spatial relationships actually existing on the ground.

CHAPTER VIII

Conclusions and Recommendations

8.1 A brief summary of the study: This study reviews three basic land cover\land use classification approaches. These approaches are: (1) supervised classification, (2) unsupervised classification, and (3) post-classification processing. These three approaches are divided into five sub groups (see figure 2.1 in chapter 2). Thus, eight different classification methods for the Vancouver metropolitan area have been evaluated and a land use map of the study area has been generated from the most suitable and accurate classification result.

This study begins by examining two traditional methods of land cover classification: unsupervised and supervised classifications. These two methods are solely based on spectral similarity or dissimilarity measures. Between these two traditional methods, the unsupervised classification approach allows the computer to group image data into spectrally similar land cover classes without any prior knowledge of the study area. These classes are spectral classes, but not information classes; thus the analyst needs to reclassify spectral classes into information classes. The supervised classification, on the other hand, produces information classes by identifying samples of known identity based on the analyst's knowledge of the study area. These samples of known identity are called *training sites* and are used to train the classifier in what to look for. In supervised classification the information classes are known before the classification process begins. Thus the supervised classification is a decision making process based upon available information. However, both for supervised and unsupervised classifications difficulty was observed in assigning spectral classes to information classes.

There are several techniques (called *classifiers*) for making these decisions. In this study I have used three supervised techniques based on three different decision rules. The three different supervised techniques evaluated in this study are: Maximum-likelihood methods, neural network analysis, and fuzzy classifications. These three techniques are based on spectral reflectances of each pixel; however, they differ in ways of assigning the information classes to each pixel. The maximum-likelihood methods use the mean and variance/covariance of the spectral response patterns of the *training sites* when classifying unknown pixels. The neural networks have an advantage over the maximum-likelihood classifiers in that they are distribution-free[1] and no prior knowledge is needed about the statistical distributions of the classes in order to assign each pixel a particular class. Compared with the maximum-likelihood classifiers, the computation of the neural networks is more complex and needs a lot of training samples to be applied successfully. Thus, the performance of the maximum-likelihood classifiers and the neural networks are more dependent on having representative and pure (i.e., not mixed, two or more land cover classes) *training sites*. In this study, these two supervised classification methods with one-pixel-to-one-class algorithms failed to deal with the association of mixed land cover classes in a single land use (i.e. the *training sites*). Fuzzy classification has been used to deal with this problem using a probability function showing how likely it is that a certain *training sites* fall in given class. The accuracy for homogeneous classes (i.e., agriculture, park and extractive) were increased, however, the accuracy for urban classes were declined comparing with neural networks. Fuzzy logic was not competent to deal with urban classes of the Vancouver metropolitan area.

A basic approach for integrating spatial contextual information with a spectral classifier involves using post-classification techniques. Post-classification techniques are based on spatial autocorrelation. Spatial autocorrelation tests whether the observed value of a variable at one locality is independent of the values of the variable at neighbouring localities. If dependence exists, the variable is said to exhibit spatial autocorrelation. Using modal filters after supervised and unsupervised classification is a naïve implementation of spatial autocorrelation. Classified data (i.e., after supervised and unsupervised classification) often manifest a salt-and-pepper appearance due to the inherent spectral variability encountered by a classification when applied on a pixel-by pixel basis. Modal filtering works as a post-classification smoothing process and is

[1] Compared with the maximum-likelihood classification, the neural networks can handle multispectral spectral data more efficiently even if the data is not normally distributed.

generally needed to weed out areas that are too small to be useful units of land cover classification. The assumption is made that these small areas are mis-classified, for one reason or another, and that they should be blended into adjacent areas.

Image segmentation also uses modal filters, however, it differs from post-classification smoothing. Image segmentation is 'unsupervised' in the sense that it is based entirely on the inherent spectral properties of the image itself, without any significant user input (apart from one or two parameters, such as gradient threshold values). Image segmentation follows two independent steps: identifying edge boundaries based on the rapid transition from one to another region of different brightness or colour value, and applying post-processing modal filtering to the segmented image (derived from edge detection). In case of supervised and unsupervised classification, a 3 by 3 modal filter was used. However, in image segmentation, polygons (with various size) identified by edge detection methods were used as modal filtering windows. Thus, compared with the supervised (using maximum-likelihood classifiers) and unsupervised classifications, the computation of image segmentation is more complex. Image segmentation has performed well for the homogeneous classes.

Post-classification processing can also be performed by integrating ancillary data with remotely sensed imagery. In this study, two sets of zoning data (agricultural and park zoning data) were included which allows individual pixels to be refined based on decision rules derived from the zoning data. This method is simple and efficient because it needs only alter 'problem' classes.

Contextual classification is a combination of two different approaches: supervised classification and post-processing. It is 'supervised' in the sense that it is based on the maximum-likelihood rules. It is 'post-processing approach' in the sense that it is based on the assumption of spatial autocorrelation. However, contextual classification is not a post-processing approach in its true sense, rather it is an integrated approach which considers the spatial information jointly with the spectral information during

Table-8.1: Overall classification results of land use classes for eight selected methods

Land cover classes	Land use classification methods								
	Traditional methods		Post-classification processing			Neural Network Analysis	Fuzzy classification	Image segmentation	Contextual classification
	Supervised classification	Unsupervised classification	Using modal filter		Using ancillary data				
			Supervised classification	Unsupervised classification					
1. Agriculture	61	41	69	45	**95***	73	91	88	87
2. Commercial	77	53	78	62	77	83	55	63	83
3. Extractive	72	59	71	60	72	84	88	85	80
4. Industrial	46	54	45	63	46	73	57	58	81
5. Lake	100	100	100	100	100	100	100	100	100
6. Park	86	83	86	81	**90***	88	91	90	91
7. Open space	52	35	51	31	70	57	71	64	69
8. Residential	84	69	86	68	89	84	80	81	91
Overall Accuracy	**71%**	**59%**	**75%**	**60%**	**82%**	**78%**	**80%**	**79%**	**85%**

* Agricultural and park zoning data used for post-classification processing

classification. Compared with the different classification methods (sub groups of the three basic classification approaches) used in this study, contextual classification is the most sophisticated classification method, which applies complex mathematical techniques to incorporate both spectral and spatial information during the classification process. Contextual classifiers were able to handle both urban and non-urban classes and produced the best classification result for this study.

8.2 Conclusions: The results of eight land cover\land use classification methods are presented in table 8.1. The following conclusions can be drawn from the observed classification results.

1) Conventional classification methods (i.e., supervised and unsupervised classification methods) have been widely used to generate land use maps. However, with the use of high spatial resolution satellite data, spectral heterogeneity, especially in urban areas, poses serious limitations to conventional per-pixel based techniques.
2) After classification (supervised and unsupervised classification), the result usually has a "salt-and-pepper" appearance (isolated and often mis-classified pixels of one category are dispersed within the area of another category). Therefore, a post-classification smoothing is generally needed to weed out areas that are too small to be useful units of land cover classification. The assumption is made that these small areas are mis-classified, for one reason or another, and that they should be blended into adjacent areas. However, the output from post-classification smoothing is generalized and sometimes loses detailed land use information. Post-classification smoothing for supervised and unsupervised classification has improved the accuracy level by 4 percent and 1 percent respectively.
3) Compared with conventional classification methods, the application of artificial neural networks to remote sensing data analysis is still in its infancy. It can be concluded, however, from the study reported here, that neural networks are able to handle multispectral spatial data more efficiently than conventional classification methods. Compared with the conventional per-pixel based

classification techniques, the artificial neural networks approach implemented for this study was 7 percent (table 8.1) more accurate than a traditional maximum likelihood approach.

4) Compared with conventional classification techniques, the fuzzy classification method has improved classification accuracy for non-urban areas (agriculture, open space and extractive lands); however, the result for urban areas is not very satisfactory (table 8.1).
5) The integration of ancillary data with remotely sensed images is particularly useful in situations where the image data alone are insufficient to produce an accurate land cover classification. The inclusion of two sets of zoning data has improved the overall accuracy of study area by 11 percent (compared with the supervised classification result, using maximum-likelihood classifiers) (table 8.1).
6) Compared with post-classification results (for supervised classification), the image segmentation has improved classification accuracy by only 4 percent. However, image segmentation is a more complex and time consuming method than simply running a modal filter after supervised classification.
7) The land cover classification accuracy obtained from the classification of satellite images using one-pixel-to-one-class conventional methods was improved by considering contextual information jointly with the spectral information. The best overall classification accuracies obtained using the eight methods were 85 percent when a contextual classification scheme was used (table 8.1). For this study the contextual classifier proved to be very efficient in terms of urban land cover classification.
8) In this study, water is the only class that was always correctly classified, since it is the only land cover that has only one land use associated with it. All of the other land use classes were misclassified to some extent because of multiple land covers associated with them.
9) Based on the eight land cover/ land use methods tested in this study the most accurate and suitable method for urban land use classification in the Vancouver metropolitan area is the contextual classification technique. A land use map of the study area has been generated using contextual classification (figure 8.1). The

accuracy level of this map is 85 percent. Compared with the 1996 GVRD land use map (table 8.2), this newly generated 1999 land use map is 16 percent more accurate (this improvement is based on the 434 sample sites). The contingency table from the GVRD land use classification was produced comparing with the 434 ground truth sites used in this study.

Table-8.2: Contingency table from GVRD land use classification, 1996

Classified land uses by GVRD	Ground Truth									Accuracy (%)	Commission error (%)	Omission error (%)
	Total	1	2	3	4	5	6	7	8			
1. Agriculture	596	445	1		8		7	38	97	65	25	35
2. Commercial	352		237		76				39	63	33	37
3. Extractive	419	9		333			41	36		88	21	12
4. Industrial	403	33	117		115			135	3	53	71	47
5. Lake	58					54	4			100	7	0
6. Park	499	4	4	9	1		420	13	48	85	16	15
7. Open space	547	183	3	26	13		20	200	102	39	63	61
8. Residential	1032	10	16	10	3		3	91	899	76	13	24
Total	3906	684	378	378	216	54	495	513	1188			

Overall Kappa = 61%
Overall Accuracy = 69%

8.2 Limitations of the Study: Land cover mapping from remotely sensed images, using digital remote sensing techniques, has inherent limitations. No map produced by a computer using digital manipulation of multispectral data is ever 100% correct (Robinove, 1981). By nature, the process of classifying such a broad range of the earth's features into specific and often simplified land cover classes introduces errors. However, these limitations can often be overcome by selecting proper classification algorithms and using statistical analysis to produce acceptably accurate land cover maps.

In retrospect, there are two limitations in this research that should be addressed as a means for improvement or to suggest potential strategies for further study. The first limitation focuses on the ground truth data acquired for accuracy assessment. The process of obtaining the ground truth data using a 1996 land use map of GVRD as a base map (as discussed in Chapter Two, Methodology and database), introduces bias with respect to inaccuracies in the land use map itself (table 8.2). However, the 1996 land use map was used only for stratifying the random sampling for the eight land cover classes, not for the

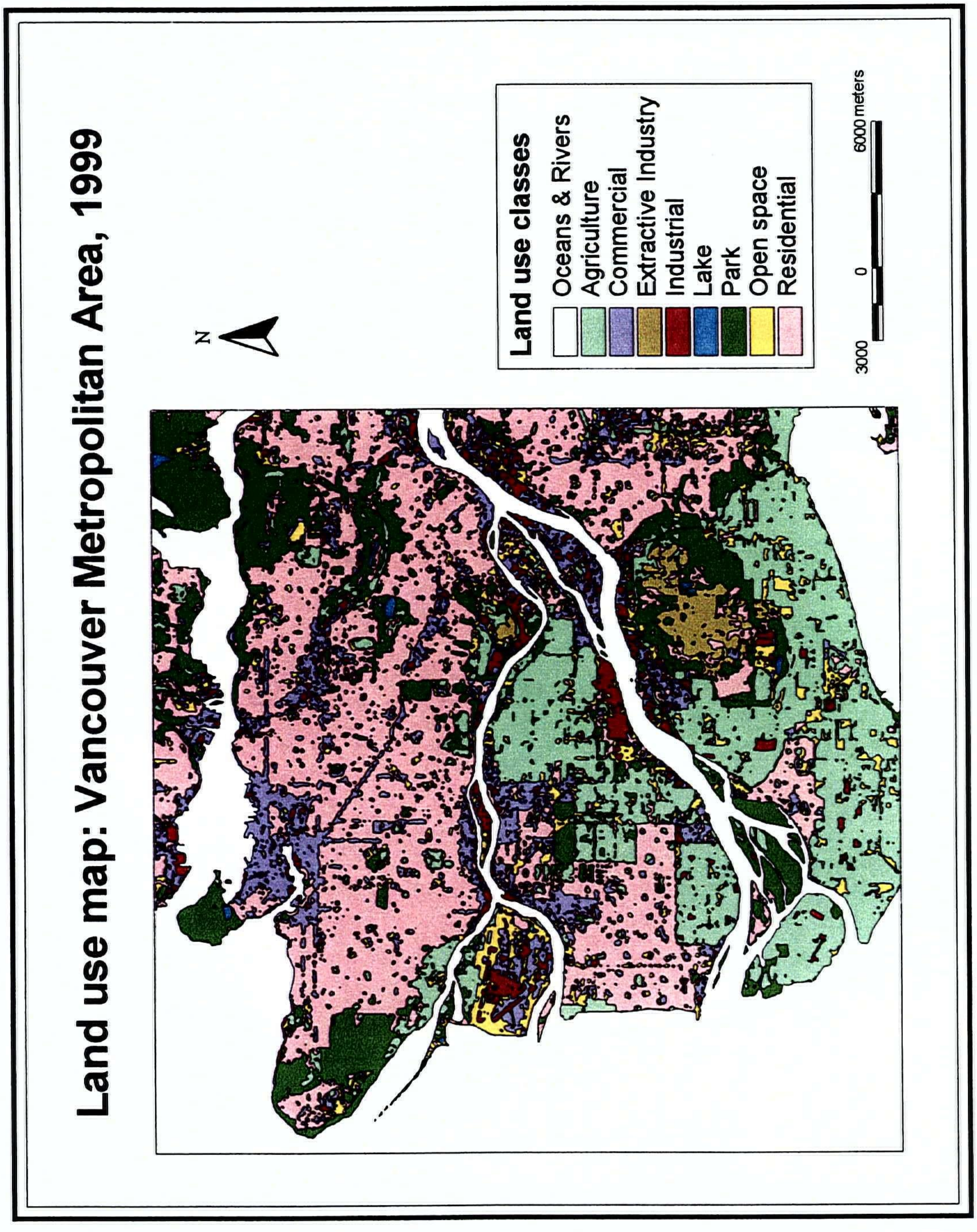

Land use map: Vancouver Metropolitan Area, 1999
N
Land use classes
Oceans & Rivers
Agriculture
Commercial
Extractive Industry
Industrial
Lake
Park
Open space
Residential
3000
0
6000 meters

Figure 8.1

ground verification itself; however, it is important to mention. One additional bias of the data utilized for ground truth is inconsistency with respect to number of the industrial and the lake ground truth sites as compared with the other land cover ground truth points. This issue has been previously addressed in Chapter Two, Methodology and database.

8.3 Recommendations for further study: There are possibilities for further study in this research, and the land use maps and contingency tables yielded by this study offer potential for further analysis.

In this study the choice of eight land use classes has significant impact on the classification results. Misclassifications have been observed between three vegetation classes (e.g., agriculture, extractive, and park) due to their spectral similarity, regardless of the classification techniques. A potential solution for this problem could be to combine the agriculture, the extractive, and the park class into one information class called 'vegetation'.

If the within-class variation of urban land cover classes is greater than the between-class variation, then it will not be possible to identify and to distinguish different urban land cover classes on the basis of spectral measures alone. Selective and successive masking of wide-coverage classes like agriculture, park or open space could be applied before classification in order to focus the discrimination process on difficult/complex land cover classes to improve classification accuracy.

The success of the contextual classification depends largely on the appropriate moving window size. If the study area includes both urban and non-urban land cover classes, a constant window size may not be able to extract sufficient spatial information for both urban and non-urban areas. Instead, a variable window size for urban and non-urban land cover classes can be used after masking out urban or non-urban areas. For example, a larger window size can be selected for areas with complex class patterns, such as in urban areas. However, for the non-urban areas (such as agricultural, park, extractive lands) a small window size can suffice.

The inclusion of ancillary data for classification improvement requires that the analyst have a detailed understanding of the land cover classes of interest and their relationship with ancillary data before attempting to improve the classification. The eight fuzzy land use layers could be used as a source of contextual knowledge before inclusion of spatial information with spectral classes.

Table-8.3: Recommended methods for eight land use classes based on the land use classification result

Methods	Land use classes							
	Agriculture	Commercial	Extractive industry	Industrial	Lake	Park	Open space	Residential
Supervised					√			
Unsupervised					√			
Modal filtering (supervised)					√			
Modal filtering (unsupervised)					√			
Neural network		√			√			
Fuzzy			√		√	√	√	
Segmentation					√			
Using ancillary data	√				√			
Contextual		√		√	√			√

Given the complexities involved in the various methods tested in this study, a combination of methods is recommended as for use by planners not trained in remote sensing. Table 8.3 presents a list of recommended methods based on the different interests (e.g., urban encroachment) of planners. For an urban planner, who is primarily concerned with urban encroachment/expansion, contextual classification would be the best choice. However, for agricultural analysis, integration of agricultural zoning data with the classified image would provide better results. If the person were an expert in remote sensing I would suggest using multi-temporal (at least two different dates in a year) satellite images for agricultural land cover analysis as some agricultural land covers are more easily discriminated during one season of the year than the other; in case of urban areas a combination of fuzzy logic with contextual classifier would be a possible option.

In conclusion, there is a need to move beyond simply mapping the physical form of urban areas, to provide indicators of their social and economic functioning. This is far from straightforward, since many of the functional properties that are of interest to urban planners - such as land use and population density - cannot be observed directly by means of remote sensing. A more complex chain of inference is required, one that incorporates ancillary spatial data and that examines the spatial and structural properties of urban areas represented in the digital image, not just their spectral characteristics.

The communication between urban and regional planners and remote sensing specialist must be improved, so that the former understand the full potential and limitations of remote sensing, while the latter can design improved satellite data-processing techniques based on the needs of urban and regional planners.

BIBLIOGRAPHY

Alford, M.P. Tuley, E. Hailstone, and J. Hailstone, (1974), "The measurement and mapping land resource data by point sampling on aerial photographs", in *Environmental Remote Sensing*, E.C. Barrett and L.F. Curtis (eds), pp. 113-126, London: Edward Arnold.

Alosno, F. G., and S. L. Soria, (1991), "Using contextual information to improve land use classification of satellite images in central Spain", *International Journal of Remote Sensing*, Vol. 12, No. 11, pp. 2227-2235.

Alpin P., P. M. Atkinson and P. J. Curran, (1999), "Fine spatial resolution simulated satellite sensor imagery for land cover mapping in the United Kingdom", *Remote sensing of Environment*, Vol. 68, pp. 206-216.

Argialas D.P. and C.A. Harlow, (1990), "Computational image interpretation models: an overview and perspective", *Photogrammetric Engineering & Remote Sensing*, Vol. 56, No. 6, pp. 871-886.

Ball, G.H., and D.J. Hall, (1965), *A Novel Method of Data Analysis and Pattern Classification*, Stanford Research Institute, Menlo Park, California.

Barbosa, P.M., Casterad, M.A. and J. Herrero, (1996), "Performance of several Landsat 5 Thematic Mapper (TM) image classification methods for crop extent estimates in an irrigation district", *International Journal of Remote Sensing*, Vol. 17, No.18, pp. 3665-3674.

Barnsley M.J and S. L. Barr, (1996), "Inferring urban land use from satellite sensor images using Kernel-based spatial reclassification", *Photogrammetric Engineering & Remote Sensing*, Vol. 62, No. 8, August, pp. 949-958.

Barnsley M.J., G.J. Sadler and J.S. Shepherd, (1989), "Spatial re-classification of remotely sensed images for urban land use monitoring", *Proceedings of Spatial Data 2000*, Oxford, 17-20 September, Remote Sensing Society, Nottingham, pp. 106-117.

Barnsley M.J., S.L. Barr and G.J. Sadler, (1991), "Spatial re-classification of remotely sensed images for urban land use monitoring", *Proceedings of Spatial Data 2000*, Oxford, 17-20 September, Remote Sensing Society, Nottingham, pp. 106-117.

Barr S. and Barnsley M., (2000), "Reducing structural clutter in land cover classifications of high spatial resolution remotely-sensed images for urban land use mapping", *Computers and Geosciences*, Vol. 26, pp. 433-449.

Benie, G.B., and K.P.B. Thomson, (1992), "Hierarchical image segmentation using local and adaptive similarity rule", *International Journal of Remote Sensing*, Vol. 13, No. 8, pp. 1559-1570.

Berlin, G. L., (1971), "Application of aerial photographs and remote sensing imagery to urban research and study", *Exchange Bibliography No. 222*, Council of Planning Libraries, Monticello, Illinois, pp. 65.

Bezdek, J. C., R. Ehrlich, and W. Full, (1984), "FCM: the fuzzy c-mean clustering algorithm", *Computers and Geoscience*, Vol. 10, pp.191-203.

Bischof, H., W. Schneider, and A.J. Pinz, (1992), "Multispectral classification of landsat-images using neural networks", *IEEE, Transactions on Geosciences and Remote Sensing*, Vol. 30, No. 3, pp. 482-490.

Booth, D. J., and Oldfield, R. B., (1989), "A comparison of classification algorithms in terms of speed and accuracy after the application of a post-classification model filter", *International Journal of Remote Sensing*, Vol. 10, No. 7, pp.1271-1276.

Burrough, P.A. and R.A McDonnell, (1998), *Principles of Geographical Information Systems*, Oxford University Press.

Campbell, James B., (1996), *Introduction to Remote Sensing*, The Guilford Press, New York, London.

Cervero, R., (1989), *America's Urban Centers: A Study of the Land Use Transportation Link,* Unwin Hyman, Boston, Massachusetts.

Cihlar, J., (2000), "Land cover mapping of large areas from satellite: status and research priorities", *International Journal of Remote Sensing*, Vol. 21, No. 6 & 7, pp. 1093-1114.

Civco, D. L. and Y. Wang, (1994), "Classification of multispectral, multitemporal, multisource spatial data using artificial neural networks", ASPRS/ACSM.

Civco, Daniel L, (1993), "Artificial neural networks for land cover classification and mapping", *International Journal of Geographical Information Systems*, Vol. 7, No. 2, pp. 173-186.

Conese, C. and F. Maselli, (1991), "Use of multi-temporal information to improve classification performance of TM scenes in complex terrain", *ISPRS Journal of Photogrammetry and Remote Sensing*, Vol. 46, No. 4, pp. 187-197.

Congalton, R.G., (1996), "Quantifying spatial uncertainty in natural resources: theory and applications for GIS and remote sensing", *International Symposium on Spatial Accuracy Assessment in Natural Resources and Environmental Sciences*, Fort Collins, Colorado, USA.

Dueker, K. J. and F. E. Horton, (1971), "Urban change detection system", *Proceedings of Seventh International Symposium on Remote Sensing of the Environment*, University of Michigan, Ann Arbor, pp. 1523-1536.

Eastman, J. R., (1999), *Guide to GIS and Image Processing*, Volume 2, Clark Labs, USA.

Ehlers, M., M.A. Jadkowski, R.R. Howard, and D.E. Brostuen, (1990), "Application of SPOT data for regional growth analysis and local planning", *Photogrammetric Engineering & Remote Sensing*, Vol. 56, No. 2, pp. 175-180.

Estes, J. E. and G.A. Thorley, (1983), "Urban/Suburban Land use Analysis" in *Manual of Remote Sensing,* American Society of Photogrammetry, Vol. II, pp. 1571-1666.

Eyton J.R., (1993), "Urban land use Classification and Modeling using Cover-type Frequencies", *Applied Geography*, Vol. 13, pp. 111-121.

Foody, G. M., and D. P. Cox, (1994), "Sub-Pixel land cover composition estimation using a linear mixture model and fuzzy membership functions", *International Journal of Remote Sensing*, Vol.15, No. 3, pp.619-631.

Foody, G. M., M. B. McCulloch, and W. B. Yates, (1995), "Classification of remotely sensed data: Issues related to training data characteristics", *Photogrammetric Engineering and Remote Sensing,* Vol. 61, No. 4, pp. 391-402.

Forster B.C., (1985), "An examination of some problems and solutions in monitoring urban areas from satellite platforms", *International Journal of Remote Sensing*, Vol. 6, pp. 139-151.

Franklin, S. E. and D. R. Peddle, (1989), "Spectral texture for improved class discrimination in complex terrain", *International Journal of Remote Sensing*, Vol. 10, No. 8, pp. 1437-1443.

Fung, Tung and King-chung Chan, (1994), "Spatial composition of spectral classes: a structural approach for image analysis of heterogeneous land-use and land-cover types", *Photogrammetric Engineering & Remote Sensing*, Vol. 60, No. 2, pp. 173-180.

Gastellu-Etchhegorry J.P., (1990), "An assessment of SPOT XS and Landsat MSS data for digital classification of near-urban land cover", *International Journal of Remote Sensing*, Vol. 11, pp. 225-235.

Golden, M., and L. Lackey, (1992), "Using ancillary data in post classification modeling to increase the accuracy of conifer species classification from landsat thematic mapper data", *GIS'92 Symposium*, Vancouver, British Columbia, Canada.

Green, N. E. and Monier R. B., (1960), "Aerial photographic interpretation of the ecological structure of the city", *Photogrammetric Engineering & Remote Sensing*, Vol. 26, pp. 770-773.

Green, N. E., (1957), "Aerial photographic interpretation of the social structure of the city", *Photogrammetric Engineering & Remote Sensing,* Vol. 23, pp. 89-96.

Griffiths, Robert J., (2001), *Developing World 01/02*, Eleventh Edition, University of North Carolina, McGraw-Hill Higher Education.

Groom G.B., R.M. Fuller and A.R. Jones, (1996), "Contextual correction: techniques for improving land cover mapping from remotely sensed images", *International Journal of Remote Sensing*, Vol. 17, No. 1, pp.69-89.

Haralick, R. M., and L.G. Shapiro, (1985), "Image segmentation techniques", *Computer Vision, Graphics, and Image Processing*, Vol. 29 (1), pp.100-132.

Harlick, R. M., (1979), "Statistical and structural approaches to texture", *Proceedings of IEEE*, Vol. 67(5), pp. 786-804.

Harris Paul M. and Stephen J. Ventura, (1995), "The integration of geographic data with remotely sensed imagery to improve classification in an urban area", *Photogrammetric Engineering & Remote Sensing*, Vol. 61, No. 8, August, pp. 993-998.

Hepner, G. F., T. Logan, N. Ritter, and N. Bryant, (1990), "Artificial neural network classification using a minimal training set: Comparison to conventional supervised classification", *Photogrammetric Engineering and Remote Sensing,* Vol. 56, No. 4, pp. 469-473.

Hodgson M.E., (1998), "What size of window for image classification? A cognitive perspective", *Photogrammetric Engineering & Remote Sensing*, Vol. 64, No. 8, August, pp. 707-807.

Homer, C.G., R.D. Ramsey, T.C. Edwards, Jr., and A. Falconer, (1997), "Landscape Cover-Type Modeling Using a Multi-Scene Thematic Mapper Mosaic", *Photogrammetric Engineering and Remote Sensing.* Vol. 63, No. 1, pp. 59-67.

Howald, K. J., (1989), "Neural network image classification", in *Proceedings ASPRS-ACSM Fall Convention - From Compass to Computer,* Cleveland, pp. 207-215, September.

Hutchinson, C. F., (1982), "Techniques for combining Landsat and ancillary data for digital classification improvement", *Photogrammetric Engineering & Remote Sensing*, Vol. 48, No. 1, pp. 123-130.

Ioka, M., and K. Masato, (1986), "Performance of Landsat-5 TM data in land cover classification", *International Journal of Remote Sensing,* Vol. 7, No. 12, pp. 1715-1728.

Jahne, B., (1995), *Digital Image Processing: Concepts, Algorithms, and Scientific Applications,* Springer-Verlag, New York.

Janssen, Lucas L.F., N.J. Marijke, and T.M., Erik, (1990), "Integrating topographic data with remote sensing for land-cover classification", *Photogrammetric Engineering & Remote Sensing*, Vol. 56, No.11, pp. 1503-1506.

Jensen, J.R. and D.L. Toll, (1982), "Detecting residential land-use development at the urban-fringe", *Photogrammetric Engineering & Remote Sensing*, Vol. 48, No. 4, pp. 629-640.

Jensen, John R., (1986), *Introductory Digital Image Processing: A Remote Sensing Perspective*, Prentice-Hall, Englewood Cliffs, New Jersey.

Justice, C.O., and J.·G Townshend, (1981), "Integrating Ground Data with Remote Sensing", in *Terrain Analysis and Remote Sensing*, Townshend J.G., editor, pp. 38-58, George Allen and Unwin, London.

Kai-Yi Huang and P. Mausel, (1993), "Spatial post-processing of spectrally classified video images by a piece wise liner classifier", *International Journal of Remote Sensing*, Vol.14, No.13, pp. 2563-2573.

Kartikeyan B., B. Gopalakrishna, M.H. Kalubarme and K.L. Majumder, (1994), "Contextual techniques for classification of high and low resolution remote sensing data", *International Journal of Remote Sensing*, Vol. 15, No. 5, pp. 1037-1051.

Kettig R.L. and D.A. Landgrebe, (1973), "Classification of multispectral of image data by extraction and classification of homogeneous objects", *IEEE Trans. Geoscience Electronics*, GE-14, pp. 19-26.

Kettig, R. L., and Landgrebe, D. A., (1976), "Classification of multispectral image data by extraction and classification of homogeneous objects", *IEEE Transactions on Geoscience Electronics*, Vol. 14, No. 1, pp. 19-26.

Key, J., A. Maslanic, and A. J. Schweiger, (1989), "Classification of merged AVHRR and SMMR arctic data with neural network", *Photogrammetric Engineering and Remote Sensing,* Vol. 55, No. 9, pp. 1331-1338.

Kivell, P. T., A.J. Parsons, and B.R.P. Dawson, (1989), "Monitoring derelict urban land: a review of problems and potentials of remote sensing techniques", *Land Degradation & Rehabilitation*, Vol. 1, pp. 5-21.

Landgrebe, David, (1997), "The evolution of landsat data analysis", *Photogrammetric Engineering & Remote Sensing*, Vol. 63, No. 7, pp. 173-180.

Lindgren, D., (1985), *Land use Planning and Remote Sensing*, Martinus Nijhoff, Dordrecht.

Luman, D.E., (1992), "Lake Michigan Ozone Study Final Report", *Lake Michigan Air Directors Consortium*, Internal Document, p. 58.

Mannan B., J. Royand A.K. Ray, (1998), "Fuzzy ARTMAP supervised classification of multi-spectral remotely sensed images", *International Journal of Remote Sensing*, Vol. 19, pp. 767-774.

Mannan, B., J. Roy, and A. K. Ray, (1998), "Fuzzy ARTMAP supervised classification of multi-spectral remotely-sensed images", *International Journal of Remote Sensing*, Vol. 19, No. 4, pp.767-774.

Martin L.R.G., P.J. Howarth and G. Holder, (1988), "Multispectral classification of land use at the rural-urban fringe using SPOT data", *Canadian Journal of Remote Sensing*, Vol. 14, pp. 72-79.

Martin L.R.G., P.J. Howarth and G. Holder, (1989), "Change-detection accuracy assessment using SPOT multispectral imagery of the rural-urban fringe", *Remote Sensing of Environment*, Vol. 36, pp. 55-66.

McCormick, Niall, (1999), *Satellite based Forest Mapping using the SILVICS Software*, User Manual, Space Application Institute, Ispra, Italy.

Nagao, M., and T. Matsuyam, (1979), "Edge-preserving smoothing", *Computer Graphics and Image Processing*, Vol. 9, pp. 394-407.

Narendra, P.M. and M. Goldberg, (1980), "Image segmentation with directed tree", *IEEE Transactions on Pattern Analysis and Machine Intelligence*, PAMI-2 (2), pp. 185-191.

Nellis, M.D., K. Lulla, and J. Jensen, (1990), "Interfacing geographic information systems and remote sensing for rural-urban fringe using SPOT data", *Photogrammetric Engineering & Remote Sensing*, Vol. 56, No. 3, pp. 329-331.

Ortiz, M.J., R. Formaggio, and J. C.N. Epiphanio, (1997), "Classification of croplands through integration of remote sensing, GIS and historical database", *International Journal of Remote Sensing*, Vol. 1, pp. 95-105.

Palacio-Prieto, J.L. and L. Luna-González, (1996), "Improving spectral results in a GIS context", *International Journal of Remote Sensing,* Vol. 17, No. 11, pp. 2201-2209.

Paola, J. D. and R. A. Schowengerdt, (1995), "A detailed comparison of backpropagation neural network and maximum-likelihood classifiers for urban land use classification", *IEEE Transactions on Geoscience and Remote Sensing*, Vol. 33, No. 4, pp. 981-996.

Pratt, W.K., (1991), *Digital Image Processing (Second Edition),* John Wiley and Sons, New York.

Quarmby, N.A. and J.L. Cushnie, (1989), "Monitoring urban land cover changes at the urban fringe from SPOT HRV imagery in South East England", *International Journal of Remote Sensing*, Vol. 10(6), pp. 953-963.

Robinson, G.S., (1977), "Edge detection by compass gradient masks", *Computer Graphics and Image Processing*, Vol. 6 (5), pp. 492-501.

Schaale, M. and R. Furrer, (1995), "Land surface classification by neural networks", *International Journal of Remote Sensing*, Vol. 16, No. 16, pp. 3003-3032.

Schmucker, K.J., (1982), Fuzzy Sets, Natural Language Computations and Risk Analysis, Computer Science Press.

Schoenmakers, R. P. H. M., Wilkinson, G. G., and Schouten, T. E., (1991), "Segmentation of remotely-sensed images: A re-definition for operational applications", *International Symposium on Geoscience and Remote Sensing*, pp. 1087-1090. IEEE.

Stuckes J., P.R. Coppin and M.E. Bauer, (2000), "Integrating contextual information with per-pixel classification for improved land cover classification", *Remote Sensing Environment*, Vol. 71, pp. 282-296.

Stuckes J., P.R. Coppin and M.E. Bauer, (2000), "Integrating contextual information with per-pixel classification for improved land cover classification", *Remote Sensing Environment*, Vol. 71, pp. 282-296.

Swain, P.H., and S.M. Davis, (1978), *Remote Sensing: The Quantitative Approach,* McGraw-Hill, New York.

Swan P. H., S. B. Verdeman and J.C. Tilton, (1981), "Contextual classification of multispectral image data", *Pattern Recognition*, Vol. 13, No. 6, pp. 429-441.

Thomas, I. L., (1980), "Spatial postprocessing of spectrally classified Landsat data", *Photogrammetric Engineering and Remote Sensing*, Vol. 46, No. 9, pp. 1201-1206.

Thompson, M. W., (1996), "A standard land-cover classification scheme for remote sensing applications in South Africa", *South Africa Journal of Science*, Vol. 92, January, pp. 34 - 42.

Tilton J.C., (1996), "Hybrid image segmentation for Earth Remote Sensing data analysis", *IEEE, Information Sciences and Technology Branch*, pp. 703-705.

Toulios L.G., N.J. Yassoglous and M. Moutsoulas, (1990), "Land use mapping in West Messinia, Greece, using satellite imagery", *International Journal of Remote Sensing*, Vol. 11, No. 9, pp. 1645-1661

Treitz, P.M., P. J. Howarth, and P. Gong, (1992), "Application of satellite and GIS technologies for land –cover and land use mapping at the rural-urban fringe: a case study", *Photogrammetric Engineering & Remote Sensing*, Vol. 58, No. 4, pp. 439-448.

Wang, F., (1990), "Fuzzy supervised classification of remote sensing images", *IEEE Transactions on Geoscience and Remote Sensing*, Vol. 28, No. 2, pp.194-201.

Welch, R., (1985), "Cartographic potential of SPOT image data", *Photogrammetric Engineering & Remote Sensing*, Vol. 51, No. 8, pp. 1085-1091.

Welch, R., M.M Remillard, and R.B. Slack, (1988), "Remote sensing and geographic information system techniques for aquatic resource evaluation", *Photogrammetric Engineering & Remote Sensing*, Vol. 54, No. 2, pp. 177-185.

Wilkinson G.G. and J. Megier, (1990), "Evidential reasoning in a pixel classification hierarchy- a potential method for integrating image classifiers and expert system rules based on geographic context", *International Journal of Remote Sensing*, Vol. 11, No. 10, pp. 1963-1968.

Wilkinson, G., (2000), "Spatial Pattern Recognition in Remote Sensing by Neural Networks", in *Geocomputational Modeling - Techniques and Applications*, M. M. Fischer and Y. Leung (editors), Springer-Verlag, Berlin, pp. 221-236.

Wilkinson, G.G., S. Folving, I. Kanellopoulos, N. McCormick, K. Fullerton, and J. Megier, (1994), "Forest mapping from multi-source Satellite data using neural network classifiers - an experiment in Portugal", *Remote Sensing Reviews*, Vol. 12, pp. 123-134.

Woodcock, C. and V. J. Harward, (1992), "Nested-hierarchical scene models and image segmentation", *International Journal of Remote Sensing*, Vol. 13, pp.3167-3188.

Wu, Xiping and James D. Westervelt, (1994), "Using neural networks to Correlate Satellite Imagery and ground-truth data", *Technical Report EC-94/28*, USACERL Special Report (SR), August.

Wulder, Mike, (1998), "Optical remote-sensing techniques for the assessment of forest inventory and biophysical parameters", *Progress in Physical Geography*, Vol. 22(4), pp. 449-476.

Yool, S.R., (1998), "Land cover classification in rugged areas using simulated moderate resolution remote sensor data and an artificial neural network", *International Journal of Remote Sensing*, Vol. 19, No. 1, pp. 85-96.

Zadeh, L.A., (1965), "Fuzzy Sets", *Information and Control*, Vol. 8, pp. 338 – 353.

Appendix-1.1: The Electromagnetic Spectrum

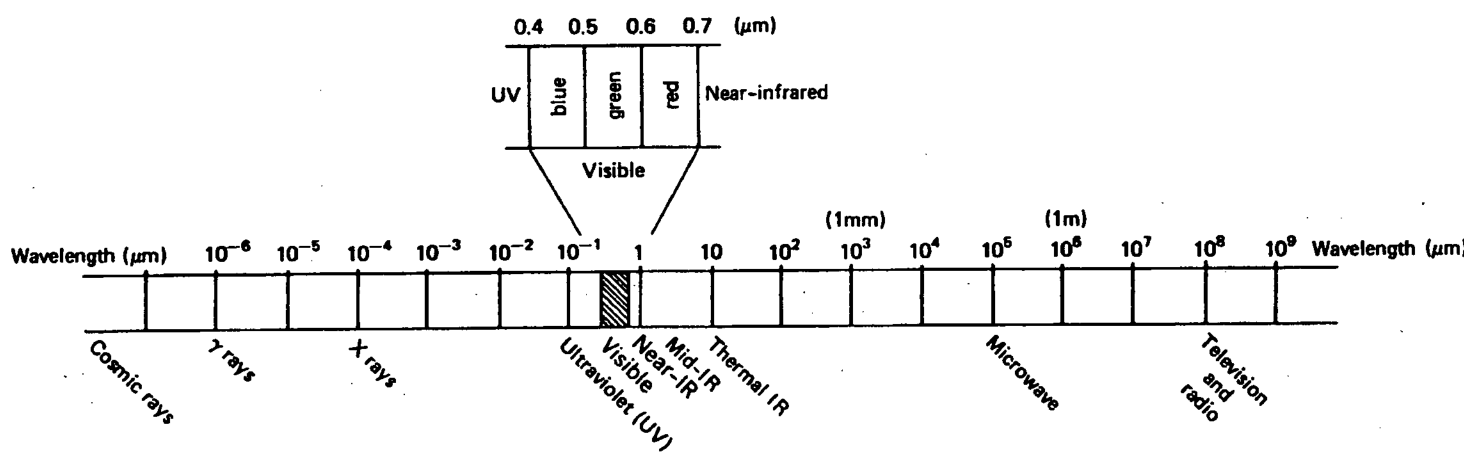

Figure 1.3 The electromagnetic spectrum.

(Source: Kiefer, R. W. et al (1994), Remote Sensing and Image Interpretation, John Wiley & Sons, New York, p. 5)